MEASUREMENT AND CONTROL OF PARTICULATE EMISSIONS FROM CATTLE FEEDLOTS IN KANSAS

by

LI GUO

B.S., Jilin Agricultural University, China, 2003
M.S., China Agricultural University, China, 2006

AN ABSTRACT OF A DISSERTATION

submitted in partial fulfillment of the requirements for the degree

DOCTOR OF PHILOSOPHY

Department of Biological and Agricultural Engineering
College of Engineering

KANSAS STATE UNIVERSITY
Manhattan, Kansas

2011

Abstract

Emissions of particulate matter (PM) are an increasing concern for large open beef cattle feedlots. Research is needed to develop science-based information on PM emissions and abatement measures for mitigating those emissions. This research was conducted to (1) measure PM concentrations emitted from large cattle feedlots, (2) compare different samplers for measuring concentrations of PM with equivalent aerodynamic diameter of 10 µm or less (PM_{10}), (3) evaluate the relative effectiveness of pen surface treatments in reducing PM_{10} emissions, and (4) predict PM control efficiency of vegetative barriers.

Concentrations of PM with equivalent aerodynamic diameter of 2.5 µm or less ($PM_{2.5}$), PM_{10}, and total suspended particulates (TSP) upwind and downwind of two large cattle feedlots (KS1, KS2) in Kansas were measured with gravimetric samplers. The downwind and net concentrations generally decreased with increasing water content (WC) of the pen surface; for effective control of PM emissions from feedlots, it appears that pen surface WC should be at least 20% (wet basis).

Three types of samplers for measuring PM_{10} concentrations in feedlots KS1 and KS2 were compared: Tapered Element Oscillating Microbalance™ (TEOM), high-volume (HV), and low-volume (LV) PM_{10} samplers. Measured PM_{10} concentration was generally largest with the TEOM PM_{10} sampler and smallest with the LV PM_{10} sampler.

A laboratory apparatus was developed for measuring the PM_{10} emission potential of pen surfaces as affected by surface treatments. The apparatus was equipped with a simulated pen surface, mock cattle hooves that moved horizontally across the pen surface, and PM_{10} samplers that collected emitted PM_{10}. Of the surface treatments evaluated, application of water (6.4 mm) and hay (723 g/m^2) exhibited the greatest percentage reduction in PM_{10} emission potential (69% and 77%, respectively) compared with the untreated manure layer.

Computational fluid dynamics (CFD) was applied to predict airflow and particle collection by a row of trees (2.2 m high × 1.6 m wide). Predicted particle collection efficiencies generally agreed with published data and ranged from less than 1% for 0.875-µm particles to approximately 32% for 15-µm particles.

MEASUREMENT AND CONTROL OF PARTICULATE EMISSION FROM CATTLE FEEDLOTS IN KANSAS

by

LI GUO

B.S., Jilin Agricultural University, China, 2003
M.S., China Agricultural University, China, 2006

A DISSERTATION

submitted in partial fulfillment of the requirements for the degree

DOCTOR OF PHILOSOPHY

Department of Biological and Agricultural Engineering
College of Engineering

KANSAS STATE UNIVERSITY
Manhattan, Kansas

2011

Approved by:

Major Professor
Ronaldo G. Maghirang

Copyright

LI GUO

2011

Abstract

Emissions of particulate matter (PM) are an increasing concern for large open beef cattle feedlots. Research is needed to develop science-based information on PM emissions and abatement measures for mitigating those emissions. This research was conducted to (1) measure PM concentrations emitted from large cattle feedlots, (2) compare different samplers for measuring concentrations of PM with equivalent aerodynamic diameter of 10 µm or less (PM_{10}), (3) evaluate the relative effectiveness of pen surface treatments in reducing PM_{10} emissions, and (4) predict PM control efficiency of vegetative barriers.

Concentrations of PM with equivalent aerodynamic diameter of 2.5 µm or less ($PM_{2.5}$), PM_{10}, and total suspended particulates (TSP) upwind and downwind of two large cattle feedlots (KS1, KS2) in Kansas were measured with gravimetric samplers. The downwind and net concentrations generally decreased with increasing water content (WC) of the pen surface; for effective control of PM emissions from feedlots, it appears that pen surface WC should be at least 20% (wet basis).

Three types of samplers for measuring PM_{10} concentrations in feedlots KS1 and KS2 were compared: Tapered Element Oscillating Microbalance™ (TEOM), high-volume (HV), and low-volume (LV) PM_{10} samplers. Measured PM_{10} concentration was generally largest with the TEOM PM_{10} sampler and smallest with the LV PM_{10} sampler.

A laboratory apparatus was developed for measuring the PM_{10} emission potential of pen surfaces as affected by surface treatments. The apparatus was equipped with a simulated pen surface, mock cattle hooves that moved horizontally across the pen surface, and PM_{10} samplers that collected emitted PM_{10}. Of the surface treatments evaluated, application of water (6.4 mm) and hay (723 g/m^2) exhibited the greatest percentage reduction in PM_{10} emission potential (69% and 77%, respectively) compared with the untreated manure layer.

Computational fluid dynamics (CFD) was applied to predict airflow and particle collection by a row of trees (2.2 m high × 1.6 m wide). Predicted particle collection efficiencies generally agreed with published data and ranged from less than 1% for 0.875-µm particles to approximately 32% for 15-µm particles.

Table of Contents

List of Figures

List of Tables

Nomenclature

$\vec{A}$	Face normal vector of the cell face
AERMOD	American Meteorological Society/Environmental Protection Agency Regulatory Model
AFO	Animal feeding operation
APS	Aerodynamic Particle Sizer
ASTM	American Society for Testing and Materials
c	An arbitrary factor to determine x_s
C_2	Inertial resistance for porous medium model (m^{-1})
$C_{1\varepsilon}$, $C_{2\varepsilon}$, $C_{3\varepsilon}$, $C_{4\varepsilon}$	Constants for $k-\varepsilon$ turbulence model
C_c	Slip correction factor
C_c	Drag coefficient
C_{pol}	Polhausen coefficient
CAFO	Concentrated animal feeding operation
CE	Particle collection efficiency of tree at certain height of barrier (%)
CE_{cell}	Particle collection efficiency of the elements of the tree in each cell
CFD	Computational fluid dynamics
CFR	Code of Federal Regulations
d_a	Equivalent aerodynamic diameter of a particle (µm)
d_e	Diameter of tree element (mm)
d_p	Particle diameter (µm)
d_i	Geometric mean diameter of particles in the j^{th} stage of the MOUDI (µm)
D_T	Turbulent diffusivity coefficient
d_{SA}	Surface area density of tree (m^{-1})
E	Hoof energy (Joule)
E_D	Collection efficiency of individual element of porous barrier due to diffusion (%)

E_I	Collection efficiency of individual element of porous barrier due to impaction (%)
F	Total particle flux to the barrier (#/s)
F_x	Any additional force (N/kg)
FEM	Federal equivalent method
FRM	Federal reference method
g_i	Gravitational vector in i^{th} direction (m/s^2)
G_b	Generation of turbulence kinetic energy due to buoyancy ($kg/m \cdot s^3$)
G_k	Generation of turbulence kinetic energy due to the mean velocity gradient ($kg/m \cdot s^3$)
GMD	Geometric mean diameter (µm)
GSD	Geometric standard deviation
H	Height of barrier (m)
HV	High-volume
k	Turbulent kinetic energy (m^2/s^2)
k_{in}	Turbulent kinetic energy of inflow (m^2/s^2)
k_r	Resistance coefficient or pressure loss coefficient
LV	Low-volume
m_j	Mass fraction of particles in the j^{th} stage of the MOUDI
MMD	Mass median diameter (µm)
MOUDI	Micro-Orifice Uniform Deposit Impactor
N_{in}, N_{out}	Particle concentration entering and emerging a cell ($\#/m^3$)
N_k	Number concentration of the k^{th} scalar or particles ($\#/m^3$)
N_{up}, N_{down}	Number concentration upwind and downwind of the barrier at certain height of barrier ($\#/m^3$)
N_x, N_z	Number of cell columns and rows for the barriers (uniform vertical and horizontal spacing)
NAAQS	National Ambient Air Quality Standards
NRC	National Research Council
P	Pressure (Pa)
PM	Particulate matter

$PM_{2.5}$	PM with equivalent aerodynamic diameter of 2.5 µm or less
PM_{10}	PM with equivalent aerodynamic diameter of 10 µm or less
Pr_t	Turbulent Prandtl number for energy
r	Weighting factor total particle collection efficiency
R	Stretching ratio from the barrier to outer boundaries
Re	Reynolds number for flow around an element
Re_p	Particle Reynolds number
RANS	Reynolds-averaged Navier-Stokes
S_i	Source term in the i^{th} direction
$S_{\Phi k}$	Source term that can be supplied by the user for each of the N scalar equations
Sc	Schmidt number
Sc_t	Turbulent Schmidt number
SE	Standard error
St	Stokes number
SIMPLE	Semi-Implicit Method for Pressure-Linked Equations
T	Absolute temperature, K
TEOM™	Tapered Element Oscillating Microbalance
TSP	Total suspended particulate
u, v	Velocity components in x and y directions (m/s)
u_0	Reference wind speed (m/s)
u_i, u_j	Air velocity in the i^{th} and j^{th} direction (m/s)
u_{in}, v_{in}	Inflow velocities in x and y directions (m/s)
u_{min}	Minimum downwind speed (m/s)
u_p	Particle velocity (m/s)
u_*	Friction velocity (m/s)
U_{cell}	Air velocity in each cell (m/s)
U_{sk}	Particle settling speed of the k^{th} particle (m/s)
UDF	User-defined function
UDS	User-defined scalar
USDA	United States Department of Agriculture

U.S.EPA	United States Environmental Protection Agency
V	Volume of each grid cell (m^3)
W	Width of barrier (m)
WC	Water content (%)
x, z	Horizontal and vertical axes
x_i, x_j	Cartesian coordinate (m)
x_{min}	Downwind distance to u_{min} (m)
x_s	Distance to u/u_0 <c (m)
X_{down}	Horizontal distance from origin to airflow outlet (m)
X_{up}	Horizontal distance from airflow inlet to the upwind edge of the barrier (m)
Y_M	Contribution of the fluctuating dilatation in compressible turbulence to the overall dissipation rate
z_0	Roughness height (m)
Z	Distance from ground to upper boundary of the domain (m)
Δx, Δz	Length of edge of each grid cell in x and z directions (m)

Greek symbols

α	Permeability of barrier (m^2)
ε	Turbulent dissipation rate (m^2/s^3)
ε_{in}	Turbulent dissipation rate of inflow (m^2/s^3)
β	Coefficient of thermal expansion
θ	Angle between the element orientation and the stream wise direction (º)
ρ	Air density (kg/m^3)
ρ_p	Particle density (kg/m^3)
μ	Air dynamic viscosity ($N \cdot s/ m^2$)
μ_t	Turbulent (or eddy) viscosity ($kg/m \cdot s$)
σ_ε	Turbulent Prandtl number for ε
σ_k	Turbulent Prandtl number for k
φ	Optical porosity

ϕ	Arbitrary scalar
ϕ_i	Passive scalar
δ	Aerodynamic porosity
ζ	Boltzmann constant (N·m/K)
λ	Mean free path (μm)
τ_p	Particle relaxation time (s)
Γ	Diffusion coefficient
Γ_D	Laminar diffusivity coefficient
Γ_k	Total diffusivity coefficient
$\vec{\psi}$	Vector field
υ	Kinematic viscosity (m^2/s)
υ_t	Local kinematic viscosity (m^2/s)

Acknowledgements

We don’t accomplish anything in this world alone. Words are limited to express my deepest gratitude, but I give my sincere appreciation to the following people and organizations that supported me for my PhD study and for the accomplishment of this dissertation.

First, special thanks to Dr. Ronaldo G. Maghirang, my advisor, who gave me the chance to study at Kansas State University (KSU) and guided me throughout the duration of my PhD program. I really appreciate his professional guidance leading me to the entrance of scientific work with support, encouragement, and patience. I thank him also for his help in my career development. Sincere thanks are given to my committee members, Dr. Joseph Harner, Dr. Larry E. Erickson, Dr. Zhongquan Zheng as well as Dr. Michael Dikeman, my outside committee chair, for their advice and contributions to the improvement of this dissertation and for serving on my graduate supervisory and examination committee.

I would like to acknowledge the support provided by USDA NIFA for the Special Research Grant “Air Quality: Reducing Air Emissions from Cattle Feedlots and Dairies (TX and KS)” through the Texas AgriLife Research and Extension Center of the Texas A&M University System and for the Grant No. 2007-35112-17853, "Impact of water sprinkler systems on air quality in cattle feedlots." Cooperation of KLA Environmental Services and feedlot managers/operators is also greatly appreciated and acknowledged.

Great thanks also are given to the BAE Air Quality Team--excellent research group, hard-working and cooperative members! Give my many thanks to Edna, our best “manager,” the first close person I met on the first day I landed in America. From that late night in the airport, our journey of working together and her endless mentoring on my research started; I was amazed by her ability in resolving problems. I thank Henry, an intelligent person, from whom I was aware that “I am a senior now;” I appreciate the time we were learning and helping each other in the classes and research projects. I thank Howell, a happy, enthusiastic and talkative person; my oral English was improved quickly since his coming. I thank Orlando, who is a big old brother; he brought me lot of fun during the field work with his humor and patience. I thank Curtis who is an amazing American and Jasper who is a knowledgeable researcher; they gave me lot of help during my lab and field work. I thank Haidee, Susana, Josephine, and Emad, who were my

"seniors." They helped me lot from my beginning life at KSU; especially Haidee, she always drove me to church and parties, and showed me different cultures. I also thank Jeremy, David, Kevin, Matt, and Katie, who helped me in my research work. Thank you guys and I will never forget those colorful days we spent in the field, lab, office and trip.

I would also like to express my gratitude to Dr. Naiqian Zhang, through whom I knew Dr. Maghirang and the PhD program in our department. I thank Dr. Zhang also for the invitations of almost every party he held since I came here. I would also like to thank the BAE Department personnel, especially Mr. Darrell Oard, Barb Moore, and Randy Erickson, for facilitating necessary documents and supplies during my PhD study. Thanks are given to Dr. Donghai Wang and Dr. Wenqiao Yuan for their warm help and consideration.

Big thanks also to Ning and Peng, who are my "siblings" at KSU. I wish to thank them for their help in my daily and academic life, their encouragement and comfort. To Jing, my close friend and roommate, I thank her for everything we shared. I would also like to thank my friends from China, Philippines and other countries for those wonderful times we spent at KSU and for making my graduate experience fun and wonderful. The lifelong friendships which we have made are truly special.

Professor Fanxi Meng, my M.S advisor at China Agricultural University, is also given my great thanks. I thank him for creating the chance for me to study abroad, both in USA and Israel, which greatly and positively influenced my life forever. I thank him also for the encouragement during the time I studied at KSU.

Finally, I offer my most sincere gratitude to my families. To my Mother and Father, I thank them for their unlimited support. I know they are proud of me, but they had much worrying about me. To my sister, Ying Guo, I am lucky to have her being around my parents when I am away. I thank her for just being there, encouraging me to succeed, and always making me happy……I love you all.

CHAPTER 1 - Introduction

1.1 Background

About 96 million cattle were raised in the U.S. in 2003 and more than 20 million are raised annually for fattening in feedlots (Rogge et al., 2006). Every year, about 18 million metric tons of manure that can cause air and water quality issues are generated from these feedlots (USDA, 2000). It has been suggested that fugitive dust and odor nuisances are the major emissions from concentrated cattle feedlots that can impair the quality of life of workers and nearby residents (Purdy et al., 2004; McGinn et al., 2002). The National Ambient Air Quality Standards (NAAQS) for particulate matter (PM) and other criteria pollutants were established to protect public health and welfare. Historically, agricultural sources, including animal feeding operations (AFOs), have been exempted from this regulation. Recently, however, agricultural sources have been included to the NAAQS regulation (NCBA, 2010; Lester, 2006).

All properties of PM depend on particle size and their health and environmental effects also depend on particle size. Coarse particles tend to be deposited in the upper airways of the respiratory tract, while PM with equivalent aerodynamic diameter of 2.5 µm or less ($PM_{2.5}$) can reach and be deposited in the smallest airways in the lungs. Consequently, U.S. EPA changed the regulation from total suspended particulates (TSP), to PM with equivalent aerodynamic diameter of 10 µm or less (PM_{10}) in 1987, and further regulates the mass concentration of $PM_{2.5}$ (Esworthy and McCarthy, 2008; U.S. EPA, 1997). Researchers (McGinn et al., 2010; Von Essen and Auvermann, 2005; Loneragan and Brashears, 2005; McGinn et al., 2002; NRC, 2003; Parnell et al., 1994) recommended long-term and short-term research needs for PM emissions from cattle feedlots, which focus on determining PM concentrations, emission rates, and dispersion to establish the potential severity of adverse impacts and the potential for developing successful mitigation and control strategies.

1.2 Characterization of Particulate Matter Emissions from Cattle Feedlots

There are many sources of dust from cattle feedlots, including traffic on unpaved roads, feed processing and delivery, vehicle exhaust, wind erosion, and cattle activity inside the pens. The major source of PM is the pen surface, composed of manure, urine, and soil. The majority of

PM emissions from the pen surface generally results from hoof action on the dry, uncompacted, pulverized layer of soil and manure (Razote et al., 2007; Auvermann et al., 2006; Purdy et al., 2004). Previous research on cattle feedlots involved measurements upwind, inside, and/or downwind of feedlots to determine the concentration, size distribution, and components of the PM emitted. Historically, a much larger database for TSP has been reported in the literature than that for PM_{10} and $PM_{2.5}$. The first PM_{10} data from cattle feedlots appeared to be those reported by Sweeten et al. (1988); limited data on $PM_{2.5}$ from feedlots have been reported in the literature.

Many factors affect the emission rate of PM from a feedlot. Cattle movement within the holding pens, wind acting on the dried pen surfaces, and vehicle travel on the alleyways contribute to PM emissions. The effect of manure on surface water, which is a function of cattle density, and the influence of weather conditions such as wind speed, precipitation, and evaporation of water are also major factors that affect PM emissions from cattle feedlots. Consequently, the pen area, weather conditions, and cattle density in pens are primary influences on PM generation (Parnell et al., 1994; Sweeten et al., 1988). Miller and Woodbury (2003) indicated that important environmental factors that contribute to dust emissions from cattle feedlots are poorly characterized.

Particulate matter is a mixture of many classes of pollutants that differ in source, formation mechanism, composition, size, and chemical, physical and biological properties. Measuring and characterizing airborne PM is a challenging task and there is no perfect method for every application, since PM is not a homogeneous pollutant. Measurement accuracy is crucial because it determines air quality trends and if a location is in compliance with air quality standards as well as for epidemiologic studies (U.S. EPA, 2004). However, no calibration standards for suspended particle mass exist and the accuracy of particle mass measurements cannot be determined at present. U.S. EPA currently defines PM measurement accuracy in terms of the agreement between a candidate sampler and a Federal Reference Methods (FRM) sampler under standardized condition for sample collection, storage, and analysis (Buser, 2004; U.S. EPA, 2004). Therefore, sampler comparisons are necessary to determine the measurement precision and the factors that influence the accuracy of sampling.

1.3 Control of Particulate Matter Emissions

Particulate matter control strategies generally fall into two categories. The first is reducing the generation rate and preventing PM emission, and include varying the stocking density (Auvermann and Romanillos, 2000a, 2000b), modifying cattle behavior relative to feeding schedule (Miller and Berry, 2005), water sprinkler systems (Razote et al., 2007; Sweeten et al., 1988; Sweeten et al., 1998), manure harvesting (Auvermann and Romanillos, 2000a), and pen surface treatments (Razote et al., 2006). The second involves edge-of-feedlot or downwind control techniques, including shelterbelts (artificial or natural) to remove and disperse particles (Adrizal et al., 2008).

Maintenance of pen surface water levels is one of the most effective ways to control dust. The water balance may be modified by adjusting stocking density (number of animals per unit pen area or animal spacing) to compensate for increases in net evaporative demand (evaporation depth less the effective or retained precipitation) (Auvermann et al., 2006). Varying the stocking density by reducing cattle spacing can reduce cattle activity, which is a major contributor to PM emission. Dust can be controlled through proper pen design and maintenance of pen surface water levels. The loose manure layer should be kept to less than 25 mm deep and pen water content to within 25% to 35% (Davis et al., 2004). However, no quantitative data are available on how effective manure management is in reducing PM emissions. Frequent manure harvesting is also labor intensive for feedlots (Davis et al., 2004). Application of water through fixed high-pressure sprinklers and water trucks are common management strategies used to reduce dust potential on feedlots (Auvermann, 2006; Sweeten et al., 1988; Sweeten et al., 1998). However installation and operation of a sprinkler system or traveling water guns are expensive (Bonifacio, 2009; Harner et al., 2008; Amosson et al., 2006, 2007). In addition, excess water used in dust control can create anaerobic conditions in the manure pack resulting in odor problems.

Organic residues, when applied on the pen surface, might help to retain and preserve water by slowing evaporation, protect the pen surface from rain by reducing its impact and slowing runoff speed, add organic matter and nutrients to the soil, and also repel insects (PM10 Inc., 2007; Auvermann et al., 2006). In addition, the residue may provide a cushioning property that reduces the hoof's shearing effect. Candidate materials include straw, waste hay, cotton,

peanut hulls, sawdust, apple pumice, lignosulfate, gypsum, and fly ash (Auvermann et al., 2006; Davis et al., 2004). However, limited research data exist on their effectiveness.

Research on porous barriers (called windbreaks, shelterbelts, vegetative barriers) started in the 1930s and focused on the reduction of wind speed and modification of microclimate based on field measurements, wind tunnel studies, or numerical simulations (Lin, 2006; Dierickx et al., 2003; Raupach et al., 2001; Cleugh, 1998; Wang and Takle, 1995; Wilson, 1985). Davis et al. (2004) indicated that trees planted along the perimeter of a feedlot will provide shelter from the wind largely containing any fugitive dust. Currently, little research is being done on the design of shelterbelt around cattle feedlots and no data are available on how effective the shelterbelts are in capturing PM emissions from cattle feedlots.

1.4 Research Objectives

The major objectives of this research are to characterize the PM emitted from cattle feedlots and investigate potential methods to control PM emissions and/or downwind concentrations from the feedlots. Specific objectives were as follows:

1. Measure the concentration and size distribution of PM emitted from large cattle feedlots;
2. Compare different samplers for measuring PM_{10} concentrations;
3. Evaluate the relative effectiveness of pen surface treatments in reducing PM_{10} emissions; and
4. Predict PM control efficiency of vegetative barriers.

1.5 Organization of Dissertation

This dissertation has seven chapters. This chapter summarizes the rationale, significance, and major objectives behind this research. Chapter 2 reviews the literature related to this research. Chapter 3 deals with the measurement of particulate matter emitted from two cattle feedlots in Kansas (specific objective 1). Chapter 4 focuses on the comparison and evaluation of PM samplers (specific objective 2). Chapter 5 discusses potential methods to control PM emissions (specific objective 3). Chapter 6 presents two-dimensional models using numerical methods to simulate the airflow and predict the collection efficiency of porous barriers (specific objective 4). Chapter 7 provides conclusions and recommendations for future work.

1.6 References

Adrizal, P.H. Patterson, R.M. Hulet, R.M. Bates, D.A. Despot, E.F. Wheeler, P.A. Topper, D.A. Anderson, and J.R. Thompson. 2008. The potential for plants to trap emissions from farms with laying hens: 2. Ammonia and dust. *J. Appl. Poultry Res.* 17(3): 398-411.

Amosson, S.H., F. Bretz, L. New, and L.K. Almas. 2007. Economic analysis of a traveling gun for feedyard dust suppression. Mobile, Ala.: Presentation at Southern Agricultural Economics Association Annual Meeting.

Amosson, S.H., B. Guerrero, and L.K. Almas. 2006. Economic analysis of solid-set sprinklers to control dust in feedlots. Orlando, Fla.: Presentation at Southern Agricultural Economics Association Annual Meeting.

Auvermann, B.W., R. Bottcher, A. Heber, D. Meyer, C.B. Parnell, Jr., B. Shaw, and J. Worley. 2006. Particulate matter emissions from animal feeding operations. In *Animal Agriculture and the Environment: National Center for Manure and Animal Waste Management White Papers*, 435-468. J.M. Rice, D.F. Caldwell, F.J. Humenik, eds. St. Joseph, Mich.: ASABE.

Auvermann, B.W., and A.Romanillos. 2000a. Effect of increased stocking density on fugitive emissions of PM_{10} from cattle feedyards. In *Proc. International Meeting of the Air and Waste Management Association*. Pittsburgh, Penn.: Air and Waste Management Association.

Auvermann, B. W., and A.Romanillos. 2000b. Manipulating stocking density to manage fugitive dust emission from cattle feedyards. In *Proc. of the Innovative Technologies for Planning Animal Feeding Operations*, 61-70. Akron, Colo.: USDA-ARS Central Great Plains Research Station.

Bonifacio, H.F. 2009. Particulate matter emissions from commercial beef cattle feedlots in Kansas. MS thesis. Manhattan, Kan.: Kansas State University.

Buser, M.D. 2004. Errors associated with particulate matter measurements on rural sources: appropriate basis for regulating cotton gins. PhD diss. College Station, Tex.: Texas A&M University.

Cleugh, H.A. 1998. Effects of windbreaks on airflow, microclimates and crop yields. *Agroforestry Syst.* 41(1): 55-84.

Davis, J.G., T.L. Stanton, and T. Haren. 2004. Feedlot manure management. Management, Livestock Series. No. 1.220. Fort Collins, Colo.: Colorado State University Cooperative Extension. Available at: http://www.cde.state.co.us/artemis/UCSU20/UCSU2062212202002INTERNET.pdf. Accessed 15 February 2010.

Dierickx, W., W.M. Cornelis, and D. Gabriels. 2003. Wind tunnel study on rough and smooth surface turbulent approach flow and on inclined windscreens. *Biosystems Eng.* 86(2):151-166.

Esworthy, R., and J.E. McCarthy. 2008. The national ambient air quality standard for particulate matter (PM): EPA's 2006 revisions and associated issues. Available at: http://congressionalresearch.com/RL34762/document.php?study=The+National+Ambient+Air+Quality+Standard+for+Particulate+Matter+PM+EPAs+2006+Revisions+and+Associated+Issues. Accessed 25 October 2009.

Harner, J.P., R.G. Maghirang, and E.B. Razote. 2008. Water requirements for controlling dust from open feedlots. In *Mitigating Air Emissions from Animal Feeding Operations Conference*. Ames, Iowa: Iowa State University.

Lester, J.C. 2006. Air Quality: Policies and standards-the evolution of agricultural air quality regulations. Washington, D.C.: Workshop on Agricultural Air Quality. Available at: http://www.ncsu.edu/airworkshop/Air_Quality_Policies_and_Standards.pdf. Accessed 29 October 2010

Lin, X. 2006. Simulation of odor dispersion around natural windbreaks. PhD diss. Ste-Anne-de-Bellevue, Quebec: McGill University.

Loneragan, G.H., and M.M. Brashears. 2005. Effects of using retention-pond water for dust abatement on performance of feedlot steers and carriage of Escherichia coli O157 and Salmonella spp. *J. Am. Veterinary Med. Assoc.* 226(8): 1378-1383.

McGinn, S.M., T.K Flesch, D. Chen, B. Crenna, O.T. Denmead, T. Naylor, and D. Rowell. 2010. Coarse particulate matter emissions from cattle feedlots in Australia. *J. Environ. Qual.* 39(3):791-789.

McGinn, S.M., K.M. Koenig, and T. Coates. 2002. Effect of diet on odorant emissions from cattle manure. *Can. J. Anim. Sci.* 82(3): 435-444.

Miller, D.N., and E.D. Berry. 2005. Cattle feedlot soil moisture and manure content: 1. Impacts on greenhouse gases, odor compounds, nitrogen losses, and dust. *J. Environ. Qual.* 34(2): 644-655.

Miller, D.N. and B.L. Woodbury. 2003. Simple protocols to determine dust potentials from cattle feedlot soil and surface samples. *J. Environ. Qual.* 32(5): 1634-1640.

NCBA. 2010. Agricultural dust and the Clean Air Act. National Cattlemen's Beef Association. Available at: http://www.beefusa.org/goveagdustandthecleanairact.aspx. Accessed 30 October 2010.

National Research Council (NRC). 2003. *Air emissions from animal feeding operations: current knowledge, future needs.* Washington D.C.: The National Academies Press.

Parnell, S.E., B.J. Lesikar, J.M. Sweeten, and R.E. Lacey. 1994. Determination of the emission factor for cattle feedyards by applied dispersion modeling. ASAE Paper No. 94-4042. St. Joseph, Mich.: ASAE.

PM10 Inc. 2007. Erosion control - mulching. Palm Desert, Calif.: PM10 Inc. Available at: http://www.pm10inc.com/erosion-control-mulching.html. Accessed 1 April 2010.

Purdy, C.W., D.C. Straus, D.B. Parker, S.C. Wilson, and R.N. Clark. 2004. Comparison of the type and number of microorganisms and concentration of endotoxin in the air of feedyards in the Southern High Plains. *Am. J. Veterinary Res.* 65(1): 45-52.

Raupach, M.R., N. Woods, G. Dorr, J.F. Leys, and H.A. Cleugh. 2001. The entrapment of particles by windbreaks. *Atmos. Environ.* 35(20): 3373-3383.

Razote, E.B., R.G. Maghirang, J.P. Murphy, B.W. Auvermann, J.P. Harner III, D.L. Oard, W.L. Hargrove, D.B. Parker, and J.M. Sweeten. 2007. Air quality measurements from a water-sprinkled beef cattle feedlot in Kansas. ASABE Paper No. 07-4108. St. Joseph, Mich.: ASABE.

Razote E.B., R.G. Maghirang, B.Z. Predicala, J.P. Murphy, B.W. Auvermann, J.P. Harner III, and W.L. Hargrove. 2006. Laboratory evaluation of the dust emission potential of cattle feedlot surfaces. *Trans. ASABE* 49(4): 1117-1124.

Rogge, W.F., P.M. Medeiros, and B.R.T. Simoneit. 2006. Organic marker compounds for surface soil and fugitive dust from open lot dairies and cattle feedlots. *Atmos. Environ.* 40(1): 27-49.

Sweeten, J.B., C.B. Parnell, R.S. Etheredge, and D. Osborne. 1988. Dust emissions in cattle feedlots. *Vet. Clin. North Am. Food Anim. Pract.* 4(3): 557-578.

Sweeten, J.M., C.B. Parnell, B.W. Shaw, and B.W. Auvermann. 1998. Particle size distribution of cattle feedlot dust emission. *Trans. ASAE* 41(5): 1477-1481.

USDA. 2000. Air Quality Research and Technology Transfer Program for Concentrated Animal Feeding Operations. Washington, D.C.: USDA Agricultural Task Force Meeting. Available at: http://www.airquality.nrcs.usda.gov/aaqtf/Documents/Old_Archives/2000/Policy/CAFO.htm. Accessed 10 November 2010.

U.S. EPA. 1997. National ambient air quality standards for particulate matter - final rule. 40 CFR part 50, Federal Register, Vol.62, No. 138. Available at: http://www.epa.gov/ttncaaa1/t1/fr_notices/pmnaaqs.pdf. Accessed 10 November 2010.

U.S. EPA. 2004. Air quality criteria for particulate matter, volume1, II. Research Triangle Park, N.C.: Office of Research and Development & National Center for Environmental Assessment-RTP office. Available at: http://publicfiles.dep.state.fl.us/OGC/GREC_PPSA-BUSSING_DISCOVERY_RESPONSES/Particulate%20Matter%20Children%20and%20Asthma/7%20of%2011/VOL_I_FINAL_PM_AQCD_OCT2004%20Part%201%20of%203.pdf. Accessed 10 November 2010.

Von Essen, S.G., and B.W. Auvermann. 2005. Health effects from breathing air near CAFOs for feeder cattle and hogs. *J. Agromedicine* 10(4): 55-64.

Wang, H., and E.S. Takle. 1995. A numerical simulation of boundary-layer flows near shelterbelts. *Boundary Layer Meteorol.* 75(1-2): 141-173.

Wilson, J.D. 1985. Numerical studies of flow through a windbreak. *J. Wind Eng. Ind. Aerodyn.* 21(2): 119-154.

CHAPTER 2 - Literature Review

2.1 Background

Air emissions from animal feeding operations (AFOs) have become a public concern because of their potential environmental effects and health impacts on humans and animals. An AFO is defined as an operation in which animals are raised and fed in a confined situation for a total of 45 days or more during a 12-month period, so large amounts of manure are generated (U.S. GAO, 2008) and odors, gases, and particulate matter (PM) are emitted. Strong odors and PM emanating from AFOs bring frequent complaints from nearby residents (Bunton et al., 2006; Bottcher, 2001).

Particulate matter may be transported from AFOs to nearby residences and cause actual or perceived health effects (Lee and Zhang, 2008; Reynolds et al., 1998). Various authors have found a relationship between respiratory diseases in children, farm workers, and residents living near AFOs and dust from AFOs (Mathisen et al., 2004; Sundblad et al., 2002; Wickens et al., 2002; Radon et al., 2007). Airborne particles may have potential health hazards to animals as well (MacVean et al., 1986). Hammond et al. (1981, 1979) indicated that PM plays a crucial role in transporting and even magnifying swine odor. Emitted fugitive PM might also occasionally reduce downwind visibility and cause local haze (Upadhyay et al., 2008; NRC, 2003)

The NRC (2003) ranked the potential importance of AFO emissions at different scales (Table 2.1). PM_{10} (PM with equivalent aerodynamic diameter, d_a, of 10 µm or less) and $PM_{2.5}$ (PM with d_a of 2.5 µm or less) are considered significant because, in urban areas, inhalation of small PM is believed to be the major cause of increased health risks (Dominici et al., 2000; Seaton et al., 1995). There are also local significant concerns for haze and health at the property line and nearest dwelling.

Table 2.1 Rank of the potential importance of AFO emissions at different scales

Emissions	Global, National, Regional	Local, Property Line, Nearest Dwelling	Primary Effects of Concern
NH_3	Major [a]	Minor	Atmospheric deposition
N_2O	Significant	Insignificant	Global climate change
NO_x	Significant	Minor	Haze
CH_4	Significant	Insignificant	Global climate change
VOCs [b]	Insignificant	Minor	Quality of human life
H_2S	Insignificant	Significant	Quality of human life
PM_{10}	Insignificant	Significant	Haze
$PM_{2.5}$	Insignificant	Significant	Health, haze
Odor	Insignificant	Major	Quality of life

[a] Relative importance of emissions from AFOs at spatial scales based on committees' informed judgment on known or potential impacts from AFOs. Rank orders from high to low importance are major, significant, minor, and insignificant. While AFOs may not play an important role for some of these, emissions from other sources alone or in aggregate may have different rankings. For example, VOCs and NO_x play important roles in the formation of tropospheric ozone, however, the role of AFOs is likely insignificant compared to other sources.
[b] VOCs: volatile organic compounds.

Source: NRC, 2003

About 96 million cattle were raised in the U.S. in 2003 and more than 20 million cattle are raised annually for fattening in feedlots (Rogge et al., 2006). Each year, about 18 million metric tons of manure that can cause air and water quality issues are generated from these feedlots (USDA, 2000a). It has been suggested that fugitive dust and odor nuisances are the major emissions from concentrated cattle feedlots that can impair the quality of life of workers and nearby residents (Purdy et al., 2004; McGinn et al., 2002).

2.2 Health Effects, Regulations, and Research Needs

2.2.1 Health effects

The main port of entry and target tissue of PM is the respiratory system. The respiratory tract, which acts as a serial filter system, includes the air passages of the nose, mouth, nasal pharynx, oral pharynx, epiglottis, larynx, trachea, bronchi, bronchioles, and alveoli (Oberdorster et al., 2005; Kreyling et al., 2004). Particles with d_a greater than 100 µm have a low probability of entering the mouth or nose in still air for humans. As particle d_a increases from 1 to 10 µm,

nasal region deposition at rest increases from 17% to 71% (ICRP, 1994) and more particles in this size range can reach the tracheobronchial (TB) and alveolar regions. The fraction of inhaled particles depositing in the extrathoracic (ET) region is quite variable and depends on particle size, flow rate, breathing frequency, and whether breathing is through the nose or the mouth (Buser, 2004). The smaller the particle, the higher the probability of a particle to hit the epithelium of the lung structure. The ET and TB regions are the target regions of particle deposition and toxicological actions for small particles 1 to 5 nm (ICRP, 1994; Kreyling et al., 2004).

Based on information on PM exposure, dosimetry, toxicology, and epidemiology, the overall weight of evidence supports the conclusion that PM, especially fine PM, is the primary contributor to a variety of adverse health effects associated with air pollution (Kaiser, 2005; U.S. EPA, 2004). Inhalation of small PM is believed to be a major cause of increased health risks and is associated with human mortality (Dominici et al., 2000; Seaton et al., 1995).

Epidemiology studies have suggested that exposure to ambient PM was associated with various acute health outcomes (U.S. EPA, 2004; Winkenwerder, 2002; Cohen, 2000; Schwartz et al., 1996). Pulmonary function is a short-term effect resulting from ambient PM exposure. Inflammatory response in the respiratory tract, exacerbation of asthma, and decreased lung functions are also outcomes of PM exposures (U.S. EPA, 2004). Winkenwerder (2002) found that individuals with asthma and other respiratory diseases, individuals with cardiovascular disease, the elderly, and children are sensitive to severe symptoms including coughing, phlegm, wheezing, shortness of breath, bronchitis, increased asthma attacks, and aggravation of lung or heart disease. A positive relationship has been found in some studies between chronic respiratory disease and increased levels of PM long term exposure (Schwartz et al., 1996). Elevated risk for lung cancer relative to living in urban areas where ambient PM levels exceed the National Ambient Air quality Standards (NAAQS) has been also indicated (Cohen, 2000).

Few studies have addressed the impact of PM and gaseous emissions from cattle feedlots. MacVean et al. (1986) found PM concentrations preceded trends in pneumonia morbidity and that there was an apparent lag time between exposure and onset of disease of 15 days in the fall and 10 days in the spring. This indicated that airborne PM may be a precursor stressor in the respiratory system, leading to pneumonia 10 to 15 days later, Subclinical bovine infections not

recognized by feedlot personnel could be aggravated by airborne PM to produce clinically recognized disease. Many reports have associated dust with feedlot dust pneumonia, which might be caused by fungal spores or other antigens in dust through hypersensitivity reactions. It may also be that dust particles cause direct irritation to the alveolar epithelium (Woolums et al., 2001). Wilson et al. (2002) indicated that an increased incidence of cattle pneumonia was associated with an increase in concentration of dust particles in the 2.0 to 3.3 µm size range in feedlots. Dust load and the numbers and types of microorganisms may be the major contributor to this. Long-term development of chronic lung disease might be increased in dairy farmers because of airborne PM exposure (Cathomas et al., 2002; Dalphin et al., 1998).

Wyatt et al. (2007) found that airway epithelial cells' release of inflammatory cytokines, IL-8 and IL-6, can be stimulated by an extract of dust obtained from ambient air downwind of cattle feeding operations and suggest that cattle feedlot dust has the potential to elevate proinflammatory cytokines in human cells. The effects of endotoxin in conjunction with the allergic and irritant properties of the dust could predispose cattle to illness. High endotoxin levels have previously been found in cattle feedlot dust samples (Wilson et al., 2002).

In general, the information about the occupational health problems in cattle feedlot workers is very limited and does not contribute to the understanding of health concerns of feedlot neighbors. Studying workers' respiratory health status may help to understand the potential health effects of dust from feedlots. There is a need to document the health status of subjects in larger samples of cattle feedlot neighbors and to make careful comparisons with residents far from cattle feedlots (Von Essen and Auvermann, 2005).

2.2.2 NAAQS

U.S. EPA (2005) has classified particles by size distribution modes (based on observed particle size distributions and formation mechanisms), sampler "cut point" (based on the inlet characteristics of specific PM sampling devices) (Table 2.2), and dosimetry or occupational health sizes, according to their entrance into various compartments of the respiratory system. U.S. EPA also has developed NAAQS for PM, which are ambient concentration limits established to protect public health (primary standards) and public well-being (secondary standards). The guidelines are expressed as "no-observed-adverse-health effects" that represent the concentration below which no adverse effects have been observed during human and animal

laboratory and clinical studies (Wanjura et al., 2008; Winkenwerder, 2002). Historically, agricultural sources, including AFOs, have been exempted from this regulation. Recently, however, agricultural sources have been included in the NAAQS regulation (NCBA, 2010; Lester, 2006).

Table 2.2 Particle size fraction terminology of sampling measurements.

Term	Description
Total Suspended Particles (TSP)	Particles measured by a high volume sampler as described in 40 CFR Part 50, Appendix B. This sampler has a cut point of aerodynamic diameters that varies between 25 and 40 µm depending on wind speed and direction.
PM_{10}	Particles measured by a sampler that contains a size fractionator designed with an effective cut point (50% collection efficiency) of 10 µm aerodynamic diameter. This measurement includes the fine particles and a subset of coarse particles, and is an indicator for particles that can be inhaled and penetrate to the thoracic region of the lung; also referred to as thoracic particles
$PM_{2.5}$	Particles measured by a sampler that contains a size fractionator designed with an effective cut point (50% collection efficiency) of 2.5 µm aerodynamic diameter. This measurement generally includes all fine particles. A small portion of coarse particles may be included depending on the sharpness of the sampler efficiency curve.
$PM_{10-2.5}$	Particles measured directly using a dichotomous sampler or by subtraction of particles measured by a $PM_{2.5}$ sampler from those measured by a PM_{10} sampler. This measurement is an indicator for the coarse fraction of thoracic particles; also referred to as thoracic coarse particles or coarse-fraction particles.

Source: U.S. EPA (2005)

The original primary and secondary NAAQS for TSP was 260 µg/m^3 based on a 24-h average. This standard was changed in 1987 with the establishment of primary and secondary PM_{10} NAAQS of 150 µg/m^3 (24-h average) and 50 µg/m^3 (annual average) (U.S. EPA, 1997). In 1997, the NAAQS was further modified to include NAAQS for $PM_{2.5}$ of 15 µg/m^3 (annual average) and 65 µg/m^3 (24-h average). Subsequent to the 2006 review of the PM NAAQS, the

PM_{10} standard was modified by removing the annual average concentration limit of 50 µg/m^3 while retaining the 24-h average standards of 150 µg/m^3. The $PM_{2.5}$ standard was also modified by lowering the 24-h average standards to 35 µg/m^3 while maintaining the annual average concentration limit of 15 µg/m^3 (Esworthy and McCarthy, 2008). The current NAAQS for PM_{10} and $PM_{2.5}$ are summarized in Table 2.3.

Table 2.3 National Ambient Air Quality Standards (NAAQS) for PM_{10} and $PM_{2.5}$

	Level (µg/m^3)	Averaging Time
PM_{10}	150	24 h [a]
$PM_{2.5}$	15	Annual [b]
	35	24 h [c]

[a] Not to be exceeded more than once per year on average over 3 years.

[b] Annual arithmetic mean, average over 3 years.

[c] 98th percentile average over 3 years.

Source: http://www.epa.gov/air/criteria.html#4

2.2.3 Research needs

The USDA (2009) indicated that, in many instances, data do not exist or are not representative of agricultural industries for the purpose of estimating emissions to the atmosphere of regulated pollutants and greenhouse gases, including fugitive dust, and that there is a need to develop practices and technologies to assist producers in preventing or mitigating air emissions. Research needs include (1) the development of emission data for agricultural production practices and effective mitigation strategies to reduce agricultural emissions and (2) the improvement of understanding of the measurement, flux, and fate and transport of PM.

Other researchers (McGinn et al., 2010; Von Essen and Auvermann, 2005; Loneragan and Brashears, 2005; McGinn et al., 2002; NRC, 2003; Parnell et al., 1994) recommended the following research needs on PM emissions from cattle feedlots. The needs focus on determining PM concentrations, emission rates, and dispersion to establish the potential severity of adverse impacts and the potential for developing successful mitigation and control strategies:

- Assess public health concerns by determining long-term concentrations within a region. Monitor PM concentrations of possible health concern at times and typical

meteorological conditions when they are likely to be highest and in places where the densities of animals and humans are likely to result in the highest degree of human exposure. Sampling methods and instruments should be evaluated and improved to accurately quantify PM.

- Minimizing environmentally important emissions requires understanding the context of emissions, the underlying mechanisms, and the relationships between emissions. An emission factor needs to be developed that provides an accurate prediction of the particulate emission from feedlots. This emission factor would permit the estimation of downwind particulate concentrations around a feedyard under various climatological conditions.
- A larger data collection period is needed to describe the longer-term feedlot PM emissions. The large dataset could be used to validate PM models that are driven by factors such as feedlot surface and ambient conditions and cattle activity. The most applicable models for PM emissions and dispersion need to be identified and validated to be used for cattle feedlots.

2.3 Characterization and Measurement

2.3.1 Measurement methods

Particulate matter is a mixture of many classes of particles that differ in source, formation mechanism, composition, size, and chemical, physical and biological properties. Measuring and characterizing airborne PM is a challenging task and there is no perfect method for every application, since PM is not a homogeneous pollutant.

Sampling methods for characterizing PM in ambient air include federal reference methods (FRMs) and federal equivalent methods (FEMs) (Buser, 2004; U.S. EPA, 1999a, 1999b; U.S. EPA, 2006). The FRMs are manual methods established by U.S. EPA for determining the PM concentration in ambient air. In these methods, a known volume of air is drawn through the sampler and the particulate fraction of interest is collected. The mass of PM is determined gravimetrically and the average ambient concentration over the sampling period is calculated. The FEMs, in the other hand, are continuous measurements of suspended PM in ambient air and allow concentrations to be tracked in real-time. Two different measurement

principles of beta-radiation and oscillating pendulum have received U.S. EPA's approval as FEMs. All measurements of air quality are expressed as mass per unit volume corrected to a reference temperature of 25 °C and a reference pressure of 760 mm Hg, except for $PM_{2.5}$. Measurements of $PM_{2.5}$ shall be reported based on actual ambient air volume measured at the actual ambient temperature and pressure at the monitoring site during the measurement period (U.S. EPA, 2006). The basic design of the FRM and FEM samplers are given in the 40 CFR Part 50 (U.S. EPA, 2006). Performance specifications for FRM and FEM samplers are listed in 40 CFR, Parts 53 and 58 (U.S. EPA, 2001a, 2001b).

A number of samplers have been designated as FRM and FEM samplers of TSP, PM_{10}, and $PM_{2.5}$ in accordance with 40 CFR Part 53 (U.S. EPA, 2010). Different samplers have different advantages and disadvantages in terms of labor cost, instrument cost, data processing requirements, size, weight, operation, maintenance requirements, and transportability (Wanjura et al., 2008; Buser, 2004; Salter and Parsons, 1999). Although some samplers do not meet the design specifications required for designation as regulatory monitors, they are used as supplements with additional measurements, e.g., saturation monitors and other PM sampling studies (Hill et al., 1999; Upadhyay et al., 2008).

Measurement accuracy is crucial because it determines air quality trends and if a location is in compliance with air quality standards as well as for epidemiologic studies (U.S. EPA, 2004). However, no calibration standards for suspended particle mass exist and the accuracy of particle mass measurements can't be determined at present. EPA currently defines PM measurement accuracy in terms of the agreement between a candidate sampler and a FRM sampler under standardized conditions for sample collection, storage, and analysis (Buser, 2004; U.S. EPA, 2004). Therefore, sampler comparisons are necessary to determine the measurement precision and factors that influence the accuracy of sampling.

Four identical PM_{10} pre-separators, along with four identical low-volume TSP samplers were tested side-by-side in a controlled laboratory chamber by Wang et al. (2005). Results showed that PM_{10} samplers over-sampled when exposed to ambient PM having mass median diameter (MMD) larger than 10 µm and under-sampled when exposed to ambient PM with MMD smaller than 10 µm. The over-sampling and under-sampling rates varied with the change of MMD and PM loading. Buser (2004) also showed that FRM PM_{10} and $PM_{2.5}$ samplers overstated the true concentrations of PM_{10} and $PM_{2.5}$, respectively, when sampling dust with

MMD larger than the sampler cutpoint. Several researchers have indicated that the tapered element oscillating microbalance (TEOM) monitor (a FEM sampler) tended to report different concentrations than those measured by gravimetric FRM samplers. Vega et al. (2003) collocated a TEOM with sequential filter sampler to measure the PM_{10} at five sites in Mexico City during February and March, 1997. Results showed significant differences between instruments that exceeded the expected uncertainties. In general, the TEOM measured higher and more variable PM_{10} than the filter sampler. Comparison of a TEOM and 2000 series Partisol was reported by Salter and Parsons (1999) for an area where airborne PM content was dominated by geological material; these two instruments showed a non-linear relationship. TSP concentrations were measured by collocated TEOM and gravimetric samplers from a Texas cattle feedlot (Wanjura et al., 2008). The TEOM sampler reported lower TSP concentrations than the collocated gravimetric TSP sampler.

Eatough et al. (2003) indicated that volatile PM makes up a considerable portion of urban fine PM and will not be measured if the sample stream is heated. Vega et al. (2003) concluded that these differences in PM concentration may be partially attributed to the loss of semi-volatile inorganic and organic material from the filters while they are in the sampler, during transport, and storage. Generally, measurement errors result from (1) cutpoint deviations associated with established tolerances and various field application parameters; (2) losses of semi-volatile components; (3) inadequate restrictions on internal particle bounce; (4) surface overloading and inlet maintenance; and (5) cations and anions, elemental composition, carbon, and organic species (U.S. EPA, 2008; Buser, 2004).

2.3.2 PM concentrations, size distribution, and emission rates in cattle feedlots

There are many sources of dust from cattle feedlots, including traffic on unpaved roads, feed processing and delivery, vehicle exhaust, wind, and cattle activity inside the pens. The major source of PM is the pen surface, composed of manure, urine, and soil. Majority of PM emissions from the corral surface generally results from hoof action on the dry, uncompacted, pulverized layer of soil and manure (Razote et al., 2007; Auvermann et al., 2006; Purdy et al., 2004). Mitloehner (2000) indicated that most dust particles can float for long periods of time and suspend in the air one to two meters above the pen surface. Dust cloud, covering the pens for hours, can form over the feedlot on days with low wind speed and high cattle activity. In windy

conditions, these particles are blown away and can contaminate the outside feedlot environment. After precipitation events, the feedlot pad gets muddy at first then hard packed, and finally powdery.

Many factors affect the emission rate of PM from a feedlot. Cattle movement within the holding pens, wind acting on the dried pen surfaces, and vehicles travelling on alleyways contribute to PM emissions. The effect of manure on pen surface water, which is a function of cattle density, and the influence of weather conditions such as wind speed, precipitation, and evaporation of soil water, are also major factors that affect PM emissions from cattle feedlots. Consequently, the pen area, weather conditions, and cattle density in pens are primary influences on PM generation (Parnell et al., 1994; Sweeten et al., 1988). Miller and Woodbury (2003) indicated that important environmental factors that contribute to dust emissions from cattle feedlots are poorly characterized. McGinn et al. (2010) pointed out that a larger data collection period is needed to describe long term feedlot PM_{10} emissions.

Previous research in cattle feedlots involved measurements upwind, inside, and/or downwind of feedlots to determine the concentration, size distribution, and component of the PM emitted. Historically, much larger database for TSP has been reported in the literature than that for PM_{10}. The first PM_{10} data from cattle feedlots appeared to be those reported by Sweeten et al. (1988); limited data on $PM_{2.5}$ from feedlots have been reported. Sweeten et al. (1988) performed particulate sampling in three feedlots with 15 complete experiments in Texas from January to December 1987. The mean net concentration (downwind concentration-upwind concentration) for 24-h TSP sampling was 412 ± 271 $\mu g/m^3$. All three feedlots exceeded the U.S. EPA and Texas Air Control Board standards for TSP on most sampling days. The mean PM_{10} downwind concentration measured by Andersen sampler was 233 $\mu g/m^3$ and about 40% of the mean TSP dust concentration for two experiments. However, the ratio of PM_{10}/TSP was just 19% measured by Wedding sampler and it collected only 47% of the amount of particulates as the Andersen sampler. The highest net dust concentration within 24-h sampling periods occurred in the late afternoon and early evening hours and the lowest net concentrations occurred after midnight until almost noon the next day.

Purdy et al. (2007) measured the PM at four commercial feedlots in Texas. Their results showed that actual or net PM_{10} concentrations generated from two feedlots were 272 $\mu g/m^3$ and 275 $\mu g/m^3$, respectively, which exceeded the 24-h NAAQS for PM_{10}. The $PM_{2.5}$ concentration

measured at one feedlot in the summer was 40 $\mu g/m^3$ and would not be in compliance for the $PM_{2.5}$ standard.

Particulate matter emitted from beef cattle feedlots was also studied in Australia by McGinn et al. (2010). The field campaign was conducted at two feedlots from 1 to 6 February 2008 and from 26 February to 4 March 2008, respectively. The 24-h PM_{10} concentrations ranged from 9 to 61 $\mu g/m^3$. This did not exceed the U.S. EPA standard but exceeded the concentration thresholds for Europe (50 $\mu g/m^3$ for 24-h mean and not more than 35 times a year) and Australia (50 $\mu g/m^3$ for 24-h mean and not more than five times a year) twice during their 10-day sampling campaign.

MacVean et al. (1986) noted that the particulates measured at the feedlot had a bimodal size distribution, which are similar with other naturally occurring dust; they observed the highest concentration in the >7.0 µm mass mean aerodynamic diameter, while the second peak was in the smallest-size fraction <1.1 um aerodynamic diameter. Hamm (2005) reported an average MMD of 16 µm with average GSD of 2.1 as measured by a Coulter Counter at a cattle feedlot in Texas.

Based on the data reported in Sweeten et al. (1988), Parnell et al. (1993) determined a mean emission factor of 4.1 kg/1000head-day for the three feedlots in Texas. The emission factor varied with time of year. The seasonal range in PM_{10} emission factors reported by Parnell et al. (1994) were 2.9 kg/1000head-day in winter, 11.6 kg/1000head-day in spring, 1.5 kg/1000head-day in summer, and 2.9 kg/1000head-day in fall. An emission factor for Texas feedlots was estimated to be 6.8 kg/1000head-day (Auvermann et al., 2006). Using a Gaussian plume model (AERMOD) and PM_{10} concentration measured by TEOM, Bonifacio (2009) estimated the PM_{10} emission factors at three feedlots in Kansas as 21 kg/1000head-day, 29 kg/1000head-day, and 48 kg/1000head-day, respectively. McGinn et al. (2010) reported PM_{10} emission factors of 60 ± 100 kg/1000head-day for a single day at one feedlot in Australia. They indicated the large emission rate may be caused by the extremely dry surface conditions and may represent an extreme emission rate situation. At another feedlot, the average PM_{10} emission rate was 31 ± 52 kg/1000head-day with 16 days of measurement. They indicated their data only illustrated the upper potential PM_{10} emission rates from dry feedlots under summer conditions in Australia.

2.4 Control Strategies for Cattle Feedlots

Particulate matter control strategies generally fall into two categories. The first is reducing the generation rate and preventing PM emission, and include varying stocking density (Auvermann and Romanillos, 2000a, 2000b), modifying cattle behavior relative to feeding schedule (Miller and Berry, 2005), water sprinkler systems (Razote et al., 2007; Sweeten et al., 1988; Sweeten et al., 1998), manure harvesting (Auvermann and Romanillos, 2000a), and pen surface treatments (Razote et al., 2006). The second involves edge-of-feedlot or downwind control techniques, including shelterbelts (artificial or natural) to remove and disperse particles (Adrizal et al., 2008).

USDA (2000b) reported that 93.1% of the large cattle feedlots and 73.5% of the small cattle feedlots implemented at least one dust control practice during the year ending June, 1999 (Table 2.4). Mechanical scrapers were the primary methods of dust control on feedlots. Also, mobile sprinklers were used frequently in feedlots with >8000 head (Table 2.4).

Table 2.4 Percent of operations that used dust control practices in any pen or on the feedlot premise during the year ending June 30, 1999, by operation capacity

	Operation Capacity (Number Head)					
	1,000 – 7,999		**8,000 or More**		**All Operations**	
Practice	Percent	SE [a]	Percent	SE [a]	Percent	SE [a]
Permanent sprinklers	8.0	1.6	17.6	1.8	10.7	1.2
Mobile sprinklers (water truck)	26.7	2.2	69.4	2.2	38.5	1.8
Mechanical scrapers	63.8	2.7	80.9	1.9	68.5	2.0
Increased cattle density	18.2	1.9	38.7	2.3	23.9	1.5
Other	3.3	1.2	5.7	1.4	4.0	0.9
Any dust control	73.5	2.6	93.1	1.1	78.9	1.9

[a] SE represents the standard error.

Source: USDA (2000b)

2.4.1 Stocking density manipulation

Maintenance of pen surface water levels is one of the most effective ways to control dust. The water balance may be modified by adjusting stocking density (number of animals per unit pen area or animal spacing) to compensate for increases in net evaporative demand (evaporation depth less effective or retained precipitation) (Auvermann et al., 2006). Varying the stocking density by reducing cattle spacing can reduce cattle activity, which is a major contributor to the PM emission. In addition, the manure layer may be more compacted if the number of cattle per unit area is increased, so that PM emission will be reduced (Romanillos and Auvermann, 1999). Mitloehner (2000) cited that increasing stocking rate from 60-100 m^2/animal to 23 m^2/animal can be used to increase the water added to the feedlot surface in the form of excreta. An experiment on a commercial feedlot in Texas showed that decreasing the cattle spacing from 13.9 to 7.0 m^2 /head reduced net PM_{10} concentrations at the corral fence line by about 20% (Auvermann et al., 2006). However, as daily net evaporation increases, the effectiveness of increased stocking density is likely to decrease (Auvermann et al., 2006). In addition, increasing the stocking density may induce behavioral problems and reduce overall feed-to-gain performance. Furthermore, the frequency of the pen surface scraping must be increased to decrease the amount of manure buildup in pens if the stocking density is increased. Extra investments and additional labor costs might be required (Rahman, et al., 2008).

2.4.2 Feeding strategies

Auvermann et al. (2006) indicated that supplemental dietary fat may increase the cohesiveness or plasticity of the resulting manure, which makes the dried manure less susceptible to shearing. However, this method is likely to be expensive and limited research has been done.

In general, the peak time for dust occurs around sunset, when the temperature starts to cool and cattle become more active (Davis et al., 2004). Changing the feeding regime of cattle to their natural feeding time can redirect the cattle away from dust-generating behaviors and reduce the aerial concentrations of fine dust (Mitloehner, 2000). Mitloehner (2000) conducted research on the feeding schedule using a total of 803 crossbred steers in a commercial feedlot. Results showed that changing the feeding regime of cattle from conventional feeding times to an alternative feeding times reduced $PM_{2.5}$ concentrations by 37% over the entire day; changing the

feeding strategy did not negatively impact production or performance. Mitloehner (2000) indicated that changing feeding times to feeding dawn, noon, and dusk impacted the normal feedlot routine. An evening shift would have to be scheduled to feed the cattle, which might generate additional costs. Another major challenge with feeding cattle in the evening is that the animals need to be fed at approximately the same time. Once feed delivery is delayed, dust generating behaviors could potentially increase.

2.4.3 Pen management

Dust can be controlled through proper pen design and maintenance of surface water levels. The loose manure layer should be kept to less than 25 mm deep and pen water content to within 25% to 35% (Davis et al., 2004). Too much water will increase odor and fly problems; too little water will promote dust problems. Frequent harvesting of loose and dry manure from the pen surface reduces the amount of material that may be pulverized by hoof action (Auvermann et al., 2006). Routine cleaning of accumulating manure also reduces odors, controls fly larvae, and minimizes the potential for surface and groundwater contamination (Davis et al., 2004). Frequency of manure removal varies widely, depending on size of lot and pen stocking rate. Pen scraping frequency of every three or four months were recommended to minimize manure accumulation and loose manure layer. A thorough pen cleaning once per year is an absolute minimum (Auvermann et al., 2006; Davis et al., 2004). However, no quantitive data are available on how effective manure management is in reducing PM emission. Frequent manure harvesting is also labor intensive (Davis et al., 2004)

2.4.4 Water application

Application of water through fixed high-pressure sprinklers and water trucks are common management strategy used to reduce dust potential on feedlots (Auvermann, 2000a; Sweeten et al., 1988; Sweeten et al., 1998). The effectiveness of sprinklers was evaluated by Carroll et al. (1974) in two comparable feedlots (one of them was not sprinkled as a control). Results showed that a program of sprinkling the pens for 2 h reduced the total dustiness by at least half. Pechan (2006) noted that watering from either sprinklers or water trucks has control efficiencies of 50% and 25% for PM_{10} and $PM_{2.5}$, respectively. Bonifacio et al., (2011) determined the PM control efficiency of a sprinkler system in a cattle feedlot in Kansas and the results showed that PM_{10}

control efficiency ranged from 32% to 80% with an overall mean of 53% (based on 24-h PM_{10} values). The effect of the sprinkler system in reducing net PM_{10} concentration lasted for one day or less.

Whereas water application is effective in controlling PM emission in feedlots, the cost of installation and operation of a sprinkler system or traveling water guns are expensive (Bonifacio et al., 2011; Harner et al., 2008; Amosson et al., 2006, 2007). The cost per marketed head per year ranged from $0.60 to $2.40 depending on feedlot turnover and type of sprinkler systems installed (Harner et al., 2008). A 30,000 head feedlot requires 2,000 L of water per day to wet the pen (Mitloehner, 2000). Access to sufficient quantities of fresh water for adequate dust control is limited in much of the High Plains region of the U.S. Although storm water retention ponds are potential sources of water for use in dust abatement programs, these ponds are generally required to contain sufficient water for dust control needs and also prevent escape of storm water from feedlots (Loneragan and Brashears, 2005). Furthermore, excess water used in dust control can create anaerobic conditions in the manure pack resulting in odor problems. In addition, Mader et al. (2007) indicated that cattle acclimatization to being sprinkled can result in slight hyperthermia even during cooler days when sprinkling would normally not be utilized.

2.4.5 Pen surface amendments

Organic residues applied on the pen surface might help to retain and preserve water by slowing evaporation, protect soil from rain by reducing its impact and slowing runoff speed, add organic matter and nutrients to the soil, and also repel insects (PM10 Inc., 2007; Auvermann et al., 2006). In addition, the residue may provide a cushioning property that reduces the hoof's shearing effect. Candidate materials include straw, waste hay, cotton, peanut hulls, sawdust, apple pumice, lignosulfate, gypsum, and fly ash (Auvermann et al., 2006; Davis et al., 2004). However, Auvermann (2003) and Razote et al. (2006) developed experimental chambers for measuring the emission potential of cattle feedlot pen surfaces. The chambers were based on the vertical action of cattle hooves on a dry, uncompacted layer of manure. Results indicated that the impact energy of cattle hooves affected PM_{10} emission potential more than the depth of the manure surface. Manure compaction, surface application of water, and topical application of crop residues greatly reduced PM_{10} emission potential. The application of 726 g/m^2 wheat straw and sawdust reduced PM_{10} emission 76% and 69%, respectively (Razote et al., 2006).

Auvermann et al. (2006) indicated that the materials must be applied frequently on pen surfaces to consistently be effective in reducing PM emission because manure is continually excreted by cattle. Additional labor costs will be necessary if the material is applied manually, although the primary materials are cheaper than water.

2.4.6 Shelterbelts

Research on porous barriers (called windbreaks, shelterbelts, vegetative barriers) started in the 1930s and focused on the reduction of wind speed and modification of microclimate based on field measurements, wind tunnel studies, or numerical simulations (Lin, 2006; Dierickx et al., 2003; Raupach et al., 2001; Cleugh, 1998; Wang and Takle, 1995; Wilson, 1985). These porous barriers have been used primarily to control snow and sand accumulation, and pesticide drift. They are also recognized to mitigate fugitive dust and odors by mixing them with clean air, though the process is still not fully understood (Lin, 2006; Malone, 2004).

Davis et al. (2004) indicated that trees planted along the perimeter of a feedlot will provide shelter from the wind largely containing any fugitive dust. Currently, little research is being done on the design of shelterbelts around cattle feedlots and no data are available on how effective the shelterbelts are in dispersing PM emissions from cattle feedlots. However, some research had been conducted in other AFOs and regions for trees, shrubs, and other vegetation as effective scavengers of both odorant gaseous and particulate pollutants from the atmosphere. Patterson and Adrizal (2005) indicated that trees can filter dust feathers, odor, and noises from AFOs and provide a visual screen from routine activities to enhance the public perception of the AFO industry. Malone (2004) reported a 3-row planting of bald cypress, Leyland cypress, and red cedar 9 m from two tunnel fans on a commercial broiler farm reduced air speed from 127 to 1.5 m/min from the front to the back of the trees. Total dust levels were reduced 53% and 50% in 2002 and 2003, respectively. Adrizal et al. (2008) indicated that vegetative buffers are capable of trapping NH_3 and PM emissions from poultry facilities and suggested the species differences of trapping and holding NH_3 and PM can be applied in practical recommendations. Tiwary et al. (2008) measured ambient PM_{10} upwind and downwind of a Hawthorn hedge at a rural location in the UK; they reported that the hedge had a PM_{10} collection efficiency of 34% on average and suggested that hedges are potentially useful barriers for capturing ambient PM_{10}.

Formation of tortuous airflow and the surface roughness are the major factors for the collection of PM by porous barriers. Tortuous airflows lead to higher turbulence and increased mixing of PM, and surface roughness increases the likelihood of particles impacting on their foliage surfaces (Tiwary et al., 2005). Early studies have led to considerable progress in understanding wind flow and turbulence characteristics (Boldes et al., 2001). However, a full understanding of aerodynamics of windbreaks is not available, even for the relatively simple artificial fence, possibly because natural barriers are irregular and difficult to characterize structurally. Besides variable topographical settings, wind speed and direction change constantly in natural settings along with conditions of atmospheric stability (Lin, 2006; Wang and Takle, 1995). Raupach et al. (2001) noted that questions related to the entrapment of particles by porous barriers are how much of the oncoming flow passes through the porous barriers and what fraction of particles in these flow are deposited on the porous barriers as well as what is the total particle deposition. Furthermore, Tyndall and Colletti (2006) indicated that natural shelterbelts still have some potential drawbacks despite its promise as a beneficial technology. For example, many years are needed before trees will become effective, several rows of trees occupy limited farm land, knowledge on tree's growth and maintenance is needed, and so on.

2.5 Vegetative Barriers - Aerodynamics and Particle Collection

When particle-laden airflow approaches porous barriers, a portion of the oncoming air passes over the barriers and a portion flows through them allowing particles to be filtered from the flow by deposition onto vegetation elements. The speed of air is reduced through the barriers (also called bleed flow), while it is accelerated over the top of the barriers. The reduced air speed and reduced particle concentration in the downwind sheltered region cause a reduction in particle deposition on the downwind surface. With increasing downwind distance, the near-surface particle concentration and surface deposition increase because flow above the barriers are mixed downwards into the sheltered region, eventually recovering approximately to their values far upwind (Raupach et al., 2001; Cleugh, 1998). Knowledge about particle deposition on individual elements, including leaves and stems, and wind flow around and through vegetative barriers will provide guidance about the likely behavior of particle deposition on porous barriers.

2.5.1 Airflow through a porous barrier

Porous barriers normally have complex structures, consisting of numerous elements, such as stems, branches, and leaves. The basic functions of porous barriers are to reduce wind speed and change its direction around the barriers. Aerodynamically, porous barriers are wind momentum sinks (pressure loss) when the rough surface interacts with the airflow above and within the barriers. Momentum is absorbed from the flow by both form and skin-friction drags on elements and transported mainly by turbulent diffusion to produce the leeward wind speed reduction (Lin, 2006; Wang and Takle, 1995; Raupach and Thom, 1981).

The efficiency of porous barriers depends on the height (H), width or thickness (W), porosity, and orientation. For most efficient results, the barriers should be oriented perpendicular to the prevailing wind direction (Lin, 2006). Raupach and Thom (1981) described the porosity by optical porosity φ and aerodynamic porosity δ. The optical porosity φ is the ratio of open surface to total surface of the porous barriers; δ, on the other hand, is the ratio of mean wind speed (bleed wind speed) immediately leeward from the bottom to the top of the porous barriers to that upwind before the barriers. The pressure loss, which results from the viscous and inertial resistance, can be measured using a wind tunnel and simulated by computational fluid dynamics (CFD) (Guan et al., 2003). For the same porosity, windbreak pressure losses can differ because of the different structure of the solid and open portions of the windbreak. Parameters, such as the leaf area index, obstacle size, roughness length or displacement height, are important in describing the canopy geometry and aerodynamics (Petroff et al., 2008).

Previous research have shown that CFD models with the turbulent $k-\varepsilon$ model and large-eddy simulation can be used to analyze windbreaks in two and three dimensions, with good prediction of the mean wind field (Packwood, 2000; Patton et al., 1998; Wang and Takle, 1995; Wilson, 1985). Lin (2006) summarized that windbreak influence extends from approximately -5 H (windward) to 30-35 H (leeward). At downwind distances of 4-6 H, wind speed reaches a minimum and at about 20H, wind speed recovers to 80% of the approaching wind speed. Furthermore, lower minimum wind speed and faster wind speed recovery was observed for very dense windbreaks compared with more porous windbreak.

2.5.2 Particle deposition on porous barriers

Neglecting advection and assuming that the mean vertical wind velocity is zero, the processes that lead to the deposition of particles on porous barriers include the transport of particles by turbulence and sedimentation and collection by the element surface of barrier. Particle collection mechanisms include diffusion, impaction, and sedimentation; other processes like diffusiophoresis, thermophoresis or electrophoresis are less important for natural plant surfaces. The collection efficiency of these mechanisms depends on wind speed and canopy structure, together with many physical and physico-chemical parameters (Petroff et al., 2008; Peters and Eiden, 1992; Bache, 1979).

Mathematical models are available to calculate the size specific deposition velocity of aerosol particles. Petroff et al. (2008) indicated that there are great differences among the predictions of those models. In addition, analytical and differential models do not behave in the same way when the canopy geometry changes. Future models must take into account the variability of vegetation element parameters, possibly through a statistical treatment.

Quinn et al. (2001) indicated that it is necessary to predict concentration levels and deposition rates to assess the impact on the local ecology of emissions of both gases and particulates. Computational techniques, including CFD and dispersion modeling methods, are valuable tools in making this assessment. CFD models have the potential to be used for the simulation of particle dispersion around porous barriers.

2.5.3 Application of CFD simulation

Computational fluid dynamics (CFD) integrates the disciplines of fluid mechanics with mathematics and computer science (Tu et al., 2008). It is dedicated to fluids in motion and how the fluid flow behavior influences processes that may include heat transfer and possibly chemical reactions in combusting flows. The physical characteristics of the fluid motion can normally be expressed by fundamental mathematical equations or governing equations. These equations are normally complex partial differential equations with no exact analytical solutions except for very simplified flow conditions, while they can be solved using high-level computer programs or software packages to attain the numerical solutions. As shown in Figure 2.1, common CFD codes, including FLUENT, consist of three main elements: pre-processor, solver, and post-processor.

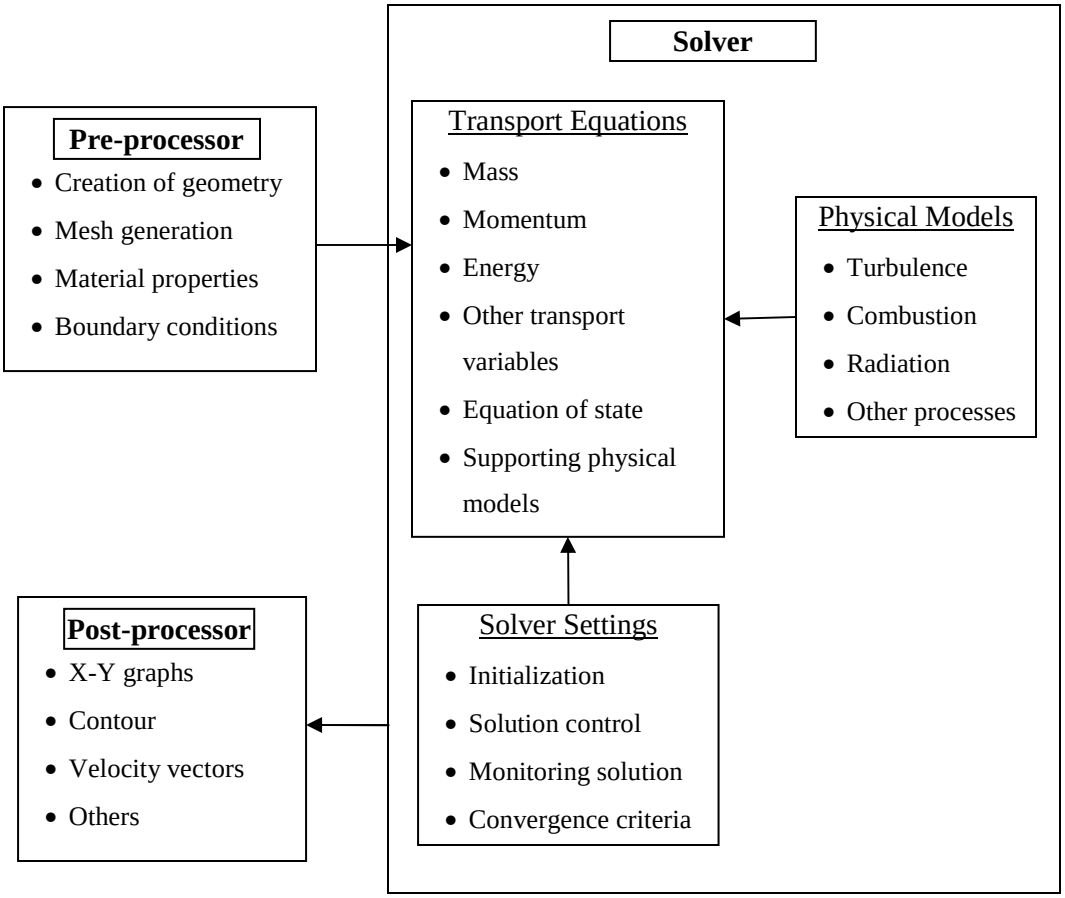

Figure 2.1 The inter-connectivity functions of the three main elements within a CFD analysis framework **(**Tu et al., 2008)

2.5.3.1 Governing equations

The governing equations are based on the conservation of mass, momentum, and energy (Tu et al., 2008). The conservation equations are related to the rate of change in the amount of that property within an arbitrary control volume to the rate of transport across the control volume surface and the rate of the production within that volume (Hirsch, 1988; Tu et al., 2008). The concepts and mathematical expressions are summarized in the following equations (Tu et al., 2008):

Generic form:

$$\underbrace{\frac{\partial \phi}{\partial t}}_{\text{local acceleration}} + \underbrace{\frac{\partial (u\phi)}{\partial x} + \frac{\partial (v\phi)}{\partial y} + \frac{\partial (w\phi)}{\partial z}}_{\text{advection}} = \underbrace{\frac{\partial}{\partial x}\left[\Gamma \frac{\partial \phi}{\partial x}\right] + \frac{\partial}{\partial y}\left[\Gamma \frac{\partial \phi}{\partial y}\right] + \frac{\partial}{\partial z}\left[\Gamma \frac{\partial \phi}{\partial z}\right]}_{\text{diffusion}} + \underbrace{S_\phi}_{\text{source term}} \quad (2.1)$$

Continuity:

$$\phi = 1;\ \Gamma = 0;\ S_\phi = 0 \quad (2.2)$$

Momentum:

$$\phi = u, v, w;\ \Gamma = \nu + \nu_T;\ S_\phi = -\frac{1}{\rho}\frac{\partial p}{\partial x} + S_u^{'}, -\frac{1}{\rho}\frac{\partial p}{\partial y} + S_v^{'}, -\frac{1}{\rho}\frac{\partial p}{\partial z} + S_w^{'} \quad (2.3)$$

Energy:

$$\phi = T;\ \Gamma = \frac{\nu}{Pr} + \frac{\nu_T}{Pr_T};\ S_\phi = S_T \quad (2.4)$$

where u, v, and w are velocity components in x, y and z directions, respectively; ϕ is general variable property per unit mass; Γ is diffusion coefficient; S_ϕ is source term; ν is the kinematic viscosity; ν_T is local kinematic viscosity; and ρ is fluid density.

2.5.3.2 Turbulence models

Most flows of engineering significance are turbulent in nature. Currently, there exist numerous turbulence models, including Reynolds averaged Navier-Stokes (RANS)-based turbulence models (i.e. linear eddy viscosity models, nonlinear eddy viscosity models), large eddy simulation, and detached eddy simulation. However, there is no single universally accepted turbulence model for all problems. The considerations to choose a turbulence model include physics encompassed in the flow, available computational resources, and amount of time available for the simulation (FLUENT Inc., 2006). Among available CFD models, the RANS approach commonly based on turbulent kinetic energy (k) closure schemes is used for engineering applications. It is increasingly used in simulations of flow and pollutant dispersion (Sabatino et al., 2007). The most widely used RANS models are two equation models, which solve two transport equations. The k-ε model is the best known among these models, which requires the solutions of k equation and dissipation of turbulent kinetic energy (ε) equation (Tu et al., 2008; Sabatino et al., 2007; Predicala, 2003; Quinn et al., 2001; Launder and Sandham, 2002).

The $k-\varepsilon$ model has been applied in majority of previous studies of flows through windbreaks yielding reasonable agreement with experimental results (Rosenfeld et al., 2010; Bourdin and Wilson, 2008; Lin, 2006; Tiwary et al., 2005). The standard $k-\varepsilon$ model (FLUENT Inc., 2006) is as follows:

$$\frac{\partial}{\partial t}(\rho k)+\frac{\partial}{\partial x_i}(\rho k u_i)=\frac{\partial}{\partial x_j}\left[\left(\mu+\frac{\mu_t}{\sigma_k}\right)\frac{\partial k}{\partial x_j}\right]+G_k+G_b-\rho\varepsilon-Y_M \tag{2.5}$$

and

$$\frac{\partial}{\partial t}(\rho \varepsilon)+\frac{\partial}{\partial x_i}(\rho \varepsilon u_i)=\frac{\partial}{\partial x_j}\left[\left(\mu+\frac{\mu_t}{\sigma_\varepsilon}\right)\frac{\partial \varepsilon}{\partial x_j}\right]+C_{1\varepsilon}\frac{\varepsilon}{k}(G_k+C_{3\varepsilon}G_b)-C_{2\varepsilon}\rho\frac{\varepsilon^2}{k} \tag{2.6}$$

where G_k represents generation of k due to the mean velocity gradients; G_b is generation of k due to buoyancy; Y_M represents contribution of the fluctuating dilatation in compressible turbulence to overall dissipation rate; $C_{1\varepsilon}$ and $C_{2\varepsilon}$ are constants; $C_{3\varepsilon}$ is constant calculated as $C_{3\varepsilon}=\tanh\left|\frac{v}{u}\right|$, in which $C_{3\varepsilon}=1$ for buoyant shear layers that main flow direction is aligned with the direction of gravity and $C_{3\varepsilon}=0$ for buoyant shear layers that are perpendicular to the gravitational vector; and σ_k and σ_ε are turbulent Prandtl numbers for k and ε, respectively. The Boussinesq hypothesis is employed to relate the Reynolds stresses to mean velocity gradients. The turbulent (or eddy) viscosity, μ_t, is computed by combining k and ε as $\mu_t=\rho C_\mu\frac{k^2}{\varepsilon}$. The model constants have the following default values: $C_{1\varepsilon}$ =1.44, $C_{2\varepsilon}$ =1.92, C_μ =0.09, σ_k =1.0 and σ_ε =1.3.

A modification of the standard $k-\varepsilon$ turbulence model is the realizable $k-\varepsilon$ model. The realizable $k-\varepsilon$ model contains a new formulation for the turbulent viscosity. In addition, the transport equation for ε is derived from an exact equation for the transport of the mean-square vorticity fluctuation (FLUENT Inc., 2006). The expression for the normal Reynolds stress in an incompressible strained mean flow is obtained by combining the Boussinesq relationship and the eddy viscosity definition as $\overline{u_i^2}=\frac{2}{3}k-2\nu_t\frac{\partial U}{\partial x_i}$. To ensure realizability, namely positivity of normal stresses and Schwarz inequality for shear stresses ($\overline{u_i'u_j'}\le\overline{u_i'^2u_j'^2}$), C_μ is sensitized to the mean flow and the turbulence parameters (k,ε).

2.5.3.3 Particle transport

The particle-laden airflow may be treated as a two-phase mixture of air and particles. Multiphase flows can be divided into two categories: (1) continuous and (2) dispersed. Each phase in continuous multiphase flows is treated as a continuous medium. The modeling and numerical issues are quite similar to single-phase flows. For dispersed multiphase flows, one of the phases is considered as a continuum and the other phase is considered as composed of discrete components. Consequently, two-phase flows may be modeled using two approaches. One is the Euler-Euler approach in which both phases (air and particles) are considered as two interpenetrating continua that are treated mathematically by solving conservation equations for both phases. Another is the Euler-Lagrange approach in which the fluid phase is treated as a continuum and the solid phase is considered as discrete particles that are dispersed in the fluid phase. The modeling of fluid-particle interactions depends on the type and number of particles. For very dilute flows, the influence of particles on the continuous phase can be neglected (one-way coupling). For dense flows, the turbulence modification by particles needs to be taken into account, and both the forcing of the particles by the flow and the forcing of the flow by the particles need to be computed simultaneously (two-way coupling) (Portela and Oliemans, 2006; Predicala, 2003).

The motion and trajectory of a discrete particle can by predicted by integrating the force balance on the particle, which is written in Lagrangian reference frame (FLUENT Inc., 2006; Predicala, 2003; Crawford, 1976):

$$\frac{du_{p_i}}{dt} = F_D(u_i - u_{p_i}) + g_i(\frac{\rho_p - \rho}{\rho_p}) + F_x \tag{2.7}$$

where $F_D = \frac{18\mu}{\rho_p D^2}\frac{C_D Re_p}{24}$ and $Re_p = \frac{\rho d_p \left|u_{p_i} - u_i\right|}{\mu}$

In the above equations, u_i is air velocity component, u_{p_i} is particle velocity, d_p is particle diameter, ρ_p is particle density, Re_p is particle Reynolds number, and g_i is gravitational acceleration, and F_x represents any additional force. The drag coefficient, C_d, is calculated according to the type of flow regime, which is determined based on Re_p (Hinds, 1999).

The trajectory is determined by stepwise integration of equation 2.7 over discrete time steps, yielding the velocity of the particle at each point along the trajectory. The trajectory itself is given by $\frac{dx_i}{dt} = u_{p_i}$.

In solving the particulate phase transport equation in Eulerian reference frame, a passive scalar transport equation (Equation 2.8) may be used with some modifications (Zhang et al., 2008; FLUENT Inc., 2006).

$$\frac{\partial \rho \phi_k}{\partial t} + \frac{\partial}{\partial x_i}(\rho u_i \phi_k - \Gamma_k \frac{\partial \phi_k}{\partial x_i}) = S_{\phi_k} \quad k = 1, 2, ..., N \tag{2.8}$$

where ϕ_k is an arbitrary scalar, and Γ_k and S_{ϕ_k} are the diffusion coefficient and the source term for each of the N scalar equations, respectively. The major weakness of the Euler-Euler approach is that it strongly depends on the models used, which are based on situations far simpler than the ones to which the simulation is usually applied. However, the Eulerian approach is preferred to discrete particle tracking (Lagrangian) calculations for reasons of computational efficiency and relative ease of integration into Eulerian-based CFD codes (Portela and Oliemans, 2006; Vlachos et al., 2002).

2.6 Summary

Review of current knowledge on particulate matter associated with open cattle feedlots indicated the following:

- Information about occupational health problems in cattle feedlot workers are very limited and does not contribute to the understanding of health concerns of feedlot neighbors. Studying the workers' respiratory health status may help to understand the potential health effects of feedlot dust.
- Current air quality regulations include the national ambient air quality standards (NAAQS) that are designed to protect public health and public well being. Historically, agricultural sources, including AFOs, have not been included in these regulations. Recently, however, agricultural sources have been targeted to be included in the NAAQS.
- Research has measured concentrations and determined emission rates of PM in large cattle feedlots. In general, PM emission rates and concentrations from cattle feedlot

vary with season, time, and location of feedlots. Important environmental factors that contribute to dust emissions from cattle feedlots are poorly characterized.

- Abatement methods for mitigating PM concentrations and/or emissions for cattle feedlots include permanent or mobile sprinklers, pen maintenance and manure harvesting, pen surface amendments, and porous barriers/shelterbelts. The most commonly used methods are water sprinkling and manure harvesting. Research is needed to establish the efficacy of abatement methods.
- Shelterbelts or vegetative barriers have been used to reduce particulate concentrations downwind of a source. Research is needed to establish their effectiveness.

2.7 References

Adrizal, P.H. Patterson, R.M. Hulet, R.M. Bates, D.A. Despot, E.F. Wheeler, P.A. Topper, D.A. Anderson, and J.R. Thompson. 2008. The potential for plants to trap emissions from farms with laying hens: 2. Ammonia and dust. *J. Appl. Poultry Res.* 17(3): 398-411.

Amosson, S.H., F. Bretz, L. New, and L.K. Almas. 2007. Economic analysis of a traveling gun for feedyard dust suppression. Mobile, Ala.: Presentation at Southern Agricultural Economics Association Annual Meeting.

Amosson, S. H., B. Guerrero, and L. K. Almas. 2006. Economic analysis of solid-set sprinklers to control dust in feedlots. Orlando, Fla.: Presentation at Southern Agricultural Economics Association Annual Meeting.

Auvermann, B.W., R. Bottcher, A. Heber, D. Meyer, C.B. Parnell, Jr., B. Shaw, and J. Worley. 2006. Particulate matter emissions from animal feeding operations. In *Animal Agriculture and the Environment: National Center for Manure and Animal Waste Management White Papers*, 435-468. J.M. Rice, D.F. Caldwell, F.J. Humenik, eds. St. Joseph, Mich.: ASABE.

Auvermann, B.W. 2003. A mechanistic model of fugitive emissions of particulate matter from cattle feedyards: Part I. Introductory evaluation. In *Proc. Air Pollution from Agricultural Operations III Conference*, 257-266. St. Joseph, Mich.: ASAE.

Auvermann, B.W., and A.Romanillos. 2000a. Effect of increased stocking density on fugitive emissions of PM_{10} from cattle feedyards. In *Proc. International Meeting of the Air and*

Waste Management Association. Pittsburgh, Penn.: Air and Waste Management Association.

Auvermann, B.W., and A. Romanillos. 2000b. Manipulating stocking density to manage fugitive dust emission from cattle feedyards. In *Proc. of the Innovative Technologies for Planning Animal Feeding Operations*, 61-70. Akron, Colo.: USDA-ARS Central Great Plains Research Station.

Bache, D.H. 1979. Particle transport within plant canopies-I. A framework for analysis. *Atmos. Environ.* 13(9): 1257-1262.

Boldes, U., J. Colman, and J.M. Di Leo. 2001. Field study of the flow behind single and double row herbaceous windbreaks. *J. Wind Eng. Ind. Aerodyn.* 89(7-8): 665-687.

Bonifacio, H.F., R.G. Maghirang, E.B. Razote, B.W. Auvermann, J.P. Harner, J.P. Murphy, L. Guo, J.M. Sweeten, and W.L. Hargrove. 2011. Particulate control efficiency of a water sprinkler system at a beef cattle feedlot in Kansas. *Trans. ASABE* 54(1): 295-304.

Bonifacio, H.F. 2009. Particulate matter emissions from commercial beef cattle feedlots in Kansas. MS thesis. Manhattan, Kan.: Kansas State University.

Bottcher, R.W. 2001. An environmental nuisance: Odor concentrated and transported by dust. *Chem. Senses* 26(3): 327-331.

Bourdin, P., and J.D. Wilson. 2008. Windbreak aerodynamics: Is computational fluid dynamics reliable? *Boundary Layer Meteorol.* 126(2): 181-208.

Bunton, B., P. O'Shaughnessy, S. Fitzsimmons, J. Gering, S. Hoff, M. Lyngbye, P. S.Thorne, J. Wasson, and M. Werner. 2006. Monitoring and modeling of emissions from concentrated animal feeding operations: Overview of methods. *Environ. Health Perspect.* 115(2): 303-307.

Buser, M.D. 2004. Errors associated with particulate matter measurements on rural sources: appropriate basis for regulating cotton gins. PhD diss. College Station, Tex.: Texas A&M University.

Carroll, J.J., J.R. Dunbar, R.L. Givens, and W.B. Goddard. 1974. Sprinkling for dust suppression in a cattle feedlot. *California Agric.* 28(3):12-14.

Cathomas, R.L., H. Bruesch, R. Fehr, W.H. Reinhart, and M. Kuhn. 2002. Organic dust exposure in dairy farmers in an alpine region. *Swiss Medical Weekly* 132(13-14):174-178.

Cleugh, H.A. 1998. Effects of windbreaks on airflow, microclimates and crop yields. *Agroforestry Syst.* 41(1): 55-84.

Cohen, A.J. 2000. Outdoor air pollution and lung cancer. *Environ. Health Perspect.* 108:743-750.

Crawford, M. 1976. *Air pollution control theory*. New York, N.Y.: McGraw-Hill.

Dalphin, J.C., M.F. Maheu, A. Dussaucy, D. Pernet, J.C. Polio, A. Dubiez, J.J. Laplante, and A. Depierre. 1998. Six year longitudinal study of respiratory function in dairy farmers in the Doubs province. *Eur. Respir. J.* 11(6): 1287-1293.

Davis, J.G., T.L. Stanton, and T. Haren. 2004. Feedlot manure management. Management, Livestock Series. No.1.220. Fort Collins, Colo.: Colorado State University Cooperative Extension. Available at: http://www.cde.state.co.us/artemis/UCSU20/UCSU2062212202002INTERNET.pdf. Accessed 15 February 2010.

Dierickx, W., W.M. Cornelis, and D. Gabriels. 2003. Wind tunnel study on rough and smooth surface turbulent approach flow and on inclined windscreens. *Biosystems Eng.* 86(2):151-166.

Dominici, F., J.M. Jonathan, and S.L. Zeger. 2000. Combining evidence on air pollution and daily mortality from the 20 largest US cities: a hierarchical modelling strategy. *J. Roy. Statistical Society: Series A (Statistics in Society)* 163(3): 263-302.

Eatough, D.J., R.W. Long, W.K. Modey, and N.L. Eatough. 2003. Semi-volatile secondary organic aerosol in urban atmospheres: Meeting a measurement challenge. *Atmos. Environ.* 37(9-10): 1277-1292.

Esworthy, R., and J.E. McCarthy. 2008. The national ambient air quality standard for particulate matter (PM): EPA's 2006 revisions and associated issues. Available at: http://congressionalresearch.com/RL34762/document.php?study=The+National+Ambient+Air+Quality+Standard+for+Particulate+Matter+PM+EPAs+2006+Revisions+and+Associated+Issues. Accessed 25 October 2009.

FLUENT Inc. 2006. FLUENT 6.3 user's guide. Lebanon, N.H.: FLUENT Inc.

Guan, D., Y. Zhang, and T. Zhu. 2003. A wind-tunnel study of windbreak drag. *Agric. For. Meteorol.* 118(1-2): 75-84.

Hamm, L.B. 2005. Engineering analysis of fugitive particulate matter emissions from cattle feedyards. MS thesis. College Station, Tex.: Texas A&M University.

Hammond, E.G., C. Fedler, and R.J. Smith. 1981. Analysis of particle-borne swine house odors. *Agric. Environ.* 6(4): 395-401.

Hammond, E.G., C. Fedler, and G. Junk. 1979. Identification of dust-borne odors in swine confinement facilities. *Trans. ASABE* 22(5):1186-1189.

Harner, J.P., R.G. Maghirang, and E.B. Razote. 2008. Water requirements for controlling dust from open feedlots. In *Mitigating Air Emissions from Animal Feeding Operations Conference*. Ames, Iowa: Iowa State University.

Hill, J.S., P.D. Patel, and J.R. Turner. 1999. Performance characterization of MiniVol $PM_{2.5}$ sampler. 92nd Annual Meeting of Air & Waste Management Association (AWMA), Paper No. 99-617. Pittsburgh, Penn.: AWMA.

Hinds, W.C. 1999. *Aerosol technology: properties, behavior and measurement of airborne particles*. New York, N.Y.: John Wiley &Sons, Inc.

Hirsch, C. 1988. *Numerical computation of internal and external flows. Volume 1: Fundamentals of numerical discretization*. Chichester, U.K.: John Wiley & Sons.

International Commission on Radiological Protection (ICRP). 1994. Human respiratory tract model for radiological protection: a report of a Task Group of the International Commission on Radiological Protection. *Ann. ICRP* 24(1-3): 1-482.

Kaiser, J. 2005. Epidemiology: Mounting evidence indicts fine-particle pollution. *Science* 307(5717): 1858-1861.

Kreyling, W.G., M. Semmler, and W. Moller. 2004. Dosimetry and toxicology of ultrafine particles. *J. Aerosol Med.* 17(2): 140-152.

Launder, B.E., and N.N. Sandham. 2002. *Closure strategies for turbulent and transitional flows*. New York, N.Y.: Cambridge University Press.

Lee, J., and Y. Zhang. 2008. Evaluation of gas emissions from animal building dusts using a cylindrical convective chamber. *Biosystems Eng.* 99(3): 403-411.

Lester, J.C. 2006. Air Quality: Policies and Standards-the evolution of agricultural air quality regulations. Washington, D.C.: Workshop on Agricultural Air Quality. Available at: http://www.ncsu.edu/airworkshop/Air_Quality_Policies_and_Standards.pdf. Accessed 29 October 2010

Lin, X. 2006. Simulation of odor dispersion around natural windbreaks. PhD diss. Ste-Anne-de-Bellevue, Quebec: McGill University.

Loneragan, G.H., and M.M. Brashears. 2005. Effects of using retention-pond water for dust abatement on performance of feedlot steers and carriage of Escherichia coli O157 and Salmonella spp. *J. Am. Veterinary Med. Assoc.* 226(8): 1378-1383.

MacVean, D.W., D.K. Franzen, T.J. Keefe, and B.W. Bennett. 1986. Airborne particle concentration and meteorologic conditions associated with pneumonia incidence in feedlot cattle. *Am. J. Veterinary Res.* 47(12): 2676-2682.

Mader, T.L., M.S. Davis, and J.B. Gaughan. 2007. Effect of sprinkling on feedlot microclimate and cattle behavior. *Int. J. Biometeorol.* 51(6):541-551.

Malone, B. 2004. Using trees to reduce dust and odor emissions from poultry farms. *In Proc. 2004—Poultry information Exchange,* 33-38. Surfers Paradise, Queensland, Australia.

Mathisen, T., S.G. Von Essen, T.A. Wyatt, and D.J. Romberger. 2004. Hog barn dust extract augments lymphocyte adhesion to human airway epithelial cells. *J. Appl. Physiol.* 96(5): 1738-1744.

McGinn, S.M., T.K. Flesch, D. Chen, B. Crenna, O.T. Denmead, T. Naylor, and D. Rowell. 2010. Coarse particulate matter emissions from cattle feedlots in Australia. *J. Environ. Qual.* 39(3):791-789.

McGinn, S.M., K.M. Koenig, and T. Coates. 2002. Effect of diet on odorant emissions from cattle manure. *Can. J. Anim. Sci.* 82(3): 435-444.

Miller, D.N., and E.D. Berry. 2005. Cattle feedlot soil moisture and manure content: 1. Impacts on greenhouse gases, odor compounds, nitrogen losses, and dust. *J. Environ. Qual.* 34(2): 644-655.

Miller, D. N. and B.L. Woodbury. 2003. Simple protocols to determine dust potentials from cattle feedlot soil and surface samples. *J. Environ. Qual.* 32(5): 1634-1640.

Mitloehner, F.M. 2000. Behavioral and environmental management of feedlot cattle. PhD diss. Lubbock, Tex.: Texas Tech University.

NCBA. 2010. Agricultural dust and the Clean Air Act. National Cattlemen's Beef Association. Available at: http://www.beefusa.org/goveagdustandthecleanairact.aspx. Accessed 30 October 2010.

National Research Council (NRC). 2003. *Air emissions from animal feeding operations: current knowledge, future needs.* Washington, D.C.: The National Academies Press.

Oberdorster, G., E. Oberdorster, and J. Oberdorster. 2005. Nanotoxicology: an emerging discipline evolving from studies of ultrafine particles. *Environ. Health Perspect.* 113(7): 823-839.

Packwood, A.R. 2000. Flow through porous fences in thick boundary layers: comparisons between laboratory and numerical experiments. *J. Wind Eng. Ind. Aerodyn.* 88(1): 75-90.

Parnell, S.E., B.J. Lesikar, J.M. Sweeten, and R.E. Lacey. 1994. Determination of the emission factor for cattle feedyards by applied dispersion modeling. ASAE Paper No. 94-4042. St. Joseph, Mich.: ASAE.

Parnell, S.E., B.J. Lesikar, J.M. Sweeten and B.T. Weinheimer. 1993. Dispersion modeling for prediction of emission factors. ASAE Paper No. 93-4554. St. Joseph, Mich.: ASAE.

Patterson, P.H., and Adrizal. 2005. Management strategies to reduce air emissions: Emphasis - dust and ammonia. *J. Appl. Poultry Res.* 14(3): 638-650.

Patton, E.G., R.H. Shaw, M.J. Judd, and M.R. Raupach. 1998. Large-eddy simulation of windbreak flow. *Boundary Layer Meteorol.* 87(2): 275-306.

Pechan, E.H. 2006. AirControlNET Version 4.1: Documentation report for U.S. Environmental Protection Agency. Pechan Report No.06.05.003/9011.002: II-645. Available at: http://www.epa.gov/ttnecas1/models/DocumentationReport.pdf. Accessed 4 April 2010.

Peters, K., and R. Eiden. 1992. Modelling the dry deposition velocity of aerosol particles to a spruce forest. *Atmos. Environ.* 26(14): 2555-2564.

Petroff, A., A. Mailliat, M. Amielh, and F. Anselmet. 2008. Aerosol dry deposition on vegetative canopies. Part I: Review of present knowledge. *Atmos. Environ.* 42(16): 3625-3653.

PM10 Inc. 2007. Erosion control - Mulching. Palm Desert, Calif.: PM10 Inc. Available at: http://www.pm10inc.com/erosion-control-mulching.html. Accessed 1 April 2010.

Portela, L.M., and R.V.A. Oliemans. 2006. Possibilities and limitations of computer simulations of industrial turbulent dispersed multiphase flows. *Flow, Turbulence and Combustion* 77(1-4):381-403.

Predicala, B.Z. 2003. Characterization and modeling of concentrations and emissions of particulate matter in swine buildings. PhD diss. Manhattan, Kan.: Kansas State University.

Purdy, C.W., R.N. Clark, and D.C. Straus. 2007. Analysis of aerosolized particulates of feedyards located in the Southern High Plains of Texas. *Aerosol Sci. Technol.* 41(5): 497-509.

Purdy, C.W., D.C. Straus, D.B. Parker, S.C. Wilson, and R.N. Clark. 2004. Comparison of the type and number of microorganisms and concentration of endotoxin in the air of feedyards in the Southern High Plains. *Am. J. Veterinary Res.* 65(1): 45-52.

Quinn, A.D., M. Wilson, A.M. Reynolds, S.B. Couling, and R.P. Hoxey. 2001. Modelling the dispersion of aerial pollutants from agricultural buildings—an evaluation of computational fluid dynamics (CFD). *Comput. Electron. Agric.* 30 (1-3): 219-235.

Radon, K., A. Schulze, V. Ehrenstein, R.T. van Strien, G. Praml, and D. Nowak. 2007. Environmental exposure to confined animal feeding operations and respiratory health of neighboring residents. *Epidemiol.* 18(3): 300-308.

Rahman, S., S. Mukhtar, and R.Wiederholt. 2008. Managing odor nuisance and dust from cattle feedlots. Fargo, N.D.: North Dakota State University Extension Service. Available at: http://www.ag.ndsu.edu/pubs/h2oqual/watnut/nm1391.pdf. Accessed 15 March 2010

Raupach, M.R., and A.S. Thom. 1981. Turbulence in and above plant canopies. *Ann. Rev. Fluid Mech.* 13: 97-129.

Raupach, M.R., N. Woods, G. Dorr, J.F. Leys, and H.A. Cleugh. 2001. The entrapment of particles by windbreaks. *Atmos. Environ.* 35(20): 3373-3383.

Razote, E.B., R.G. Maghirang, J.P. Murphy, B.W. Auvermann, J.P. Harner III, D.L. Oard, W.L. Hargrove, D.B. Parker, and J.M. Sweeten. 2007. Air quality measurements from a water-sprinkled beef cattle feedlot in Kansas. ASABE Paper No. 07-4108. St. Joseph, Mich.: ASABE.

Razote E.B., R.G. Maghirang, B.Z. Predicala, J.P. Murphy, B.W. Auvermann, J.P. Harner III, and W.L. Hargrove. 2006. Laboratory evaluation of the dust emission potential of cattle feedlot surfaces. *Trans. ASABE* 49(4): 1117-1124.

Reynolds, S.J., D.Y. Chao, P.S. Thorne, P. Subramanian, P.F. Waldron, M. Selim, P.S. Whitten, and W.J. Popendorf. 1998. Field comparison of methods for evaluation of vapor/particle phase distribution of ammonia in livestock buildings. *J. Agric. Safety Health* 4(2): 81-93.

Rogge, W.F., P.M. Medeiros, and B.R.T. Simoneit. 2006. Organic marker compounds for surface soil and fugitive dust from open lot dairies and cattle feedlots. *Atmos. Environ.* 40(1): 27-49.

Romanillos, A., and B.W. Auvermann. 1999. Effect of stocking density on fugitive PM_{10} emissions from a cattle feedyard. ASABE Section Meeting Paper No. 99-4192. St. Joseph, Mich.: ASABE.

Rosenfeld M., G. Marom, and A. Bitan. 2010. Numerical simulation of the airflow across trees in a windbreak. *Boundary Layer Meteorol.* 135(1): 89-107.

Sabatino, S.D., R. Buccolieri, B. Pulvirenti, and R. Britter. 2007. Simulations of pollutant dispersion within idealised urban-type geometries with CFD and integral models. *Atmos. Environ.* 41(37): 8316-8329.

Salter, L.F. and B. Parsons. 1999. Field trials of the TEOM and Partisol for PM_{10} monitoring in the St Austell China clay area, Cornwall, U.K. *Atmos. Environ.* 33(13): 2111-2114.

Schwartz, J., D.W. Dockery, and L.M. Neas. 1996. Is daily mortality associated specifically with fine particles? *J. Air Waste Manage. Assoc.* 46(10): 927-939

Seaton, A., W. MacNee, K. Donaldson, and D. Godden. 1995. Particulate air pollution and acute health effects. *The Lancet* 345(8943): 176-178.

Sundblad, B.M., B.M. Larsson, L. Palmberg, and K. Larsson. 2002. Exhaled nitric oxide and bronchial responsiveness in healthy subjects exposed to organic dust. *Eur. Respir. J.* 20(2): 426-431.

Sweeten, J.B., C.B. Parnell, R.S. Etheredge, and D. Osborne. 1988. Dust emissions in cattle feedlots. *Vet. Clin. North Am. Food Anim. Pract.* 4(3): 557-578.

Sweeten, J.M., C.B. Parnell, B.W. Shaw, and B.W. Auvermann. 1998. Particle size distribution of cattle feedlot dust emission. *Trans. ASAE* 41(5): 1477-1481.

Tiwary, A., H.P. Morvan, and J.J. Colls. 2005. Modelling the size-dependent collection efficiency of hedgerows for ambient aerosols. *J. Aerosol Sci.* 37(8): 990-1015.

Tiwary, A., A. Reff, and J.J. Colls. 2008. Collection of ambient particulate matter by porous vegetation barriers: Sampling and characterization methods. *J. Aerosol Sci.* 39(1): 40-47.

Tu, J, G.H. Yeoh, and C. Liu. 2008. *Computational fluid dynamics: a practical approach.* Amsterdam: Butterworth-Heinemann.

Tyndall, J., and J. Colletti. 2006. Mitigating swine odor with strategically designed shelterbelt systems: a review. *Agroforestry Syst*. 69(1): 45-65.

Upadhyay, J.K., B.W. Auvermann, A.N. Paila, and N. Hiranuma. 2008. Open-path transmissometry to determine atmospheric extinction efficiency associated with feedyard dust. *Trans. ASABE* 51(4): 1433-1441.

USDA. 2000a. Air quality research and technology transfer program for concentrated animal feeding operations. Washington, D.C.: USDA Agricultural Task Force. Available at: http://www.airquality.nrcs.usda.gov/aaqtf/Documents/Old_Archives/2000/Policy/CAFO.htm. Accessed 10 November 2010.

USDA. 2000b. Feedlot 99-Part I. Baseline reference of feedlot management practices, 1999. Washington, D.C.: USDA Animal and Plant Health Inspection Service & Veterinary Services. Available at: http://www.aphis.usda.gov/animal_health/nahms/feedlot/downloads/feedlot99/Feedlot99_dr_PartI.pdf. Accessed 11 November 2010.

USDA. 2009. Agriculture and food research initiative competitive grants program-FY 2009 program announcement. Washington, D.C.: USDA Cooperative State Research, Education, and Extension Service. Available at: http://www.csrees.usda.gov/funding/afri/pdfs/program_announcement.pdf. Accessed 29 October 2010.

U.S. EPA. 1997. National ambient air quality standards for particulate matter - final rule. 40 CFR part 50, Federal Register, Vol.62, No. 138. Available at: http://www.epa.gov/ttncaaa1/t1/fr_notices/pmnaaqs.pdf. Accessed 10 November 2010.

U.S. EPA. 1999a. Compendium of methods for the determination of inorganic compounds in ambient air, Chapter IO-1: Continuous measurement of PM_{10} suspended particulate matter (SPM) in ambient air-overview. Cincinnati, Ohio: Center for Environmental Research Information Office of Research and Development. Available at: http://www.epa.gov/ttnamti1/files/ambient/inorganic/overvw1.pdf. Accessed 10 November 2010.

U.S. EPA. 1999b. Compendium of methods for the determination of inorganic compounds in ambient air, Chapter IO-2: Integrated sampling of suspended particulate matter (SPM) in ambient air-overview. Cincinnati, Ohio: Center for Environmental Research Information

Office of Research and Development. Available at: http://www.epa.gov/ttnamti1/files/ambient/inorganic/overvw2.pdf. Accessed 10 November 2010.

U.S. EPA. 2001a. Ambient air monitoring reference and equivalent methods. 40 CFR, part 53. Available at: http://www.access.gpo.gov/nara/cfr/waisidx_08/40cfr53_08.html. Accessed 10 November 2010.

U.S. EPA. 2001b. Ambient air quality surveillance. 40 CFR, Part 58. Available at: http://www.access.gpo.gov/nara/cfr/waisidx_08/40cfr58_08.html. Accessed 10 November 2010.

U.S. EPA. 2004. Air quality criteria for particulate matter, volume1, II. Research Triangle Park, N.C.: Office of Research and Development & National Center for Environmental Assessment-RTP office. Available at: http://publicfiles.dep.state.fl.us/OGC/GREC_PPSA-BUSSING_DISCOVERY_RESPONSES/Particulate%20Matter%20Children%20and%20Asthma/7%20of%2011/VOL_I_FINAL_PM_AQCD_OCT2004%20Part%201%20of%203.pdf. Accessed 10 November 2010.

U.S. EPA. 2005. Review of the national ambient air quality standards for particulate matter: policy assessment of scientific and technical information. Research Triangle Park, N.C.: Office of Air Quality Planning and Standards. Available at: http://www.epa.gov/ttn/naaqs/standards/pm/data/pmstaffpaper_20050630.pdf. Accessed 10 November 2010.

U.S. EPA. 2006. National primary and secondary ambient air quality standards- final rule. 40 CFR, part 50, Federal Register, Vol.71, No. 200. Available at: http://www.epa.gov/ttnnaaqs/standards/pm/data/fr20061017.pdf. Accessed 10 November 2010.

U.S. EPA. 2008. Integrated science assessment for particulate matter—first external review draft. Research Triangle Park, N.C.: Office of Research and Development. Available at: http://cfpub.epa.gov/ncea/cfm/recordisplay.cfm?deid=201805. Accessed 10 November 2010.

U.S. EPA. 2010. List of designated reference and equivalent methods. Research Triangle Park, N.C.: Human Exposure & Atmospheric Sciences Division. Available at: http://www.epa.gov/ttnamti1/files/ambient/criteria/reference-equivalent-methods-list.pdf. Accessed 30 March, 2010.

U.S. GAO. 2008. Concentrated animal feeding operations: EPA needs more information and a clearly defined strategy to protect air and water quality from pollutants of concern. Washington, D.C.: Government Accountability Office. Available at: http://www.gao.gov/new.items/d08944.pdf. Accessed 11 November 2010.

Vega, E., E. Reyes, A. Wellens, G. Sanchez, J.C. Chow, and J.G. Watson. 2003. Comparison of continuous and filter based mass measurements in Mexico City. *Atmos. Environ.* 37 (20): 2783-2793.

Vlachos, N., E. Mourouglou, and A.G. Konstandopoulos. 2002. Development of fluent user-defined functions for the modeling of particle transport in non-isothermal gas flows. Advanced Process Modeling and Simulation Tools. Thermi, Thessaloniki, Greece: 2002 workshop of CPERI.

Von Essen, S.G., and B.W. Auvermann. 2005. Health effects from breathing air near CAFOs for feeder cattle and hogs. *J. Agromedicine* 10(4): 55-64.

Wang, H., and E.S. Takle. 1995. A numerical simulation of boundary-layer flows near shelterbelts. *Boundary Layer Meteorol.* 75(1-2): 141-173.

Wang, L., J.D. Wanjura, C.B. Parnell, R.E. Lacey, and B.W. Shaw. 2005. Performance characteristics of a low-volume PM_{10} sampler. *Trans. ASAE* 48(2): 739-748.

Wanjura, J.D., B.W. Shaw, C.B. Parnell, Jr., R.E. Lacey, and S.C. Capareda. 2008. Comparison of continuous monitor (TEOM) and gravimetric sampler particulate matter concentrations. *Trans. ASABE* 51(1): 251-257.

Wickens, K., J.M. Lane, P. Fitzharris, R. Siebers, G. Riley, J. Douwes, T. Smith, and J. Crane. 2002. Farm residence and exposures and the risk of allergic diseases in New Zealand children. *Allergy* 57(12): 1171-1179.

Wilson, S.C., J. Morrow-Tesch, D.C. Straus, J.D. Cooley, W.C. Wong, F.M. Mitloehner, and J.J. McGlone. 2002. Airborne microbial flora in a cattle feedlot. *Appl. Environ. Microbiol.* 68(7): 3238-3242.

Wilson, J.D. 1985. Numerical studies of flow through a windbreak. *J. Wind Eng. Ind. Aerodyn.* 21(2): 119-154.

Winkenwerder, W. 2002. Environmental exposure report-particulate matter, final report. Available at: http://www.gulflink.osd.mil/particulate_final/index.htm#vi. Accessed 2 November 2009.

Woolums, A.R., T.A. McAllister, and G.H. Loneragan. 2001. Interstitial pneumonia in feedlot cattle: noninfectious causes. *Compendium on Continuing Education for the Practicing Veterinarian* 23(9): S86-S93.

Wyatt, T.A., R.E, Slager, J. DeVasure, B.W. Auvermann, M.L. Mulhern, S.Von Essen, T. Mathisen, A.A. Floreani, and D.J. Romberger. 2007. Feedlot dust stimulation of interleukin-6 and -8 requires protein kinase C epsilon in human bronchial epithelial cells. *Am. J. Physiology-Lung Cell. Mol. Physiol.* 293(5): L1163-L1170.

Zhang, N., Z.C. Zheng, and R.G. Maghirang. 2008. Numerical simulation of smoke clearing with nanoparticle aggregates. *Int. J. Numer. Methods Eng.* 74(4): 601-618.

CHAPTER 3 - Concentrations and Size Distribution of Particulate Matter Emitted from Large Cattle Feedlots

3.1 Abstract

Particulate matter (PM) emitted from cattle feedlots can impact air quality in rural communities, yet little is known about factors controlling their emissions. The concentrations of PM (i.e., $PM_{2.5}$, PM_{10}, and TSP) upwind and downwind at two large cattle feedlots (KS1, KS2) in Kansas were measured with gravimetric samplers from May 2006 to October 2009 (at KS1) and from September 2007 to April 2008 (at KS2). The mean downwind and net (i.e., downwind – upwind) mass concentrations of $PM_{2.5}$, PM_{10}, and TSP varied seasonally, indicating the need for multiple-day, seasonal sampling. The downwind and net concentrations were closely related to the water content of the pen surface. The $PM_{2.5}/PM_{10}$ and $PM_{2.5}$/TSP ratios at the downwind sampling location were also related to the water content of the pen surface, humidity, and temperature. Measurement of the particle size distribution downwind of the feedlot with a cascade impactor showed geometric mean diameter ranging from 7 to 18 µm, indicating that particles that were emitted from the feedlots were generally large in size.

3.2 Introduction

The increasing size and geographic concentration of animal feeding operations, including beef cattle feedlots, has led to public concern about emissions of particulate matter (PM), ammonia, volatile organic compounds, and odor. Open beef cattle feedlots generate fugitive dust, including total suspended particulates (TSP), PM with equivalent aerodynamic diameter of 10 µm or less (PM_{10}), and PM with equivalent aerodynamic diameter of 2.5 µm or less ($PM_{2.5}$). Although there have been no direct studies on feedlot personnel health problems, several researchers indicated that dust generated from cattle feedlots has the potential to cause a number of health hazards in humans and livestock (Rogge et al., 2006; Purdy et al., 2004; MacVean et al., 1986). Sweeten et al. (2000) indicated that dust from cattle feedlot surfaces, alleys, and roads can annoy neighbors and irritate feedlot employees. In addition, particulates with bound ammonia and odorous compounds can be emitted from feedlots to nearby residences and can

cause actual or perceived health effects (Lee and Zhang, 2008; Reynolds et al., 1998). As more stringent air quality standards are developed, there is a need to characterize and control PM emissions from cattle feedlots and to assess the effectiveness of abatement measures for mitigating those emissions.

Particle size is important in characterizing the physical behavior and potential health effects of PM. Removal processes, atmospheric residence times, and contribution of light scattering to visibility degradation are affected by particle size (U.S. EPA, 2005; Hinds, 1999). The formation and growth of particles might be influenced by several processes, and they are sensitive to a number of environmental parameters including humidity, temperature, reactive trace gas concentrations (Lammel et al., 2004; Wehner et al., 2002), and possibly wind speed. Therefore, it is necessary to understand the particle size distribution and mass concentrations at critical size ranges for investigating health effects posed by PM emissions from cattle feedlot and monitoring the transport and fate of PM. Moreover, to develop or improve control methods, it is necessary to know factors that influence PM emissions.

Dry, warm conditions and active cattle behavior are the principal contributors to dust emission from cattle feedlots (Wilson et al., 2002). In general, fugitive dust emitted from feedlots is mainly from the un-compacted and pulverized manure layer associated with animal activity, especially from late afternoon to early evening. Other sources of dust include feed mills, loading and unloading of feed trucks, vehicle exhaust, unpaved roads, and winds (Wu et al., 2008; Razote et al., 2007a, 2007b; Auvermann et al., 2006). Cattle feedlots may contribute to secondary PM by emissions of ammonia and nitric oxide that subsequently leads to secondary aerosol formation (Rogge et al., 2006; NRC, 2003; Wilson et al., 2002), although there is little evidence showing this occurs at the local scale (Hiranuma et al., 2010). Information on the spatial, temporal, and physical characteristics of the emission sources are needed to distinguish their contributions to ambient particulate matter concentrations. Accurate emission inventories are also needed to provide accurate inputs to air quality modeling.

Currently, there is little information on either concentration or particle size distribution of PM from cattle feedlots and almost all of the published data have been from Texas (Purdy et al., 2007; Sweeten et al., 1998; Sweeten et al., 1988). Based on cattle feedlots in Texas, the mean net TSP was 412 (± 271) $\mu g/m^3$ (15 occasions measured seasonally in 1987) with PM_{10} concentrations of 19% to 40% of TSP (Sweeten et al., 1998; Sweeten et al., 1988).In a related

study, Purdy et al. (2007) reported that the downwind $PM_{2.5}/PM_{10}$ ratio was close to 10%. From the limited data available, dust from cattle appears to be large with over half larger than PM_{10}. However, more measurements are needed to further characterize and understand PM emissions from open-lot beef cattle feedlots (Razote et al., 2008). The objectives of this study were to: (1) measure the mass concentration and size distribution of PM emitted from two large cattle feedlots in Kansas and (2) determine the effects of weather conditions and pen surface water content on the mass concentrations.

3.3 Materials and Methods

3.3.1 Feedlot description and sampling locations

Two large cattle feedlots in Kansas (i.e., KS1 and KS2) were considered in this study. The feedlots were within 40 km of each other. The first feedlot, KS1, had approximately 30,000 head of cattle and a total pen area of about 50 ha. It had a water sprinkler system for dust control with an application rate of 5 mm/day (5 L/m^2-day). The system was normally operated from April to October and during prolonged dry periods. It had a total of 179 sprinkler heads; a group of three sprinkler heads was turned on simultaneously every 6 min and 6 h were required to cycle through all sprinkler heads. In addition, pens at KS1 were scraped two to three times per year and manure was removed from the pens at least once a year. The second feedlot, KS2, had approximately 25,000 head of cattle and a total pen area of 68 ha. Pens were also scraped five to six times per year and manure was removed from each pen two to three times per year. For both feedlots, feed was processed and mixed in the feed mill, loaded on feed trucks, and delivered to the pens three times a day. Prevailing wind directions at the sites were south in summer and north in winter (Fig. 3.1a). Annual mean values of precipitation at KS1 and KS2 were approximately 573 mm and 671 mm, respectively.

Particulate samplers (2100 Mini-Partisol, Thermo Fisher Scientific, Franklin, MA) were set up at the north and south perimeters of each feedlot (Fig. 3.1b). For KS1, the north sampling location was about 5 m away from the closest pen and the south sampling location was about 30 m away from the closest pen (Fig. 3.1b). For KS2, the north and south sampling locations were approximately 40 m and 60 m away from the closest pens, respectively. These locations were selected so that samplers are able to capture particulates coming from the feedlots; in addition, power availability, and access to the sampling locations were considered.

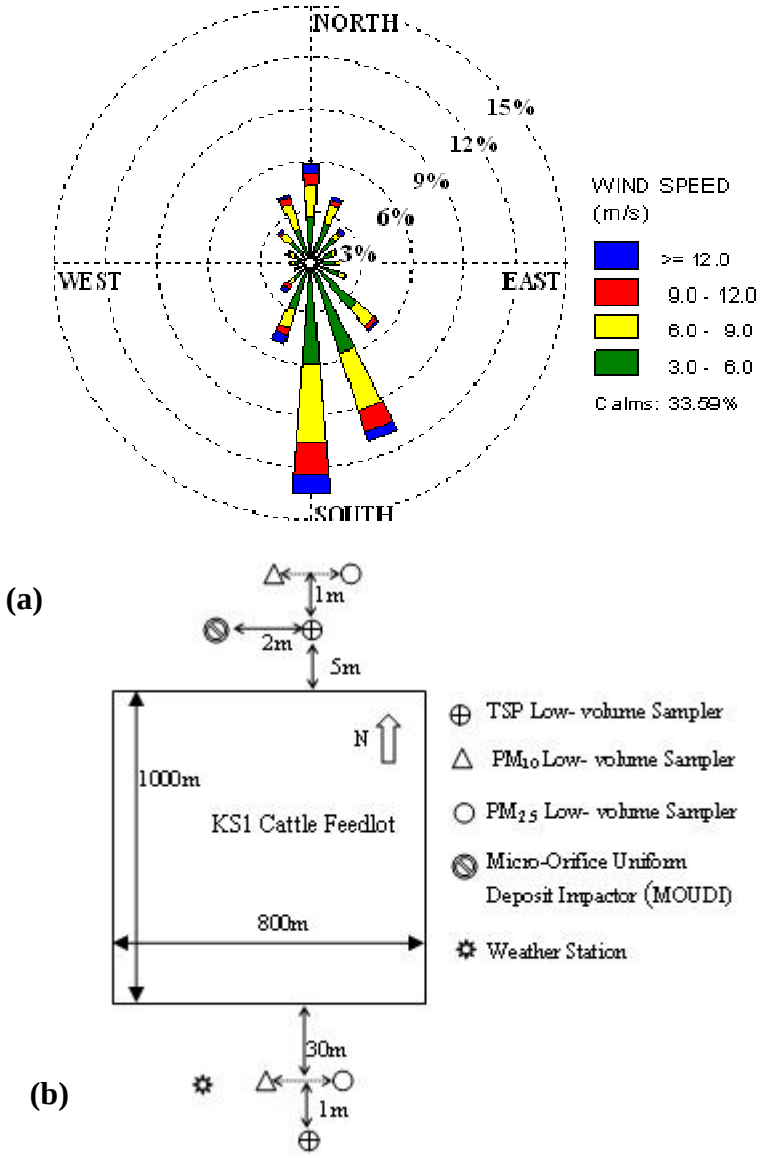

Figure 3.1 (a) Wind rose statistics from May 2006 to October 2009 (hourly data from total time period); (b) Schematic diagram showing sampler locations at feedlot KS1.

Each feedlot was equipped with a weather station (Campbell Scientific Inc., Logan, UT) to measure and record at 20-min intervals wind speed, wind direction, pressure, temperature, precipitation, and relative humidity. Weather data from a local weather station were also collected. In addition to the low-volume samplers, a Micro-Orifice Uniform Deposit Impactor or MOUDI (Model 100/110, MSP corporation, Shoreview, MN) was set up in the prevailing downwind location of KS1 to measure the particle size distribution.

3.3.2 Air sampling and measurement

The mass concentrations of TSP, PM_{10}, and $PM_{2.5}$ were measured with low-volume samplers (air sampling flow rate of 5 L/min) equipped with size-selective inlets for TSP, PM_{10}, and $PM_{2.5}$. Samplers were placed side by side with a minimum distance of about 1 m from each other (Figure 3.1b). These samplers are gravimetric samplers that yield time-integrated mass concentration of PM. During measurement, ambient air is drawn into the size-selective inlet of the sampler using a vacuum pump and PM is collected on the collection filter. The mass of the collected PM is determined by subtracting the gross weight of the filter from its tare weight. The mass of PM is then divided by the sampling flow volume to get the mass concentration of PM. Flow rate is critical for particle fractionation and calculation of mass concentration. For the samplers, the flow control system uses a temperature and pressure compensated mass flow control scheme to maintain a constant volumetric flow rate of 5 L/min (Rupprecht & Patashnick Co, Inc., 2004). Filters used for low-volume samplers were either a Pallflex TX40 or a PTFE filter (Whatman Inc., Clifton, NJ). All filters were conditioned in a laboratory conditioning chamber (25 °C, 40% relative humidity) for 24 h before weighing, before and after sampling, to minimize the effect of humidity.

Particle size distribution at the prevailing downwind sampling location of KS1 (generally, the north sampling location) was measured with the MOUDI. The MOUDI is an 8-stage cascade impactor that is based on the principle of inertial impaction using multiple-nozzle-stages in series. Particles larger than the cut-size of the stage are collected on the impaction plate when the particle laden air impinges on the plate, while the smaller particles will proceed to next stage. It was operated with air sampling flow rate of 30 L/min. It used 34-mm aluminum foils for the impaction stages and 34-mm PTFE filters for the bottom stage. In accordance with the manufacturer's recommendation, the aluminum foils were sprayed with thin layer of grease to minimize particle bounce and then heated for about 90 min in an oven with temperature of 65^{o}C.

Field sampling events were conducted monthly from May 2006 to October 2009 at KS1 and from September 2007 to April 2008 at KS2. Since 2007, fifteen and three 5-day intensive sampling events were conducted at KS1 and KS2, respectively. The 5-day sampling events were conducted mostly from March to November (13 out of the 15 events for KS1). Each sampling event normally included from 2 to 10 sampling runs. For each sampling run, sampling duration was generally 12 h. In cases when expected concentrations were small (e.g., winter or after rain

events), sampling duration was 24 h to ensure that measurable amounts of PM were collected on the filters. The total numbers of sampling runs for the low-volume samplers were 185 and 40 for KS1 and KS2, respectively. Because of sampler malfunctions and/or power outages, the actual numbers of sampling runs ranged from 126 to 177 for KS1 and from 1 to 39 for KS2. The MOUDI sampler was used from July 2007 to July 2009 for a total of 43 sampling runs (each run had a duration of 24 h).

During each sampling run, manure samples were collected from three to five different pens for the determination of water content (WC) of pen surfaces in the feedlots. These samples were normally taken right after the start of each sampling run and when the sprinkler heads in the pens from which samples were being collected were not running. Approximately 2.5 to 5 cm upper layer of manure was collected from two to three spots between the center of the pen to the feed apron. The collected samples from each pen were placed in a zipped plastic bag. The WC of the manure sample was determined using the ASTM D 2216-98 oven-drying method (ASTM, 2002).

Data on the operation of the sprinkler system, including when the system was operated and the daily amount of water used for sprinkling, were obtained from the feedlot operator. In this research, the water sprinkler system at KS1 was operated during 60 sampling runs out of 185 total sampling runs. The amount of water applied ranged from 0 to 5.2 mm for each run.

3.3.3 Data analysis

Measured PM values were first screened on the basis of wind direction. Since the samplers were strategically set up north and south of the feedlots, measured values were considered acceptable if the wind direction was from 120^{o} to 240^{o} (i.e., the north sampling site was the downwind location) at least 80% of the time (Guerra et al., 2006). If the wind direction was within the 120^{o} to 240^{o} range but less than 80% of the time or outside the 120^{o} to 240^{o} range at least 20% of the time, the PM data were excluded in the analysis. Tables 3.1 and 3.2 summarize the numbers of acceptable sampling runs.

Table 3.1 Numbers of acceptable sampling runs and 24-h values for the low-volume samplers.

		Feedlot KS1		Feedlot KS2	
		Number of acceptable sampling runs	Number of 24-h values	Number of acceptable sampling runs	Number of 24-h values
Downwind (typically north sampling location)	$PM_{2.5}$	47	21	11	3
	PM_{10}	69	28	10	3
	TSP	71	28	6	3
Upwind (typically south sampling location)	$PM_{2.5}$	44	20	6	2
	PM_{10}	61	28	10	3
	TSP	59	27	0	0
Net (Downwind – Upwind)	$PM_{2.5}$	30	15	4	2
	PM_{10}	49	25	8	2
	TSP	49	25	0	0

Table 3.2 Numbers of acceptable sampling runs for each month for KS1.

Month	TSP		PM_{10}			$PM_{2.5}$			With Rain	With Sprinkling
	Down wind	Net	Down wind	Net	24-h Concentration ≥150 µg/m³	Down wind	Net	24-h Concentration ≥35 µg/m³		
01	1	0	1	1	0	1	1	0	0	0
02	1	1	1	1	0	0	0	0	0	0
03	4	3	4	3	1	2	2	1	0	0
04	3	3	4	1	0	2	1	0	0	0
05	7	5	7	5	1	5	4	1	1	3
06	7	5	7	4	0	2	1	0	0	6
07	16	8	15	9	1	11	7	1	0	17
08	12	9	10	8	1	10	7	1	1	7
09	7	5	7	6	0	6	2	0	1	4
10	6	6	7	6	0	4	3	0	1	2
11	4	4	4	4	0	2	2	0	0	0
12	3	0	2	1	0	2	0	0	0	0
Total	71	49	69	49	4	47	30	4	4	39

All PM concentration data were converted to standard conditions of temperature (25^{o}C) and pressure (760 mmHg). From the screened data, the $PM_{2.5}/PM_{10}$, $PM_{2.5}$/TSP, and PM_{10}/TSP ratios for each sampling run at each sampling location were calculated. The frequency distribution, which is the tabulation of raw data obtained by dividing it into size ranges and computing the number of data elements falling within each size range (Karaca et al., 2006), was used to describe the population of these ratios within certain ranges. In addition, from the pre-screened data, the corresponding 24-h mass concentrations were calculated by taking into account the mass concentrations in successive runs within 24 h. Then, from the 24-h data sets, the net concentration (i.e., difference between downwind and upwind concentrations) was determined. Table 3.2 also shows the numbers of acceptable data set for the 24-h means and the net concentrations for the low-volume samplers.

Particle size distribution data from the MOUDI were also screened for acceptability in the analysis based on wind direction. There were 14 acceptable sampling runs (out of 43 total sampling runs) for the MOUDI sampler. For each of the MOUDI data sets, the geometric mean diameter (GMD) and geometric standard deviation (GSD) were obtained using Equations 3.1 and 3.2, respectively (Hinds, 1999).

$$GMD = \exp\left(\frac{\sum\left(m_j \ln d_j\right)}{\sum m_j}\right) \tag{3.1}$$

$$GSD = \exp\left(\frac{\sum\left\{m_j\left[\ln\left(\frac{d_j}{GMD}\right)\right]^2\right\}}{\sum m_j}\right)^{0.5} \tag{3.2}$$

where GMD is the geometric mean diameter of the sample, µm; d_j is the geometric mean diameter of particles in the j^{th} stage of the MOUDI, µm; m_j is the mass fraction of particles in the j^{th} stage of the MOUDI; and GSD is the geometric standard deviation.

The following statistical analyses were conducted using SAS (version 9.1.3, SAS Institute Inc., Cary, NC) and Excel (Microsoft Corp, Redmond, WA):

1. Paired t-test procedure to determine significant difference between the upwind and downwind sampling locations in PM concentrations and ratios (i.e., $PM_{2.5}/PM_{10}$, $PM_{2.5}$/TSP, and PM_{10}/TSP).
2. The CONTRAST statement in SAS GLM procedure was used to contrast the mean concentrations and ratios between the day and evening sampling.
3. Correlation analysis on mass concentrations (i.e., $PM_{2.5}$, PM_{10}, and TSP) and PM ratios (i.e., $PM_{2.5}/PM_{10}$, $PM_{2.5}$/TSP, and PM_{10}/TSP).
4. Correlation analysis on log-transformed PM concentrations as well as PM ratios with weather conditions (i.e., humidity, temperature, wind speed, and precipitation), and amount of water applied by the water sprinkler system. Log-transformed PM concentrations provided better correlation with factors compared with untransformed concentrations.
5. Regression analysis using the backward selection procedure to identify the factors that could predict the mass concentration.

For all analyses, a 5% level of significance was used except for the regression analysis of backward selection which used 10% significance level.

3.4 Results and Discussion

3.4.1 Particle size distribution

The mean GMD of the particles as measured by the MOUDI at the downwind sampling location of KS1 was 13.0 µm, ranging from 7.0 µm to 18.2 µm. The relatively large GMD value indicates that the PM emitted from feedlot KS1 was dominated by coarse particles. The mean GSD was 2.4 (ranging from 2.1 to 3.8) indicating a relatively broad particle size distribution. The observed size distribution is similar to those in previous research on cattle feedlots. Hamm (2005) reported an average mass median diameter of 16 µm with average GSD of 2.1, while Sweeten et al. (1988) reported mean GMD of 9.5 (standard deviation, SD=1.5) µm and mean GSD of 2.1 (SD=0.06); both studies were from cattle feedlots in Texas and Coulter Counters were used for the analysis of particle size distribution.

3.4.2 PM mass concentrations and ratios

The PM concentrations at the upwind and downwind sampling locations of the feedlots varied with season with the highest concentrations observed between March and November (Fig. 3.2). Overall mean downwind concentrations were 34, 105, and 262 $\mu g/m^3$ for $PM_{2.5}$, PM_{10} and TSP at KS1 respectively, while they were 24, 88, and 185 $\mu g/m^3$, respectively, at KS2 (Table 3.3). These values were within the ranges of published values for cattle feedlots. Sweeten et al. [19] reported mean downwind concentrations of 700 $\mu g/m^3$ (range of 97-1,685 $\mu g/m^3$) and 285 $\mu g/m^3$ (range of 11-866 $\mu g/m^3$) for TSP and PM_{10}, respectively. Purdy et al. (2007) reported mean upwind and downwind PM_{10} concentrations of 94 $\mu g/m^3$ and 269 $\mu g/m^3$ and corresponding $PM_{2.5}$ concentrations of 14 $\mu g/m^3$ and 25 $\mu g/m^3$, respectively, from four cattle feedlots in Texas. The primary and secondary 24-h national ambient air quality standards (NAAQS) for PM_{10} is 150 $\mu g/m^3$ and is not to be exceeded more than once per year on average over a three year period and the $PM_{2.5}$ 24-h concentration must not exceed 35 $\mu g/m^3$ over a three year period (U.S.EPA, 2006). In 4 out of 28 samples for PM_{10} and 4 out of 21 samples for $PM_{2.5,}$ the measured 24-h concentration exceeded the NAAQS (Fig. 3.3). These cases occurred in March, May, July, and August) when pen surfaces were generally dry (Table 3.2), with pen surface WC generally less than 16%. Note that the sampling locations were 5 m from the closest pen in KS1, representing a worst case. If measurements were carried out at the property lines, a few hundred meters further away from the pens, it is likely that the concentrations would have been considerably lower because of particle dispersion and settling (Todd et al., 2004).

Table 3.3 also presents the net concentrations, which are the downwind concentrations adjusted for upwind or background concentrations to reflect the contribution of the feedlot only (Sweeten et al., 1998). The overall mean net mass concentrations of TSP, PM_{10}, and $PM_{2.5}$ at KS1 were 201, 76, and 25 $\mu g/m^3$, respectively. For KS2, only two cases of 24-h net mass concentrations were obtained; the upwind TSP data were not available because of TSP sampler malfunction. The net mass concentrations of PM_{10} and $PM_{2.5}$ at KS2 were 80 and 17 $\mu g/m^3$, respectively.

The PM mass concentrations during the day and night sampling periods for KS1 were also compared. Results showed that there were no significant differences in mean concentrations between the day and night sampling periods (P=0.09) except for TSP (P=0.04) (Table 3.4). The mean net concentration of TSP during the day (6AM to 6PM) was less than that at night (6PM to

6AM). However, earlier research using high resolution sampling has shown that the highest concentrations of dust occurs between 6PM and 11PM (Razote et al., 2008; Wilson et al., 2002; Sweeten et al., 1988), during which cattle are generally more active and atmospheric conditions are relatively stable.

Table 3.3 Downwind and upwind 24-h PM concentration values.

		Feedlot KS1			Feedlot KS2		
		n[a]	Mean ($\mu g/m^3$)	SE[b] ($\mu g/m^3$)	n[a]	Mean ($\mu g/m^3$)	SE[b] ($\mu g/m^3$)
Downwind	$PM_{2.5}$	21	34	7	3	24	9
Sampling	PM_{10}	28	105	14	3	88	12
Location	TSP	28	262	42	3	185	23
Upwind	$PM_{2.5}$	20	16	1	2	11	7
Sampling	PM_{10}	28	39	5	3	73	55
Location	TSP	27	58	7	-	-	-
	$PM_{2.5}$	15	25	13	2	17	4
Net (Downwind-Upwind)	PM_{10}	25	76	16	2	80	13
	TSP	25	201	40	-	-	-

[a] n represents the number of 24-h values.

[b] SE represents the standard error.

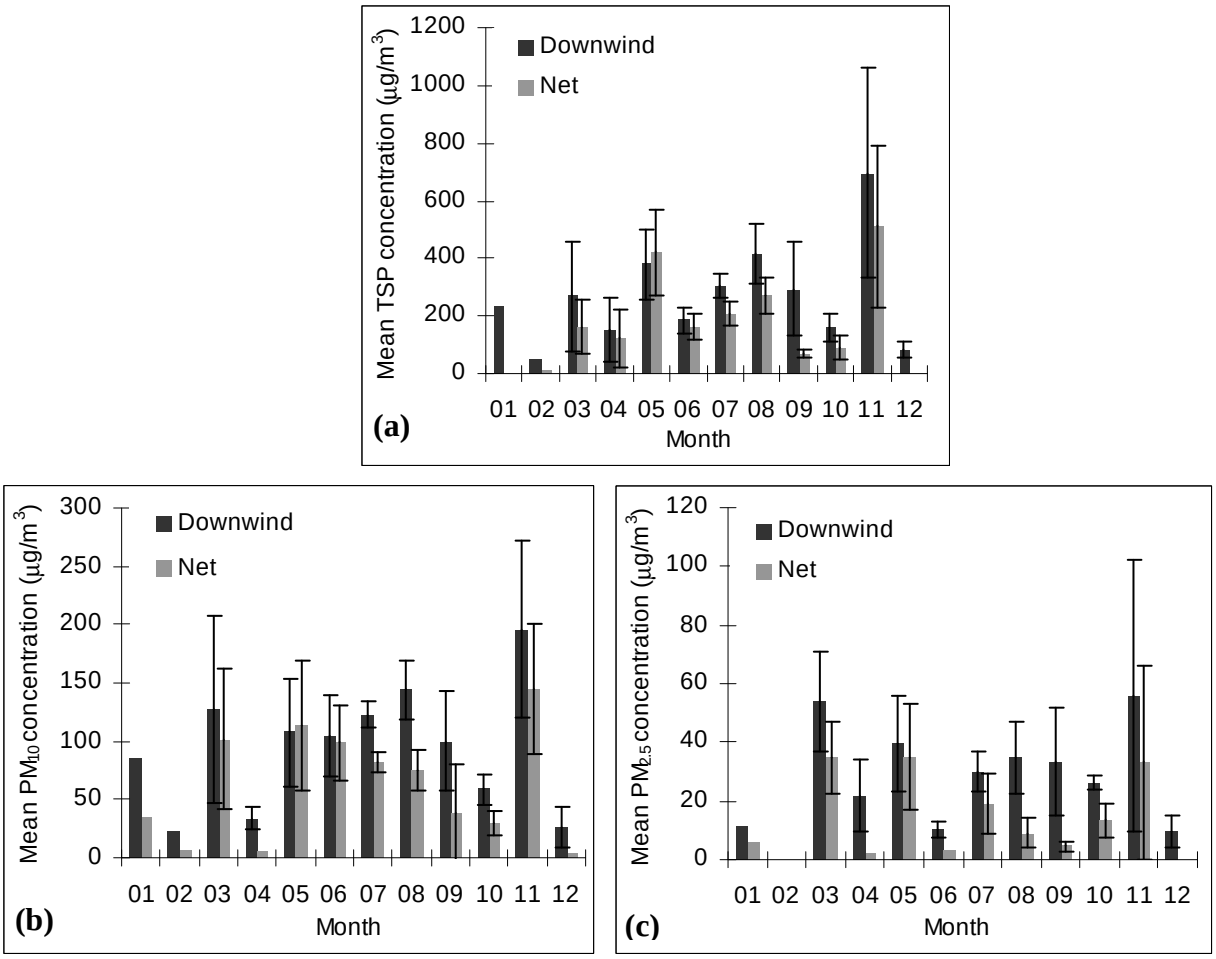

Figure 3.2 Mean PM concentrations of (a) TSP, (b) PM_{10}, and (c) $PM_{2.5}$.

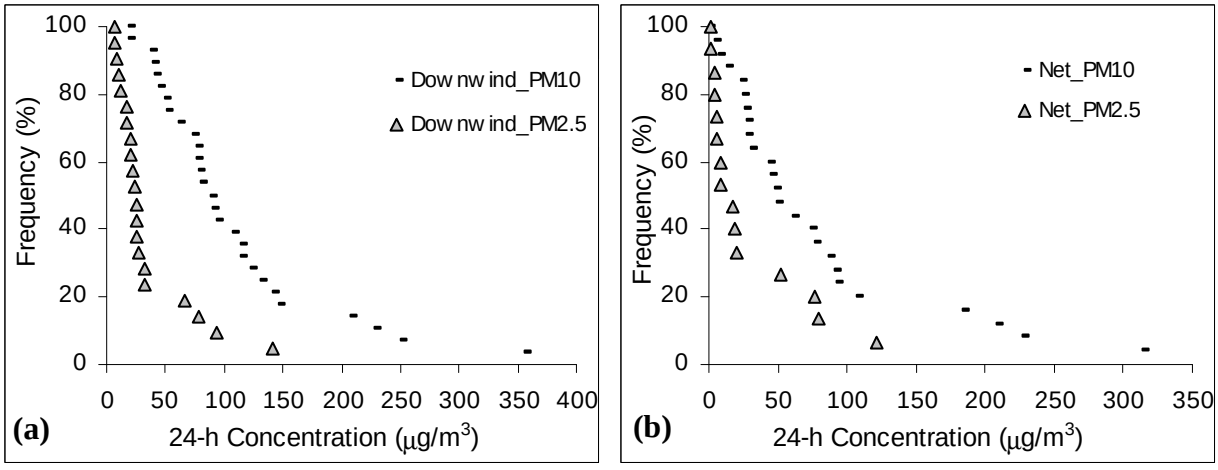

Figure 3.3 Cumulative frequencies of 24-h concentration vs. 24-h concentration for (a) downwind values and (b) net values at feedlot KS1.

Table 3.4 Descriptive statistics of PM concentrations during the day and night sampling periods for feedlot KS1.

		Day Sampling Period (6AM to 6PM)			Night Sampling Period (6PM to 6AM)		
		n	Mean ($\mu g/m^3$)	SE ($\mu g/m^3$)	n	Mean ($\mu g/m^3$)	SE ($\mu g/m^3$)
Downwind	$PM_{2.5}$*	23	25 [a]	6	22	36 [a]	7
Sampling	PM_{10}*	37	104 [a]	13	30	111 [a]	18
Location	TSP*	39	286[a]	50	30	322[a]	57
Upwind	$PM_{2.5}$*	22	21 [a]	5	21	17 [a]	2
Sampling	PM_{10}*	38	57 [a]	12	22	37 [a]	6
Location	TSP*	36	124 [a]	34	23	77 [a]	18
	$PM_{2.5}$*	11	13 [a]	6	16	19 [a]	6
Net (Downwind-Upwind)	PM_{10}*	27	71 [a]	12	21	74 [a]	18
	TSP*	27	202 [a]	50	23	237[b]	47

* Row means followed by the same letter are not significantly different at the 0.05 level of significance.

Previous research indicated that PM ratios may allow the estimation of long-term fine PM concentrations using available TSP or PM_{10} data (Lall et al., 2004; Gehrig et al., 2003). For KS1, the mean $PM_{2.5}/PM_{10}$, $PM_{2.5}$/TSP, and PM_{10}/TSP ratios at the downwind sampling location were significantly ($P<0.05$) smaller than the corresponding ratios at the upwind sampling location (Table 3.5). The frequency distribution of PM ratios at the downwind locations showed smaller ratios occurred more often than upwind sampling location in which frequencies were distributed more uniformly (Fig. 4a and 4b). $PM_{2.5}/PM_{10}$, $PM_{2.5}$/TSP, and PM_{10}/TSP ratios with ranges of 0.1-0.3, less than 0.1, and 0.3-0.4, respectively, had higher frequency observed. These results suggest that the contribution of fine and coarse particles from the feedlot was not as equally distributed compared with the upwind areas and that the PM emitted from the feedlots was dominated by coarse particles. This finding is consistent with the MOUDI results, in which the mean GMD was 13.0 µm and consistent with previous studies that reported GMD ranging from 9.5-16.0 µm (Sweeten et al., 1998; Sweeten et al., 1988).

Table 3.5 Descriptive statistics of PM ratios at the downwind and upwind sampling locations for feedlots KS1 and KS2.

		Feedlot KS1		Feedlot KS2		Urban Areas (Published Data)
		Downwind	Upwind	Downwind	Upwind	
$PM_{2.5}/PM_{10}$	n	46	44	10	5	
	Mean*	0.29[a]	0.44[b]	0.38	0.39	0.54[1]
	SE	0.02	0.04	0.05	0.11	
$PM_{2.5}$/TSP	n	46	42	6		
	Mean*	0.10[a]	0.28[b]	0.18		0.30[1]
	SE	0.01	0.03	0.04		
PM_{10}/TSP	n	67	55	5		
	Mean*	0.41[a]	0.54[b]	0.53		0.50[2]
	SE	0.02	0.03	0.04		

* Row means followed by the same letter are not significantly different at the 0.05 level of significance.

[1] Source: Lall et al. (2004)

[2] Source: Cicero-Pernandez et al. (1993)

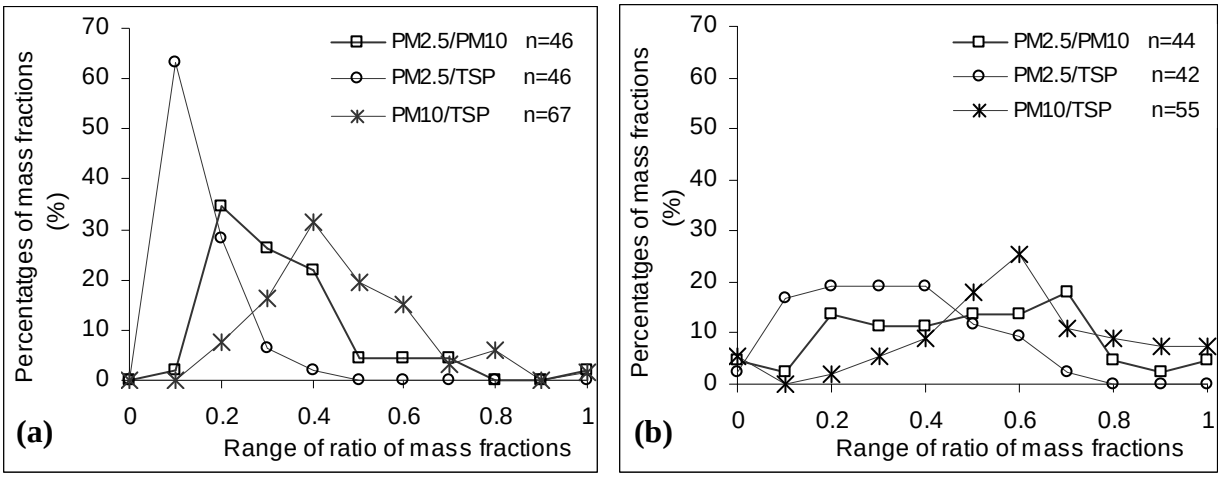

Figure 3.4 Frequencies of mass fractions at the (a) downwind and (b) upwind sampling locations of feedlot KS1.

In comparison, PM measurements in urban environments showed the $PM_{2.5}/PM_{10}$, $PM_{2.5}$/TSP and $PM_{2.5}/PM_{10}$ ratios typically run higher with average of 0.54, 0.30, and 0.50,

respectively (Lall et al., 2004; Cicero-Pernandez et al., 1993). Studies in Swiss and Asian regions also showed that fine PM had greater portion in urban and industrial areas (Gehrig et al., 2003; Cohen et al., 2002; Gehrig et al., 2000), primarily because the major source of PM in these areas is burning of fossil fuels by transportation and industrial sources.

The data from KS2 were limited and may not be representative of the long trend of PM ratios (Table 3.5). The mean $PM_{2.5}/PM_{10}$, $PM_{2.5}$/TSP, and PM_{10}/TSP ratios obtained at the downwind sampling location of feedlot KS2 were 0.38, 0.18, and 0.53, respectively. Only the $PM_{2.5}/PM_{10}$ ratio was available at the upwind sampling location of feedlot KS2 (Table 3.5).

The $PM_{2.5}/PM_{10}$, $PM_{2.5}$/TSP, and PM_{10}/TSP ratios at KS1 were also analyzed by sampling period (i.e., day vs. night). There were no significant differences ($P>0.05$) between day time (6AM to 6PM) and night time (6PM to 6AM) for mean values of $PM_{2.5}/PM_{10}$ ($P=0.7$) and $PM_{2.5}$/TSP ($P=0.3$), indicating that the fraction of fine and coarse particles varied only slightly between day and night.

Statistical analysis showed significant correlations among $PM_{2.5}$, PM_{10}, and TSP concentrations at both the downwind and upwind sampling locations of KS1 (Table 3.6). There was also strong correlation between the $PM_{2.5}/PM_{10}$ and $PM_{2.5}$/TSP ratios at both the downwind and upwind sampling locations (correlation coefficients of 0.71 and 0.82, respectively) as well as $PM_{2.5}$/TSP and PM_{10}/TSP ratios (correlation coefficients of 0.51 and 0.60, respectively), while there were no significant correlations for the other PM ratios. The ratios had significant correlations with PM mass concentrations for $PM_{2.5}$/TSP and PM_{10} as well as TSP at the upwind sampling location, and for PM_{10}/TSP and $PM_{2.5}$ at the downwind sampling location.

Table 3.6 Correlation matrix of concentrations and ratios for the downwind and upwind sampling locations of feedlot KS1.

		$PM_{2.5}$	**PM_{10}**	**TSP**	**$PM_{2.5}/PM_{10}$**	**$PM_{2.5}$/TSP**	**PM_{10}/TSP**
Downwind	$PM_{2.5}$	1.00	0.89*	0.91*	0.21	0.02	-0.33*
	PM_{10}		1.00	0.91*	-0.17	-0.26	-0.14
	TSP			1.00	0.03	-0.26	-0.40
	$PM_{2.5}/PM_{10}$				1.00	0.71*	-0.16
	$PM_{2.5}$/TSP					1.00	0.51*
	PM_{10}/TSP						1.00
Upwind	$PM_{2.5}$	1.00	0.74*	0.89*	0.25	-0.02	-0.30
	PM_{10}		1.00	0.69*	-0.26	-0.46*	0.15
	TSP			1.00	-0.14	-0.39*	-0.25
	$PM_{2.5}/PM_{10}$				1.00	0.82*	0.10
	$PM_{2.5}$/TSP					1.00	0.60*
	PM_{10}/TSP						1.00

* Significant at the 0.05 level.

3.4.3 Effects of weather conditions and pen surface water content

The PM mass concentrations and ratios would likely depend on weather conditions and feedlot pen surface characteristics. In general, the PM emitted from cattle feedlots results from hoof action on the dry, uncompacted, pulverized layer of manure on the corral surface (Razote et al., 2007a; Auvermann et al., 2006). As such, weather conditions and pen surface characteristics (i.e., depth, degree of compaction, and moisture content) are important determinants of the PM emission potential of the pen surface (Funk et al., 2008; Auvermann et al., 2006). To identify factors associated with variation of PM concentrations, the weather conditions (i.e., humidity, temperature, wind speed, and precipitation), water content of the pen surface, and the amount of water applied by the water sprinkler system were further analyzed. For the 82 acceptable sampling runs at the downwind sampling location of feedlot KS1, average temperature was 21 ^{o}C (range of -13 to 40 ^{o}C); average relative humidity was 57% (range of 20% to 91%); and average wind speed was 6 m/s (range of 1 to 22 m/s). There were 4 runs in which there was rainfall (maximum amount of 3 mm) and 39 runs in which the water sprinkler system was operated (maximum amount of water applied was 5 mm).

Pen surface WC showed significant correlation with the log-transformed PM concentrations and ratios except for PM_{10}/TSP (Table 3.7). The amount of water used by sprinkler system was significantly and positively correlated to the log-transformed PM_{10} and TSP concentrations, possibly because the sprinkler system was normally operated when dust events were occurring or expected to occur. For weather conditions, significant correlation was observed between wind speed and ln(TSP), temperature and ln(TSP), humidity and ln(TSP), temperature and ln(PM_{10}), and humidity and ln(PM_{10}). Precipitation was not significantly correlated with concentrations and ratios. The lack of significant correlation between precipitation and concentrations or ratios could be due to relatively small number of cases in this study; however, a rainfall event, depending on the amount and intensity, can reduce the PM concentration due to reduction in emission rate from the wet surface and also the wash-out process in the near-surface atmosphere (Holst et al., 2008).

Table 3.7 Correlation coefficients for concentrations and ratios for the downwind sampling location of feedlot KS1 with weather conditions, pen surface water content, and amount of water applied by the sprinkler system.

	n	Humidity (%)	Temperature (ºC)	Wind speed (m/s)	Precipitation (mm)	Pen Surface Water Content (%)	Amount of Water Used by Sprinkler (mm)
Ln($PM_{2.5}$)	47	-0.02	0.01	0.20	0.22	-0.40*	0.28
Ln(PM_{10})	69	-0.38*	0.33*	0.23	-0.11	-0.67*	0.39*
Ln(TSP)	71	-0.29*	0.24*	0.27*	-0.13	-0.60*	0.37*
$PM_{2.5}$/PM_{10}	46	0.37*	-0.15	0.09	0.18	0.43*	-0.14
$PM_{2.5}$/TSP	46	0.24	-0.01	0.08	0.02	0.49*	-0.04
PM_{10}/TSP	67	-0.04	0.12	-0.18	0.09	0.04	-0.13

* Significant at the 0.05 level.

The backward variable selection procedure in regression analysis was used to determine the independent predictors of the concentrations and PM ratios (Guyon and Elisseeffe, 2003; Nally, 2000). The R^2 values, parameter estimates and intercept of the multi-variable regression

model are summarized in Table 3.8. Factors that significantly influenced TSP concentration included pen surface WC and wind speed; those that influenced PM_{10} concentration were humidity, temperature, pen surface WC, and amount of water used by sprinkler. Pen surface WC was the only factor that significantly influenced the $PM_{2.5}$ concentration. For the $PM_{2.5}/PM_{10}$ ratio, humidity and pen surface WC were the significant factors; and for $PM_{2.5}$/TSP ratio, pen surface WC and amount of water used by sprinkler were the significant parameters.

Table 3.8 Factors selected in backward selection model for the concentrations and ratios at the downwind sampling location of feedlot KS1[†].

			Parameter estimates				
	R^2	**Intercept**	Humidity (%)	Temperature (°C)	Wind speed (m/s)	Pen Surface Water Content (%)	Amount of Water Used by Sprinkler (mm)
Ln($PM_{2.5}$)	0.16	3.6	-	-	-	-0.03	-
Ln(PM_{10})	0.51	6.1	-0.01	-0.02	-	-0.05	0.2
Ln(TSP)	0.44	5.8	-	-	0.05	-0.05	-
$PM_{2.5}/PM_{10}$	0.24	-2.3	0.01	-	-	0.02	-
$PM_{2.5}$/TSP	0.22	-3.0	-	-	-	0.03	0.1

[†]All variables left in the regression models are significant at the 0.1 level.

Statistical analysis indicated that the pen surface WC had the greatest effect on PM concentrations, particularly PM_{10} and TSP, which were reduced when WC was increased. The decrease in concentration with increasing WC of the pen surface is likely due to reduction in emission rates from the pen surfaces. The presence of water in the manure surface is expected to enhance the strength of surface crusts and also increase the mass of particles and surface tension, thereby decreasing particle suspension and transport. Figures 3.5a, 3.5b, and 3.5c plot the net concentrations of TSP, PM_{10}, and $PM_{2.5}$, respectively, as a function of pen surface WC. In general, net TSP and PM_{10} concentrations decreased exponentially with increasing WC. The relationship between net $PM_{2.5}$ concentration and pen surface WC was not as clear, possibly because pen surface WC < 20% for all of the acceptable sampling runs for net $PM_{2.5}$ concentration.

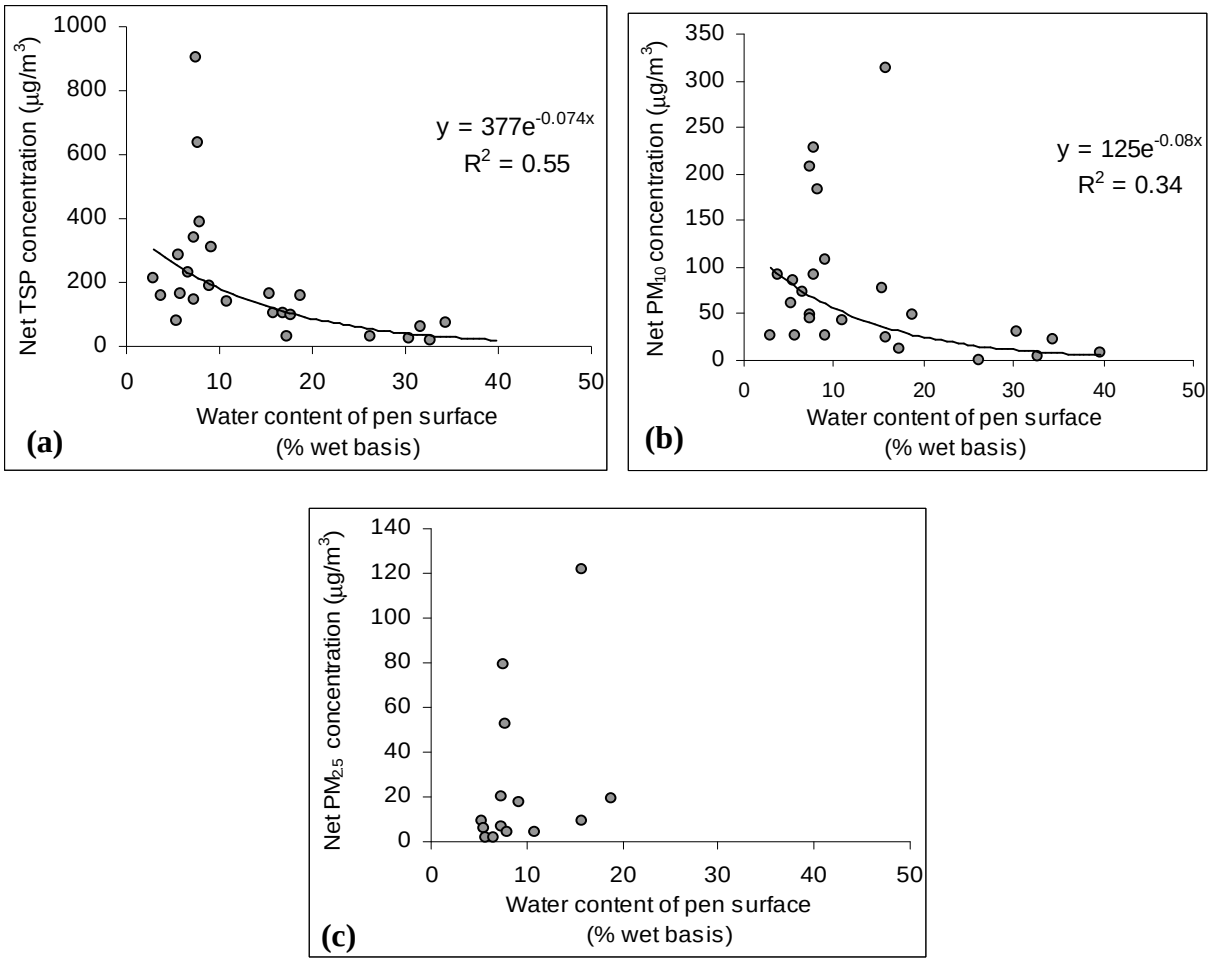

Figure 3.5 Plots of the net 24-h mass concentrations of (a) TSP, (b) PM_{10}, and (c) $PM_{2.5}$ vs. pen surface water content at feedlot KS1.

Results indicate that the threshold value of pen surface WC for PM control is about 20% (Fig. 3.5). Comparison of the mean net concentrations in cases in which WC≥20% and WC<20% showed mean percentage difference of over 80% for TSP and PM_{10}; for net $PM_{2.5}$ concentrations, all acceptable cases has WC<20% (Fig. 3.5). When downwind concentrations were considered (data not shown), comparison of cases in which WC≥20% and WC<20% resulted in mean percentage differences or reductions of 79%, 72%, and 78% for TSP, PM_{10}, and $PM_{2.5}$, respectively. The critical threshold WC of 20% is similar to previous findings and recommendations. Sweeten et al. (1988) indicated that the WC should be in the range between 26% and 41% depending on surface conditions, while Miller and Berry (Miller and Berry, 2005), from laboratory experiments, determined water contents above 35% best in controlling dust but

noted that organic matter content of the feedlot surface also played a large role (Miller and Berry, 2005; Miller and Woodbury, 2003). Other researchers have also suggested that the pen surface WC should be maintained at 20 to 40 % on the basis of odor and dust control as well as the economy of treatment (Auvermann et al., 2006; Miller and Berry, 2005; DPI&F Note, 2003).

3.5 Conclusions

The following conclusions can be drawn from this research:

- The downwind and net mass concentrations of $PM_{2.5}$, PM_{10}, and TSP as well as their ratios varied seasonally, indicating the need for multiple-day, seasonal sampling. The mass concentration of TSP and PM_{10} were closely related to the pen surface water content. The mass concentration of $PM_{2.5}$ also was related to the water content, but not to the same degree. For PM control, the water content of pen surface should be at least 20%.
- The ratios of $PM_{2.5}/PM_{10}$, $PM_{2.5}$/TSP, and PM_{10}/TSP at the downwind sampling location were generally less than those upwind. In addition, measurement of the particle size distribution at the downwind edge of the feedlot with a cascade impactor (MOUDI) showed geometric mean diameter ranging from 7 to 18 μm, indicating that particles that are emitted from the feedlots were generally large in size.

3.6 References

ASTM. 2002. D2216-98: Standard test method for laboratory determination of water (moisture) content of soil and rock by mass. In *Annual Book of American Society for Testing Materials Standards*. Philadelphia, Penn.: ASTM.

Auvermann, B.W., R. Bottcher, A. Heber, D. Meyer, C.B. Parnell, Jr., B. Shaw, and J. Worley. 2006. Particulate matter emissions from animal feeding operations. In *Animal Agriculture and the Environment: National Center for Manure and Animal Waste Management White Papers*, 435-468. J.M. Rice, D.F. Caldwell, F.J. Humenik, eds. St. Joseph, Mich.: ASABE.

Cicero-Pernandez, P., W.A. Thistlewaite, Y.I. Falcon, and I.M. Guzman. 1993. TSP, PM_{10} and PM_{10}/TSP ratios in the Mexico City Metropolitan area: a temporal and spatial approach. *J. Expo. Anal Environ. Epidemiol.* 3 suppl. 1: 1-14.

Cohen, D.D., D. Garton, E. Stelcer, T. Wang, S. Poon, J. Kim, S.N. Oh, H.J. Shin, M.Y. Ko, F. Santos, L. Esquerra, V. T. Bac, P.D. Hien. 2002. Uematsu, M.. 2002. Characterization of $PM_{2.5}$ and PM_{10} fine particle pollution in several Asian regions; 16th Int. Clean Air Conf. Christchurch, N.Z., 18-22 Aug 2002.

DPI&F Note. 2003. Environmental scientists and engineers feedlot waste management series: Dust control. Available at: http://www2.dpi.qld.gov.au/environment/5243.html. Accessed 1st March 2009.

Funk, C.V., H.I. Reuter, C. Hoffmann, W. Engel, and D. Oetti. 2008. Effect of moisture on fine dust emission from tillage operations on agricultural soils. *Earth Surf. Process. Landforms* 33 (12): 1851-1863.

Gehrig, R., and B. Buchmann. 2003. Characterizing seasonal variations and spatial distribution of ambient PM_{10} and $PM_{2.5}$ concentrations based on long-term Swiss monitoring data. *Atmos. Environ.* 37: 2571-2580.

Gehrig, R., and P. Hofer. 2000. Parallel measurements of PM_{10} and total suspended particles (TSP)--estimation of PM_{10}-characteristics from TSP data. *Gefahrstoffe Reinhaltung Der Luft* 60 (10): 389-394.

Guerra, S.A., D.D. Lane, G.A. Marotz, R.E. Carter, and C.M. Hohl. 2006. Effects of wind direction on coarse and fine particulate matter concentrations in Southeast Kansas. *J. Air Waste Manage. Assoc.* 56 (11): 1525-1521.

Guyon, I., and A. Elisseeffe. 2003. An introduction to variable and feature selection. *J. Machine Learning Res.* 3: 1157-1182.

Holst, J., H. Mayer, and T. Holst. 2008. Effect of meteorological exchange conditions on PM_{10} concentration. *Meteorologische Zeitschrift* 17 (3): 273-282.

Hamm, L.B. 2005. Engineering analysis of fugitive particulate matter emissions from cattle feedyards. MS thesis. College Station, Tex.: Texas A&M University.

Hiranuma, N., S. Brooks, D. Thornton, and B. Auvermann. 2010. Atmospheric ammonia mixing ratios at an open-air cattle feeding facility; *J. Air Waste Manage. Assoc*. 60(2): 210-218.

Hinds, W.C. 1999. *Aerosol technology: properties, behavior and measurement of airborne particles*. New York, N.Y.: John Wiley &Sons, Inc.

Karaca, F., O. Alagha, and F. Erturk. 2005. Statistical characterization of atmospheric PM_{10} and $PM_{2.5}$ concentrations at a non-impacted suburban site of Istanbul, Turkey. *Chemosphere* 59 (8), 1183-1190.

Lall, R., M. Kendall, K. Ito, and G. D. Thurston. 2004. Estimation of historical annual $PM_{2.5}$ exposure for health effects assessment. *Atmos. Environ.* 38 (31): 5217-5226.

Lammel, G., F. Schneider, E. Bruggemann, T. Gnauk, A. Rohrl, and P. Wieser. 2004. Aerosols emitted from a livestock farm in southern Germany. *Water, Air, Soil Pollut.* 154(1-4): 313-330.

Lee, J., and Y. Zhang. 2008. Evaluation of gas emissions from animal building dusts using a cylindrical convective chamber. *Biosystems Eng.* 99(3): 403-411.

MacVean, D.W., D.K. Franzen, T.J. Keefe, and B.W. Bennett. 1986. Airborne particle concentration and meteorologic conditions associated with pneumonia incidence in feedlot cattle. *Am. J. Veterinary Res.* 47(12): 2676-2682.

Miller, D.N., and E.D. Berry. 2005. Cattle feedlot soil moisture and manure content: 1. Impacts on greenhouse gases, odor compounds, nitrogen losses, and dust. *J. Environ. Qual.* 34(2): 644-655.

Miller, D. N. and B. L. Woodbury. 2003. Simple protocols to determine dust potentials from cattle feedlot soil and surface samples. *J. Environ. Qual.* 32(5): 1634-1640.

MSP Corporation. 2006. Model 100/110 MOUDI™ user guide. Shoreview, MN: MSP Corp.

Nally, R. 2000. Regression and model-building in conservation biology, biogeography and ecology: The distinction between-and reconciliation of - 'predictive' and 'explanatory' models. *Biodiversity and Conservation* 9(5): 655-671.

National Research Council (NRC). 2003. *Air emissions from animal feeding operations: current knowledge, future needs.* Washington, D.C.: The National Academies Press.

Purdy, C.W., R.N. Clark, and D.C. Straus. 2007. Analysis of aerosolized particulates of feedyards located in the Southern High Plains of Texas. *Aerosol Sci. Technol.* 41(5): 497-509.

Purdy, C.W., D.C. Straus, D.B. Parker, S.C. Wilson, and R.N. Clark. 2004. Comparison of the type and number of microorganisms and concentration of endotoxin in the air of feedyards in the Southern High Plains. *Am. J. Veterinary Res.* 65(1): 45-52.

Razote, E.B., R.G. Maghirang, L. Guo, J.G. Tallada, B.W. Auvermann, J.P. Harner III, and W.L Hargrove. 2008. TEOM measurements of PM_{10} and $PM_{2.5}$ concentrations at cattle feedlots in Kansas. ASABE Paper No. MC08108. St. Joseph, Mich.: ASABE.

Razote, E.B., R.G. Maghirang, J.P. Murphy, B.W. Auvermann, J.P. Harner III, D.L. Oard, W.L. Hargrove, D.B. Parker, and J.M. Sweeten. 2007a. Ambient PM_{10} concentrations at a beef cattle feedlot in Kansas. ASABE Paper No.701P0907cd. St. Joseph, Mich.: ASABE.

Razote, E.B., R.G. Maghirang, J.P. Murphy, B.W. Auvermann, J.P. Harner III, D.L. Oard, W.L. Hargrove, D.B. Parker, and J.M. Sweeten. 2007b. Air quality measurements from a water-sprinkled beef cattle feedlot in Kansas. ASABE Paper No. 07-4108. St. Joseph, Mich.: ASABE.

Reynolds, S.J., D.Y. Chao, P.S. Thorne, P. Subramanian, P.F. Waldron, M. Selim, P.S. Whitten, and W.J. Popendorf. 1998. Field comparison of methods for evaluation of vapor/particle phase distribution of ammonia in livestock buildings. *J. Agric. Safety Health* 4(2): 81-93.

Rogge, W.F., P.M. Medeiros, and B.R.T. Simoneit. 2006. Organic marker compounds for surface soil and fugitive dust from open lot dairies and cattle feedlots. *Atmos. Environ.* 40(1): 27-49.

Rupprecht & Patashnick Co, Inc. 2004. Operating manual, Mini-Partisol model 2100 air sampler, Revision B. Albany, N.Y.: Rupprecht & Patashnick Co., Inc.

Sweeten, J. M., C.B. Parnell, B. W. Auvermann, B. W. Shaw, and R. E. Lacey. 2000. *Livestock feedlots. In: Air Pollution Engineering Manual*. W. T. Davis (ed.). N.Y.: Wiley.

Sweeten, J.M., C.B. Parnell, B.W. Shaw, and B.W. Auvermann. 1998. Particle size distribution of cattle feedlot dust emission. *Trans. ASAE* 41(5): 1477-1481.

Sweeten, J.B., C.B. Parnell, R.S. Etheredge, and D. Osborne.1988. Dust emissions in cattle feedlots. *Vet. Clin. North Am. Food Anim. Pract.* 4(3): 557-578.

Todd, R.W. W. Guo, B.A. Stewart, and C. Robinson. 2004. Vegetation, phosphorus, and dust gradients downwind from a cattle feedyard. *J. Range Manage.* 57 (3): 291-299.

U.S. EPA. 2006. National primary and secondary ambient air quality standards- final rule. 40 CFR, part 50, Federal Register, Vol.71, No. 200. Available at: http://www.epa.gov/ttnnaaqs/standards/pm/data/fr20061017.pdf. Accessed 10 November 2010.

U.S. EPA. 2005. Review of the national ambient air quality standards for particulate matter: policy assessment of scientific and technical information. Research Triangle Park, N.C.:

Office of Air Quality Planning and Standards. Available at: http://www.epa.gov/ttn/naaqs/standards/pm/data/pmstaffpaper_20050630.pdf. Accessed 10 November 2010.

Wehner, B., W. Birmili, T. Gnauk, and A. Wiedensohler. 2002. Particle number size distributions in a street canyon and their transformation into the urban-air background: measurements and a simple model study. *Atmos. Environ.* 36(13): 2215-2223.

Wilson, S.C., J. Morrow-Tesch, D.C. Straus, J.D. Cooley, W.C. Wong, F.M. Mitloehner, and J.J. McGlone. 2002. Airborne microbial flora in a cattle feedlot. *Appl. Environ. Microbiol.* 68(7): 3238-3242.

Wu, S.Y., S. Krishnan, Y. Zhang, and V. Aneja. 2008. Modeling atmospheric transport and fate of ammonia in North Carolina - Part II: Effect of ammonia emissions on fine particulate matter formation. *Atmos. Environ.* 42 (14), 3437-3451.

CHAPTER 4 - Field Comparison of PM_{10} Samplers

4.1 Abstract

Fugitive emissions of particulate matter with equivalent aerodynamic diameter of 10 µm or less (PM_{10}) are an increasing concern for concentrated animal feeding operations, including open-lot beef cattle feedlots. Various federal reference method (FRM) and equivalent samplers can be used to measure PM_{10} concentrations. This research compared the performance of Tapered Element Oscillating Microbalance™ (TEOM), FRM high-volume (HV), and low-volume (LV) PM_{10} samplers in measuring PM_{10} concentrations in the vicinity of large cattle feedlots in Kansas. Each of the three samplers was installed at the downwind and upwind perimeters of two commercial cattle feedlots (KS1 and KS2). Samplers were operated from May 2006 to February 2008 at KS1 and from February 2007 to February 2008 at KS2. PM_{10} concentration ranged from < 10 to 832 µg/m^3 at KS1 and from < 10 to 713 µg/m^3 at KS2. Comparison of collocated PM_{10} samplers showed that measured PM_{10} concentration was generally largest with the TEOM PM_{10} sampler and smallest with the LV PM_{10} sampler. Differences in PM_{10} concentration among samplers were affected by location and duration of sampling, season, and slightly by weather conditions.

4.2 Introduction

Fugitive emissions of particulate matter (PM), ammonia, and odor are an increasing concern for animal feeding operations (AFOs), including open-lot beef cattle feedlots and dairies. Dust generated from cattle feedlots has potential to cause a number of respiratory problems in humans as well as livestock (Purdy et al., 2004). Inhalation of fine PM is believed to be the major cause of increased health risks (Seaton et al., 1995). As a result, PM_{10} (PM with equivalent aerodynamic diameter of 10 µm or less) and $PM_{2.5}$ (PM with equivalent aerodynamic diameter of 2.5 µm or less) are being regulated (Purdy et al., 2007). For example, primary and secondary 24-h national ambient air quality standards for PM_{10} are 150 µg/m^3 and not to be exceeded more than once per year on average over 3 years (Chow et al., 2006).

Measuring PM_{10} in cattle feedlots is necessary to investigate health effects posed by PM_{10} emissions, monitor transport and fate of PM_{10}, and assess effectiveness of PM abatement measures. The Federal Reference Method (FRM) and Federal Equivalent Method (FEM) of measuring PM emissions are recommended by the U.S. EPA (U.S.EPA, 1987). The FRM is a gravimetric technique in which particles are collected on a filter that is exposed for 24 h (Bulpitt and Price, 2006). The equivalent PM measurement methods, including the Tapered Element Oscillating Microbalance (TEOM), have been used to provide direct PM mass measurement for near real-time continuous data acquisition (Meyer et al., 2000; U.S. EPA, 2004).

Measurement technologies for PM are affected by the complexity of PM emissions. Actual constituents and particle size vary with geographical location and meteorological conditions (National Research Council, 2003). Inorganic, semi-volatile or volatile components, hydrogen sulfide, and ammonium nitrate may be present in the particulate phase and may be lost with time and location (Allen et al., 1997; Jerez et al., 2006). Currently, effectiveness of the measurement method is one of the more important issues in PM quantification and control, and analytical methods, including consideration of sampling uncertainties, should be fully understood (Chow, 1995; Bulpitt and Price, 2006). Several instruments are currently being used to measure PM_{10} concentration. Comparison of these samplers is needed to determine agreement of these samplers and improve various designs that influence what is actually being measured.

The major objective of this study was to compare PM_{10} concentrations measured by three different PM_{10} samplers (i.e., low-volume [LV], FRM high-volume [HV], FEM TEOM) under field conditions. Performance of similar PM_{10} samplers placed in two commercial cattle feedlots in Kansas was also evaluated. Results may provide an understanding of the PM_{10} measurement techniques as well as improve PM_{10} measurement in future studies.

4.3 Materials and Methods

4.3.1 Description of PM_{10} samplers

This study considered the FRM HV PM_{10} sampler (Thermo Fisher Scientific, Franklin, MA), LV PM_{10} sampler (2100 Mini-Partisol, Thermo Fisher Scientific, Franklin, MA), and TEOM PM_{10} sampler (Series 1400a, Thermo Fisher Scientific, Franklin, MA; EPA designation No. EQPM-1090-079). The LV and HV PM_{10} samplers with PM_{10} size-selective inlets are gravimetric measurements that yield time-integrated mass concentration of PM_{10}. During

measurement, ambient air is drawn into the size-selective inlet of the sampler using a vacuum pump. As ambient air passes through a filter, PM is collected on the filter. Mass of the collected PM is calculated by subtracting the gross weight of the sample filter from its tare weight. Mass of PM_{10} is then divided by the sampling flow volume to get the mass concentration of PM_{10}.

Flow rate is critical for particle fractionation and calculation of mass concentration. For the HV sampler, the flow rate of 1130 L/min is controlled by venturi (Thermo Electron Corp., 2003). For the LV sampler, the flow control system uses a temperature and pressure compensated mass flow control scheme to maintain a constant volumetric flow rate of 5 L/min (Rupprecht & Patashnick Co., Inc., 2004a).

The TEOM PM_{10} sampler, a FEM sampler for PM_{10} measurement, is also a filter-based mass measurement technique. An inertial balance directly measures the mass collected on the filter cartridge every 2 s by monitoring the corresponding frequency changes of a tapered element. The sample flow passes through the filter and then continues through the hollow tapered element on its way to an active volumetric flow control system and vacuum pump. The total airflow rate of 16.67 L/min is separated into a filter flow rate of 3 L/min and auxiliary flow rate of 13.67 L/min. The airstream for the filter flow is heated to 50 ^{o}C to remove particle-bound water (Rupprecht & Patashnick Co., Inc., 2004b; Jerez et al., 2006). The TEOM system has near real-time data output and near real-time mass measurement capability. Furthermore, it eliminates possible filter handling errors that might happen with manual and gravimetric methods (Green and Fuller, 2006).

4.3.2 Site description

Measurements were conducted at the upwind and downwind perimeters of two cattle feedlots, herein referred to as KS1 and KS2, in Kansas. KS1 is located approximately 40 km southwest of KS2. Prevailing wind directions at the sites were from south-southeast in summer and north-northwest in winter. Annual average precipitation in KS1 and KS2 were approximately 627 mm and 608mm, respectively. Cattle capacities of KS1 and KS2 are 30,000 and 25,000 head, respectively. For both feedlots, feed was processed and mixed in the feed mill, loaded on feed trucks and delivered to the pens three times a day. The major source of PM emission for both feedlots was the pen surface. As the cattle moves around the pen, the accumulated manure on the pen surface is ground into smaller sizes that can be subsequently

suspended in the air. This is generally more pronounced during the late afternoon to early evening hours when the cattle are most active. For PM control, KS1 has a solid set sprinkler system that was normally operated from May to October and during times when there was a prolonged dry period. In addition, pens at KS1 were scraped year round and manure was harvested at least twice a year. At KS2, pens were also scraped year round and manure was harvested five to six times a year. The soil at KS2 was generally clay loam, resulting in better compaction of the base soil and better scraping of the pens compared to KS1, which had sandy soil.

A set of TEOM PM_{10}, HV $PM_{10,}$ and LV PM_{10} samplers was set up along the north and south perimeters of KS1 in April 2006 (Fig. 4.1). Similarly, TEOM PM_{10} and HV PM_{10} samplers were set up in February 2007 and LV PM_{10} samplers were set up in September 2007 at the north and south perimeters of KS2. To compare similar samplers, two identical HV PM_{10} and LV PM_{10} samplers were used from April to December 2006 and from July and August 2007, respectively, at both of the north and south sampling locations of KS1. In addition, there were two identical TEOM PM_{10} samplers at the south sampling location of KS1 from January to July 2007.

A weather station was installed at the south sampling location of KS1 and north sampling location of KS2 to obtain meteorological information. Weather data from a local weather station were also collected.

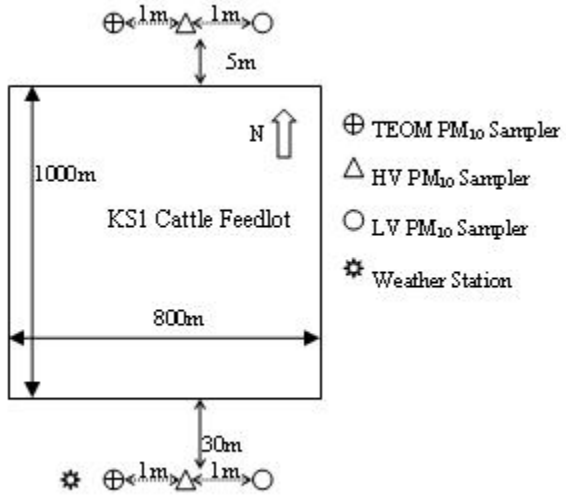

Figure 4.1 Schematic diagram showing the location of the PM_{10} samplers and the weather station at KS1 (not drawn to scale)

4.3.3 Air sampling

At each sampling location, samplers were placed side by side with a minimum distance of about 1 m from each other (Fig. 4.1). Intensive sampling campaigns (approximately 24 h) were conducted monthly from May 2006 to February 2008, and six 5-day intensive sampling events were conducted for the months of July to October 2007 and February 2008. For each run, the sampling duration was from 2 h to 24 h (107 runs with duration of 6 h or greater; 13 runs had a duration less than 6 h at KS1; 57 runs had a duration of at least 6 h at KS2). The sampling duration was initially from 2 h to 4 h and was increased to 6 h to 24 h, particularly during events of low concentration, to increase the mass of PM collected on the filter

Filters used for HV PM_{10} samplers were 20 cm × 25 cm, type A/E glass fiber filters (Gelman Sciences, Ann Arbor, MI), and either Pallflex TX40 or PTFE filters (Whatman Inc., Clifton, NJ) were used for the LV PM_{10} samplers. All filters were conditioned in the conditioning chamber (25 °C, 40% relative humidity (RH) for 24 h before weighing, before and after sampling, to minimize the effect of humidity. Field blank filters were used for the HV and LV samplers for quality control of the data. Blank filters were handled in the same way as the other filters, the only difference was that blank filters were placed in the samplers and then taken out without turning on the pump (i.e., no sampled air going through the filter). Blank filters were used in 79% and 62% of the total runs for the HV and LV samplers, respectively. The average difference in the initial and final weight of the blank filters was approximately 1 mg for the HV samplers and 0.03 mg for the LV samplers. On the average, the mean values of the change in mass of the field blanks as percentage of the particulate mass on the collection filters were 7% (6% for the north or downwind location and 8% for the south or upwind location) and 26% (21% for the north location and 31% for the south location) for the HV and LV samplers respectively. In accordance with U.S. EPA's recommendation (U.S. EPA, 1998), the field blanks were not used for correction but as a quality control check to detect weight changes due to filter handling. For example, if the weight change was large, contamination during transportation or at the sampling site may be occurring; appropriate troubleshooting and corrective actions should be taken.

4.3.4 Data analysis

The data analyzed were measurements taken from May 2006 to February 2008 for KS1 and from February 2007 to February 2008 for KS2. Data collected when there was a power failure or when instruments had operational problems were discarded. The TEOM values were arithmetically averaged according to the starting and ending time of intensive sampling (e.g., for the 12 h HV/LV sampling duration of 6 am to 6 pm, the mass concentrations measured by TEOM from 6 am to 6 pm were averaged to get the TEOM mass concentration for this run). In some cases, negative values on the TEOM data were observed. These negative values could be due to the nature of particles or instrument malfunction. In accordance with the manufacturer's recommendation, "small" negative values (i.e., 0 to -10 $\mu g/m^3$), which are likely due to the nature of particles, were considered in the calculation of mean values. "Large" negative values (i.e., <-10 $\mu g/m^3$) are likely due to instrument malfunction and were discarded in the calculation. Overall, about 14.4% of TEOM raw data had negative values. Of these, about 7.4% (5% for the north or downwind location and 10% for the south or upwind location) had values that are less than <-10 $\mu g/m^3$ and 7.0% (6% for the north location and 8% for south location) had values that are within the 0 to -10 $\mu g/m^3$. On the basis of the national ambient air quality standards for PM, all measurements were converted to standard conditions of temperature (25 ^oC) and pressure (760 mm Hg) (U.S.EPA, 2006). Mass concentration data from samplers were compared in pairwise (y versus x) fashion. In this paper, for the comparison of different samplers, concentrations measured by the HV sampler were selected as the reference or the "x" variable (Krieger et al., 2007; Knight and Moore, 1987a, 1987b). The "y" variable represented concentration data from the TEOM or LV samplers. The HV sampler was selected as the reference because it is a FRM sampler. The terms "oversampling" and "undersampling" were then based on the HV sampler as the reference. Comparability was evaluated by linear regression (LR) of y and x with zero intercept. For excellent agreement between samplers, the slope should be close to unity (1 ± 0.1) with a high R^2 value (≥ 0.94) (Salter and Parsons, 1999; Predicala and Maghirang, 2003; Vega et al., 2003; Chow et al., 2006). Paired t-tests and correlation analyses were also used. The presence of outliers might cause regression errors. Data points with vertical distance from the regression line exceeding four times the standard error (SE) of estimate were eliminated (Cornbleet and Gochman, 1979; Lee et al., 2005). Five and two outliers were eliminated in the comparison of TEOM vs. HV samplers at KS1 and KS2, respectively. Three

and two outliers were excluded from the comparison of LV vs. HV samplers at KS1 and KS2, respectively.

The slope (b), R^2 value, and other statistical parameters were generated through Excel (Microsoft Corp, Redmond, WA) and SAS (version 9.1.3, SAS Institute Inc., Cary, NC).

4.4 Results and Discussion

4.4.1 Comparison of similar PM_{10} samplers

A total of 60, 41, and 28 data points measured by similar HV, LV, and TEOM samplers were obtained. As shown in Table 4.1, maximum values for the two HV samplers were 395 $\mu g/m^3$ and 390 $\mu g/m^3$; minimum values were 9 $\mu g/m^3$ and 8 $\mu g/m^3$; and mean values with standard error of mean were both equal to 99 ± 13 $\mu g/m^3$. For the two LV samplers, maximum concentrations were 337 $\mu g/m^3$ and 302 $\mu g/m^3$; minimum values were 0 $\mu g/m^3$ and 13 $\mu g/m^3$; and average values were 80 ± 11 $\mu g/m^3$ and 77 ± 9 $\mu g/m^3$. For the TEOM samplers, the average mass concentrations were based on the sampling duration of the HV or LV samplers. Respective maximum values were 145 $\mu g/m^3$ and 181 $\mu g/m^3$; minimum values were 6 $\mu g/m^3$ and 3 $\mu g/m^3$; and average values were 37 ± 6 $\mu g/m^3$ and 36 ± 8 $\mu g/m^3$.

The t-test of paired samples for means with 95% confidence showed that Pearson correlations were all 0.97 for HV, LV, and TEOM samplers. The P (T<=t) values were greater than 0.05, indicating that similar samplers were highly correlated and there were no significant differences between similar samplers. Figure 4.2 shows regression lines with slopes of 0.99, 0.90, and 1.05 with R^2 values around 0.98 for HV, 0.97 for LV, and 0.96 for TEOM samplers, respectively.

Table 4.1 Comparison of similar PM_{10} samplers.

Sampler	n	Min µg/m^3	Max µg/m^3	Mean (±SE[†]) µg/m^3	R^2	b[‡]	SE_b[‡]	Paired t-test P-value
HV 1	60	9	395	99(±13)	0.98	0.99	0.02	P>0.05
HV 2		8	390	99(±13)				
LV 1	41	0	337	80(±11)	0.97	0.90	0.02	P>0.05
LV 2		13	302	77(±9)				
TEOM1	28	6	145	37(±6)	0.96	1.05	0.04	P>0.05
TEOM2		3	181	36(±8)				

[†] SE is the standard error of the mean

[‡] b is the slope, SE_b is the standard error of b.

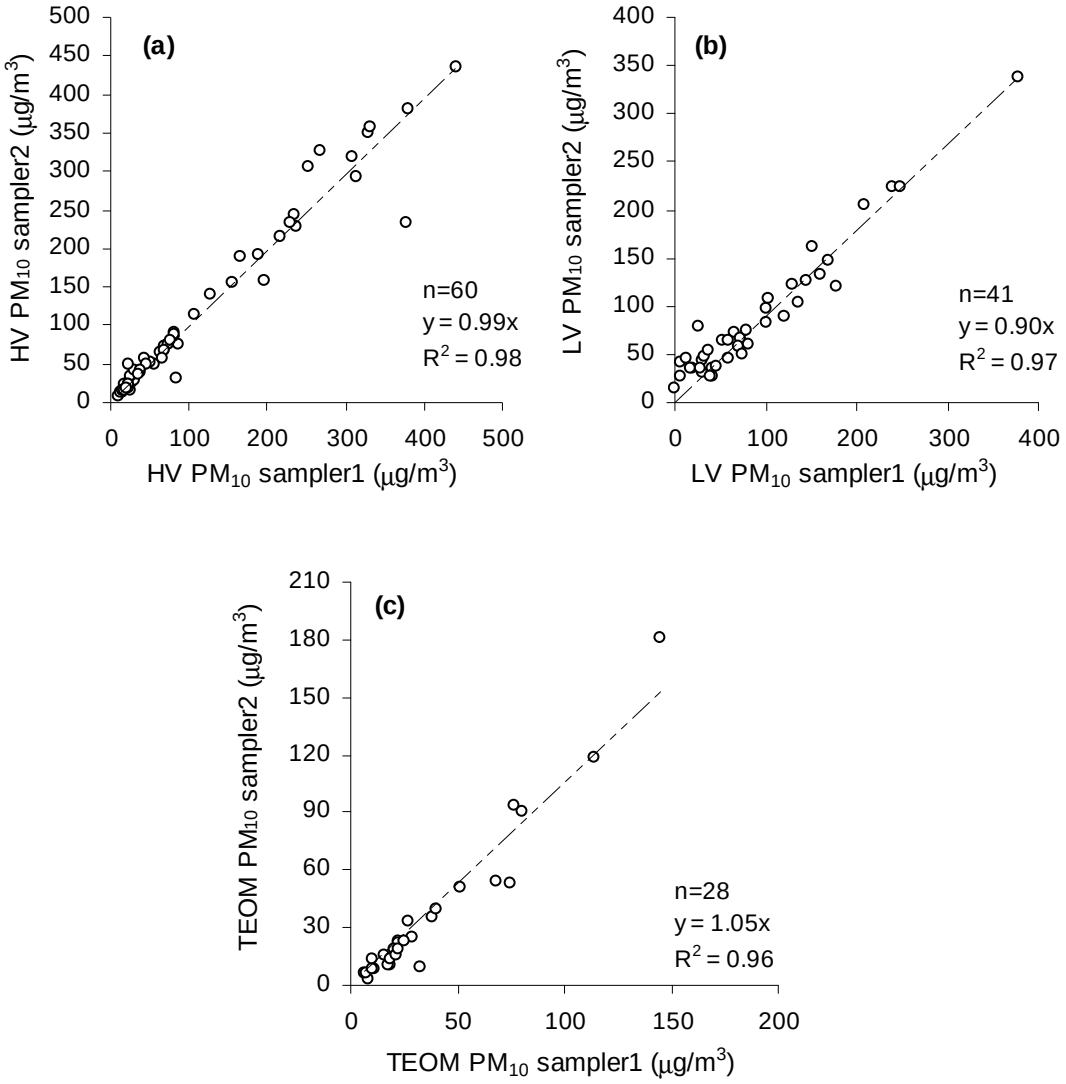

Figure 4.2 Plots of PM_{10} concentrations for similar samplers at feedlot KS1: (a) high-volume (HV) PM_{10} samplers, (b) low-volume (LV) PM_{10} samplers, and (c) Tapered Element Oscillating Microbalance (TEOM) PM_{10} samplers.

4.4.2 Comparison of TEOM and high-volume (HV) PM_{10} samplers

There were 208 and 98 pairs of mass concentration data measured by HV and TEOM samplers at KS1 and KS2, respectively (Table 4.2). At KS1, maximum values of mass concentrations were 537 µg/m^3 and 505 µg/m^3 for the HV and TEOM samplers, respectively; minimum values were less than 10 µg/m^3; and corresponding mean values were 76 ± 7 µg/m^3 and 86 ± 7 µg/m^3. At KS2, corresponding maximum values of concentrations were 611 µg/m^3

and 713 µg/m^3; minimum values were also less than 10 µg/m^3; and average values were 47 ± 9 µg/m^3 and 55 ± 10 µg/m^3 for HV and TEOM samplers, respectively.

Pearson correlations of 0.96 and 0.90 in t-tests of paired samples indicate that concentrations measured by HV and TEOM samplers at KS1 and KS2 were highly correlated. Slopes of the linear regression (Fig. 4.3a and 4.3b) were 1.07 and 1.04 with R^2 values of 0.95 and 0.85 for KS1 and KS2, respectively. Comparing KS1 and KS2, the p-value was 0.6 indicating that there was no significant difference in the correlations of mass concentration measured by TEOM and HV samplers between KS1 and KS2. Accordingly, a combined regression line (Fig. 4.3c) was obtained with a slope of 1.06 and R^2 value of 0.93 suggesting that the TEOM tended to oversample when compared with the HV sampler. The p-value obtained by t-test of paired two samples for means was less than 0.05, indicating that there was significant difference between mean concentrations measured by HV and TEOM samplers.

Table 4.2 Comparison of different PM_{10} samplers.

Sampler	n	Min µg/m^3	Max µg/m^3	Mean (±SE†) µg/m^3	R^2	b‡	SE_b‡	Paired t-test P-value
HV-KS1	208	4	537	76(±7)	0.95	1.07	0.02	P<0.05
TEOM-KS1		5	505	86(±7)				
HV-KS2	98	3	611	47(±9)	0.85	1.04	0.04	P<0.05
TEOM-KS2		5	713	55(±10)				
HV-KS1	190	2	832	96(±9)	0.88	0.53	0.01	P<0.05
LV-KS1		0	393	64(±5)				
HV-KS2	63	3	611	68(±13)	0.88	0.59	0.03	P<0.05
LV-KS2		3	313	52(±7)				

† SE is the standard error of the mean

‡ b is the slope, SE_b is the standard error of b.

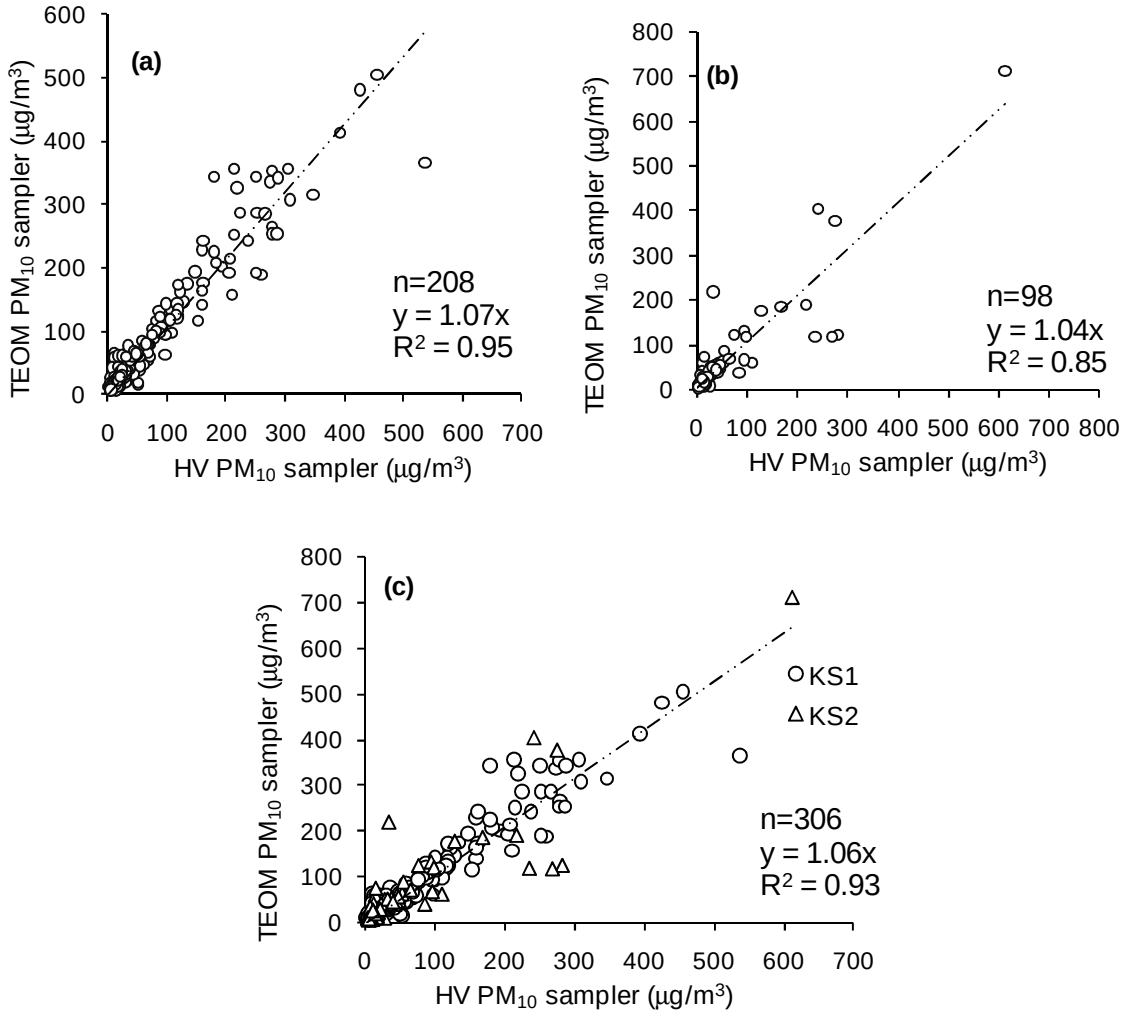

Figure 4.3 Comparison of Tapered Element Oscillating Microbalance (TEOM) and high-volume (HV) PM_{10} samplers for two feedlots: (a) KS1, (b) KS2, and (c) combination of KS1 and KS2.

Since the samplers in this study were placed at two different sampling locations and sampling was conducted in different seasons, better understanding of the performance of these samplers could be made by analyzing the data in groups according to location (i.e., north vs. south) and sampling time (i.e., winter vs. summer). As shown in Table 4.3, for the comparison of TEOM and HV samplers at the south sampling locations of KS1 and KS2, slopes were 1.12 and 1.35 with R^2 values of 0.96 and 0.98, respectively. For the north sampling locations of KS1 and KS2, slopes were 1.04 and 0.99, respectively with R^2 values of 0.95 and 0.83. These results suggest that TEOM samplers had a greater tendency to oversample at the south sampling location than at the north sampling location.

Table 4.3 Comparison of different PM_{10} samplers for different locations.

		TEOM vs. HV				LV vs. HV			
		n	R^2	b†	SE_b†	n	R^2	b†	SE_b†
KS1	N	102	0.95	1.04	0.02	58	0.96	0.50	0.01
	S	106	0.96	1.12	0.02	58	0.93	0.61	0.02
KS2	N	44	0.83	0.99	0.07	31	0.91	0.53	0.03
	S	54	0.98	1.35	0.03	32	0.95	0.85	0.04

† b is the slope, SE_b is the standard error of b.

To determine the effect of season, mass concentration data during winter (December to February) and summer (June to August) were extracted for analysis. Because of limited amount of data, the data from KS1 and KS2 were combined. For the comparison of TEOM and HV samplers, the slope 0.94 with an R^2 value of 0.96 in winter. In summer, the slope was 1.01 with an R^2 value of0.93 (Table 4.4). This shows that TEOM slightly tended to oversample in summer and undersample in winter compared with the HV sampler.

Table 4.4 Comparison of different PM_{10} samplers for different seasons.

		n	**R^2**	**b†**	**SE_b†**
Summer	TEOM vs. HV	117	0.93	1.01	0.03
Winter		70	0.96	0.94	0.02
Summer	LV vs. HV	34	0.94	0.49	0.02
Winter		49	0.77	0.90	0.07

† b is the slope, SE_b is the standard error of b.

Effects of meteorological conditions were examined between pairs of measurements at KS1. KS2 was not considered because of limited available weather data taken directly from KS2. During the intensive sampling periods, ambient relative humidity (RH) ranged from 20% to 95% with a mean value of 58.5%; air temperature ranged from -5.9 ^oC to 41.8 ^oC with a mean value of 20.1 ^oC; and wind speed ranged from 0 m/s to 9.0 m/s, with a mean value of 3.4 m/s. Figure 4.4

shows that differences of mass concentration varied only slightly with RH, wind speed, and ambient temperature, with Pearson correlation coefficients of -0.09, 0.20 and 0.09 respectively. There was a slight decrease of concentration difference with RH and an increasing trend of concentration with ambient temperature, as well as wind speed, as shown in Figure 4.4.

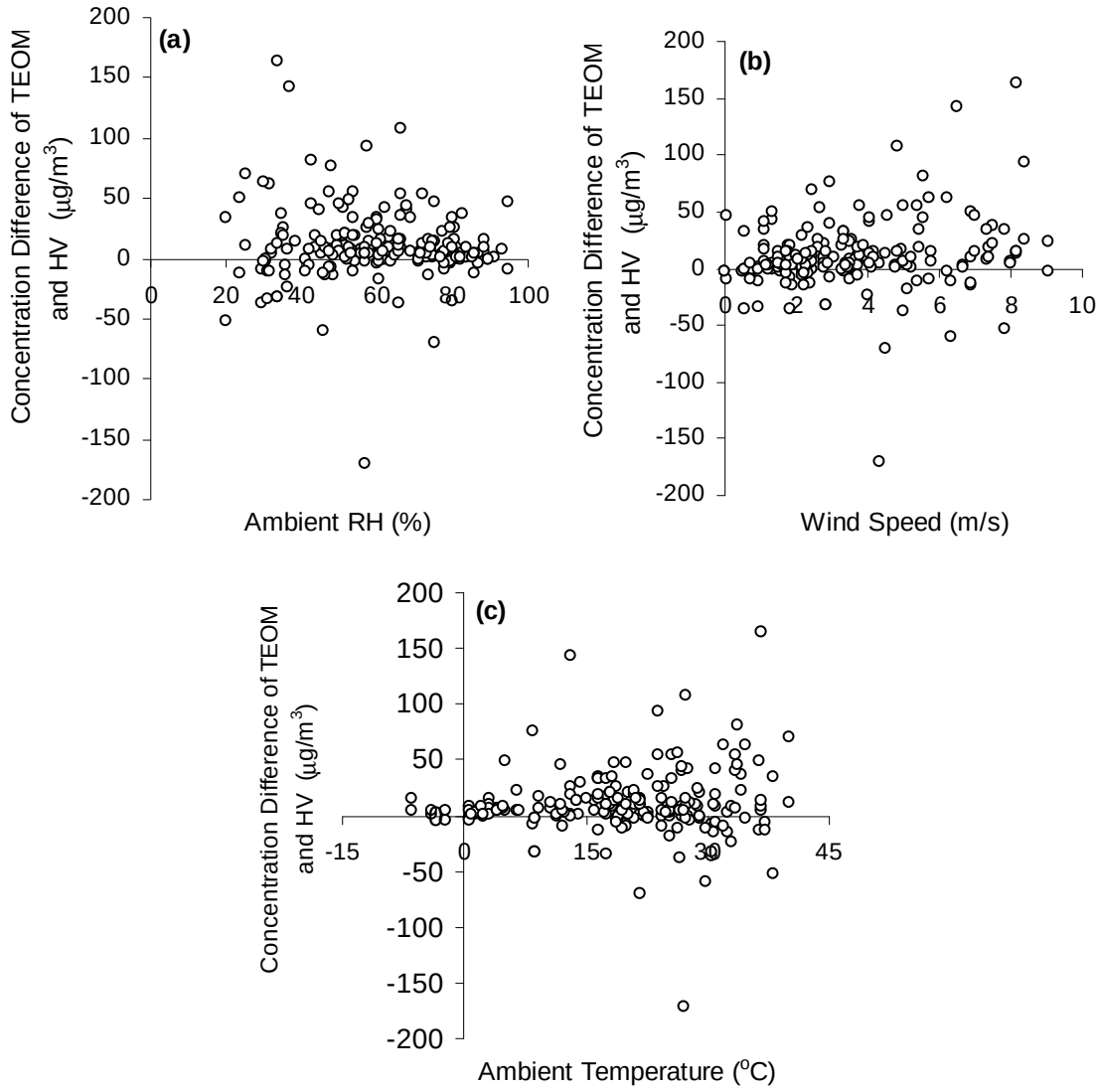

Figure 4.4 Effects of weather conditions on the difference of Tapered Element Oscillating Microbalance (TEOM) and high-volume (HV) PM_{10} mass concentrations: (a) ambient relative humidity (RH), (b) wind speed, and (c) ambient temperature.

The above results indicate that, in general, the TEOM PM_{10} samplers measured higher concentration by approximately 6% than the FRM HV PM_{10} sampler. Under similar conditions, such relationship can be used to correct for sampler bias. Sampler performance is affected by many factors, including sampler characteristics (e.g., sampler inlet design, operating principles), particle characteristics (e.g., shape, size distribution, chemical composition), and weather conditions (e.g., wind speed, temperature). Specific reasons to explain differences in measured concentrations between the TEOM and HV samplers are difficult to ascertain from this study. Previous researchers have observed both undersampling and oversampling by the TEOM compared with the gravimetric method. For example, Vega et al. (2003) measured ambient PM_{10} concentrations from five sites in Mexico City and observed that the TEOM measured larger PM_{10} concentrations than the gravimetric method. They attributed the larger TEOM PM_{10} concentration to re-entrainment of larger particles from the unclean TEOM PM_{10} sampler inlet. In this study, routine cleaning of the TEOM PM_{10} inlet was conducted during the sampling period; thus, the possibility of re-entrainment was reduced. Other researchers (e.g., Bulpitt and Price, 2006) have observed undersampling of the TEOM and attributed it to the loss of semi-volatile organic compounds and particle-bound water during sampling.

Chow et al. (2006) noted that particulate monitors have higher comparability when particles are chemically stable, small in size, and when the particles having diameters similar to the sampling inlet cut point are not dominant. Other researchers (Wang, et al., 2005; Wanjura, 2005; Buser et al., 2007) also reported that changes in particle size distribution and concentration of PM_{10} resulted in various oversampling and undersampling errors. In this study, the particle size distribution at the downwind sampling location was measured with two cascade impactors; the mean mass median diameter (MMD) was 12 µm, which was larger than the 10-µm cut point of the size-selective inlet. The larger MMD might have caused the TEOM PM_{10} sampler to measure higher values (Buser, et al., 2007) than the HV sampler. Note that collection efficiency of the PM_{10} samplers may be affected by the inlet cut point and velocity of impaction (McFarland, et al., 1984; Shaw et al., 1983). O'Shaughnessy et al. (2007) suggested that particle shape, density, and other physical factors have a greater effect on sampler bias than environmental factors.

4.4.3 Comparison of low-volume (LV) and high-volume (HV) PM_{10} samplers

As shown in Table 4.2, there were 190 and 63 pairs of mass concentrations measured by HV and LV samplers at KS1 and KS2, respectively. For KS1, maximum mass concentrations measured by HV and LV were 832 $\mu g/m^3$ and 393 $\mu g/m^3$; minimum values were less than 10 $\mu g/m^3$; and average values were 96 ± 9 $\mu g/m^3$ and 64 ± 5 $\mu g/m^3$, respectively. For KS2, maximum values were 612 $\mu g/m^3$ and 313 $\mu g/m^3$; minimum values were less than 10 $\mu g/m^3$; and average values were 68 ± 13 $\mu g/m^3$ and 52 ± 7 $\mu g/m^3$.

Concentrations measured by LV and HV samplers were highly correlated with Pearson correlations of 0.91 and 0.92 in the paired t-test for KS1 and KS2, respectively. Correlation was improved for sampling durations of 12 h or longer at KS1, which had a Pearson correlation of 0.97. Longer sampling duration seemed to improve correlation of the LV with the HV sampler. This was one reason why the sampling duration was increased from 2 h to 6 h to at least 12 h since August 2007. Figure 4.5 summarizes the relationship between the LV and HV samplers. A significant difference was observed with p-values less than 0.05 and low slopes of about 0.5 in the regression lines. Analysis also indicated that there was no significant difference in the correlation of mass concentration measured by LV and HV samplers between KS1 and KS2 ($P > 0.05$). Combined data measured by LV and HV samplers at KS1 and KS2 had a linear function with slope of 0.53 and R^2 value of 0.93 (Fig. 4.5c). Unlike the TEOM, which seemed to have the tendency to oversample compared with the HV sampler, the LV samplers tended to significantly undersample compared with the HV samplers.

The effects of sampling location and season on the performance of the LV and HV samplers are summarized in Tables 4.3 and 4.4, respectively. Regardless of sampling location and season, the LV samplers tended to undersample compared with the HV samplers. The difference in performance between the LV and HV samplers were affected by sampling location and season. For example, the degree of undersampling of the LV sampler compared with the HV sampler was greater in summer than in winter as indicated by the smaller regression coefficient in summer than in winter (0.49 vs. 0.90). Also, the degree of undersampling was greater for the north sampling location than for the south sampling location. Similar to the TEOM-HV sampler comparison, the difference in concentration between the LV and HV samplers were only slightly affected by weather conditions, including RH, wind speed, and temperature.

In general, the LV PM_{10} sampler showed much smaller concentration (by about 47%) compared with the HV PM_{10} sampler. Under similar conditions, such relationship could be used to account for sampler bias. Similar to the comparison between the TEOM and HV samplers, it is likely that the results were due to the interaction between inherent sampler characteristics and particle size distribution (Wang et al, 2005; Buser et al., 2007). It should be noted that the LV samplers were likely more prone to experimental errors than the HV samplers because of the small amounts of PM_{10} that were collected on the filters as a result of lower sampling flow rate (5 L/min). While there appears to have no guidelines on the lower concentration limit for PM_{10}, there is a guideline for $PM_{2.5}$ (U.S.EPA. 1998). Based on the guideline, the estimated amount of dust that must be collected on the filters is about 48 μg. In this study, approximately 86% out of 154 data points for the LV samplers collected on the north (downwind) location and 74% out of 152 data points collected on the south (upwind) location had mass values $\geq$ 48 μg.

It should also be noted that the HV PM_{10} sampler was used as the reference, primarily because it was a FRM sampler. The HV PM_{10} sampler has sampler bias in itself, as documented by several researchers (e.g., Buser et al., 2007), particularly if the particles being sampled are large. Clearly, there is a need to further evaluate the performance of the samplers considered in this study as affected by particle characteristics and operating conditions.

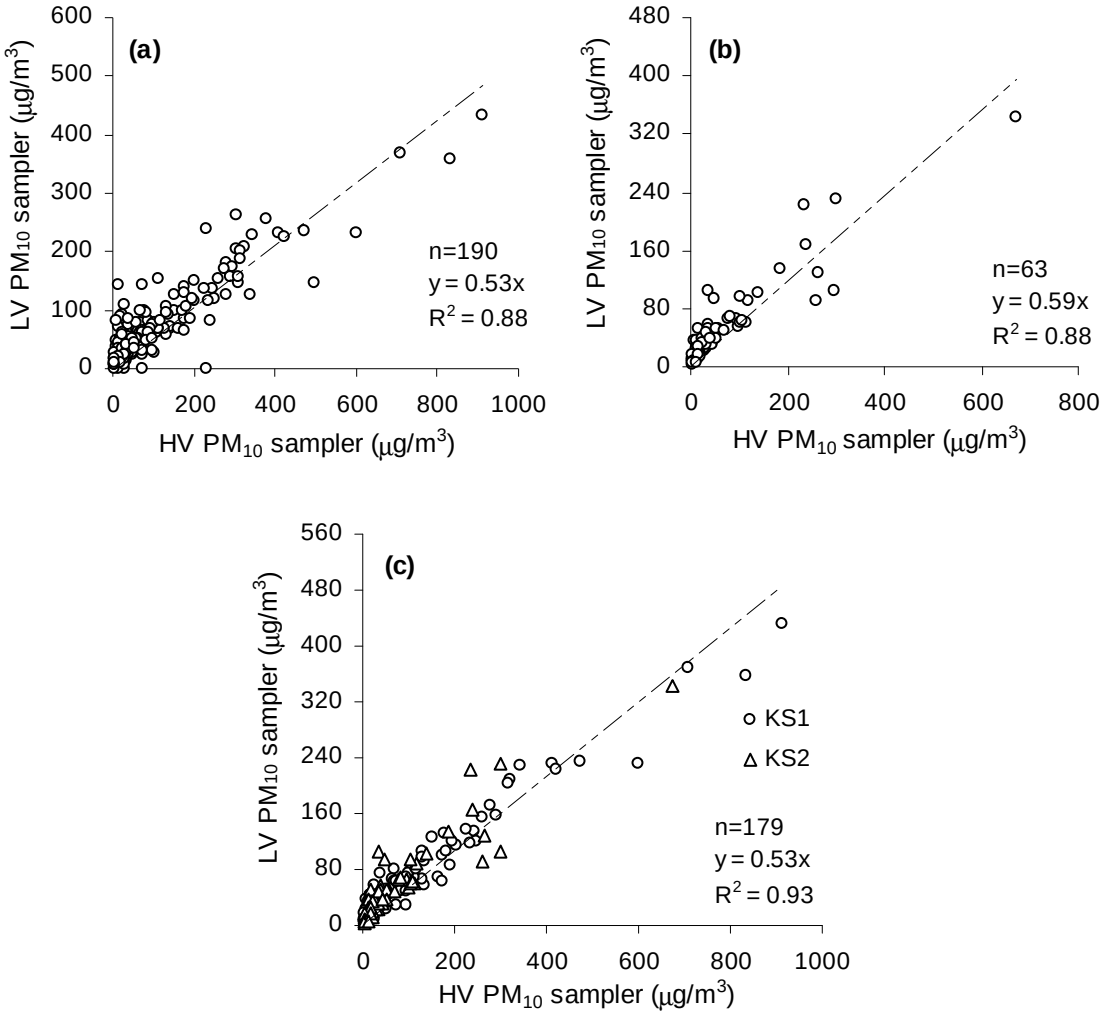

Figure 4.5 Comparison of high-volume (HV) and low-volume (LV) PM_{10} samplers: (a) for feedlot KS1, (b) for feedlot KS2, and (c) combination of KS1 and KS2 with sampling duration ≥ 12 h.

4.5 Conclusions

This research compared three types of PM_{10} samplers. The following conclusions were drawn:

- Collocated PM_{10} samplers showed similar trends but significant differences in concentrations.
- The TEOM PM_{10} sampler (a federal equivalent method sampler) had great correlation with the federal reference method high-volume PM_{10} sampler. In general, the TEOM tended to oversample PM_{10} (by approximately 6%) compared with the high-volume sampler.

- The low-volume PM_{10} sampler tended to undersample (by about 47%) compared with the high-volume sampler.
- Differences in PM_{10} concentration among samplers slightly decreased with an increase in relative humidity and decreased with an increase in wind speed and ambient temperature.

4.6 References

Allen, G., C. Sioutas, P. Koutrakis, R. Reiss, F.W. Lurmann, and P.T. Roberts.1997. Evaluation of the TEOM method for measurement of ambient particulate mass in urban areas. *J. Air Waste Manage. Assoc.* 47(6): 682-689.

Bulpitt, S., and M. Price. 2006. The composition of PM_{10} as collected by a conventional TEOM, a modified TEOM and a partisol gravimetric monitor at a kerbside site in the north east of England. *Environ. Monit. Assess.* 121(1-3): 479-489.

Buser, M.D., C.B. Parnell, B.W. Jr., Shaw, and R.E. Lacey. 2007. Particulate matter sampler errors due to the interaction of particle size and sampler performance characteristics: Ambient PM_{10} samplers. *Trans. ASABE* 50 (1):229-240.

Chow, J.C.1995. Measurement methods to determine compliance with ambient air-quality standards for suspended particles. *J. Air Waste Manage. Assoc.* 45(5): 320-328.

Chow, J.C., J.G. Watson, D.H. Lowenthal, L.A. Chen, R. J. Tropp, K. Park, and K.A. Magliano. 2006. $PM_{2.5}$ and PM_{10} mass measurements in California's San Joaquin Valley. *Aerosol Sci. and Technol.* 40(10): 796-810.

Cornbleet, P.J., and N. Gochman. 1979. Incorrect least-squares regression coefficients in method-comparison analysis. *Clin. Chem.* 25: 432-438.

Green, D., and G.W. Fuller. 2006. The implications of Tapered Element Oscillating Microbalance (TEOM) software configuration on particulate matter measurements in the UK and Europe. *Atmos. Environ.* 40(29): 5608-5611.

Jerez, S.B., Y. Zhang, J.W. McClure, L. Jacobson, A. Heber, S. Hoff, J. Koziel, and D. Beasley. 2006. Comparison of measured total suspended particulate matter concentrations using tapered element oscillating microbalance and a total suspended particulate sampler. *J. Air Waste Manage. Assoc.* 56(3): 261-270.

Knight, G., and E. Moore. 1987a. Comparison of dust samplers: statistical analysis techniques. *Am. Ind. Hyg. Assoc. J.* 48(4): 344-353.

Knight, G., and E. Moore. 1987b. Comparison of respirable dust samplers for use in hard rock mines. *Am. Ind. Hyg. Assoc. J.* 48(4): 354-368.

Krieger, U.K., S. Rupp, E. Hausammann, and T. Peter. 2007. Simultaneous measurements of PM_{10} and PM_1 using a single TEOM™. *Aerosol Sci. and Technol.* 41(11): 975-980.

Lee, J.H., P.K. Hopke, T.M. Holsen, and A.V. Polissar. 2005. Evaluation of continuous and filter-based methods for measuring $PM_{2.5}$ mass concentration. *Aerosol Sci. and Technol.* 39(4): 290-303.

Meyer, M.B., H. Patashnick, J.L. Ambs, and E. Rupprecht. 2000. Development of a sample equilibration system for the TEOM continuous PM monitor. *J. Air Waste Manage. Assoc.* 50(8): 1345-1349.

McFarland, A.R., C.A. Oritiz, and R.W. Bertch Jr. 1984. A 10µm cutpoint size-selective inlet for hi-vol samplers. *J. Air Pollut. Control Assoc,* 34(5): 544-547.

National Research Council (NRC). 2003. *Air emissions from animal feeding operations: current knowledge, future needs.* Washington, D.C.: The National Academies Press.

O'Shaughnessy, P.T., J. Lo, V. Golla, J. Nakatsu, M.I. Tillery, and S. Reynolds. 2007. Correction of sampler-to-sampler comparisons based on aerosol size distribution. *J. Occup. Environ. Hyg.* 4(4): 237-245.

Predicala, B.Z., and R.G. Maghirang, 2003. Field comparison of inhalable and total dust samplers for assessing airborne dust in swine confinement barns. *Appl. Occup. Environ. Hyg.* 18(9); 694-701.

Purdy, C.W., R.N. Clark, and D.C. Straus. 2007. Analysis of aerosolized particulates of feedyards located in the southern high plains of Texas. *Aerosol Sci. and Technol.* 41(5): 497-509.

Purdy, C.W., D.C. Straus, D.B Parker, S.C. Wilson, and R.N. Clark. 2004. Comparison of the type and number of microorganisms and concentration of endotoxin in the air of feedyards in the Southern High Plains. *Am. J. Vet. Res.* 65(1): 45-52.

Rupprecht & Patashnick Co, Inc., 2004a. Operating manual, Mini-Partisol model 2100 air sampler, Revision B. Franklin, Mass.: Thermo Fisher Scientific.

Rupprecht & Patashnick Co, Inc., 2004b. Operating manual, TEOM series 1400a ambient particulate (PM-10) monitor air sampler, Revision B. Franklin, Mass.: Thermo Fisher Scientific.

Salter, L.F., and B. Parsons. 1999. Field trials of the TEOM and partisol for PM_{10} monitoring in the ST Austell china clay area, Cornwall, UK. *Atmos. Environ.* 33(13): 2111-2114.

Seaton, A., W. MacNee, K. Donaldson, and D. Godden. 1995. Particulate air pollution and acute health-effects. *Lancet* 345(8943):176-178.

Shaw, R.W., R.K. Stevens, C.W. Lewis, and J.H. Chance. 1983. Comparison of aerosol sampler inlets. *Aerosol Sci. and Technol.* 2: 53-67.

Thermo Electron Corporation. 2003. Instruction manual, high volume PM_{10} air sampler, P/N 100042-00. Franklin, Mass.: Thermo Fisher Scientific.

U.S. EPA. 1987. 40CFR50, Revisions to the National ambient air quality standards for particulate matter and appendix J--reference method for the determination of particulate matter as PM_{10} in the atmosphere. Federal Reg. 50(126): 24364, 24664-24669.

U.S. EPA. 1998. Monitoring PM2.5 in ambient air using designated reference or class I equivalent methods. Quality Assurance Guidance Document2.12. Research Triangle Park, N.C.: National Center for Environmental Assessment, U.S. Environmental Protection Agency.

U.S. EPA. 2004. Air quality criteria for particulate matter. EPA/600/P-99/002aF. Research Triangle Park, N.C.: National Center for Environmental Assessment, U.S. Environmental Protection Agency.

U.S. EPA. 2006. National primary and secondary ambient air quality standards- final rule. 40 CFR, part 50, Federal Register, Vol.71, No. 200. Available at: http://www.epa.gov/ttnnaaqs/standards/pm/data/fr20061017.pdf. Accessed 10 November 2010.

Vega, E., E. Reyes, A. Wellens, G. Sanchez, J.C. Chow, and J.G. Watson. 2003. Comparison of continuous and filter based mass measurements in Mexico City. *Atmos. Environ.* 37(20): 2783-2793.

Wang, L., J.D. Wanjura, C.B. Parnell, R.E. Lacy, and B.W. Shaw. 2005. Performance characteristics of a low-volume PM_{10} sampler. *Trans. ASABE* 48 (2): 739-748.

Wanjura, J.D. 2005. Engineering approaches to address errors in measured and predicted particulate matter concentrations. MS thesis. College Station, Tex.: Texas A&M University.

CHAPTER 5 - Laboratory Evaluation of Dust Control Effectiveness of Pen Surface Treatments for Cattle Feedlots

5.1 Abstract

Emission of particulate matter (PM) is one of the major air-quality concerns for large beef cattle feedlots. Effective treatments on the uncompacted soil and manure mixture of the pen surface may help in reducing PM emission from the feedlots. A laboratory apparatus was developed for measuring dust emission potential of cattle feedlot surfaces as affected by surface treatments. The apparatus was equipped with a simulated pen surface, four mock cattle hooves, and samplers for PM with equivalent aerodynamic diameter of 10 µm or less (PM_{10}). The simulated pen surface had a layer of dry, loose feedlot manure with a compacted soil layer underneath. Mock hooves were moved horizontally on the manure layer to simulate the horizontal action of cattle hooves on the pen surface. High-volume PM_{10} samplers were used to collect emitted dust. Effects of hoof speed, depth of penetration, and surface treatments with independent candidate materials (i.e., sawdust, wheat straw, hay, rubber mulch, and surface water application) on PM_{10} emission potential of the manure layer were investigated. Results showed that PM_{10} emission potential increased with increasing depth of penetration and hoof speed. Of the surface treatments evaluated, application of water (6.4 mm) and hay (723 g/m^2) exhibited the greatest percentage reduction in PM_{10} emission potential (69% and 77%, respectively) compared with the untreated manure layer. This study indicated application of hay or other mulch materials on the pen surface might be good alternative methods to control dust emission from cattle feedlots.

5.2 Introduction

Emission of particulate matter (PM) is one of the major environmental challenges for large open cattle feedlots. The pen surface is a major source of PM emission from cattle feedlots; other sources include unpaved roads and feed processing areas (Auvermann et al., 2006; Razote et al., 2007). Factors that influence PM emissions from pen surfaces include pen surface characteristics [i.e., water content (WC); presence of loose, uncompacted manure layer], degree

of cattle activity, pen cleaning and other activities in the feedlot such as pen cleaning, and weather conditions. Of the above factors, the WC of the pen surface is probably one of the most important (Miller and Woodbury, 2003). Field studies have shown that dust concentrations downwind of feedlots decreased with increasing pen surface WC (Razote et al., 2007; Sweeten et al., 1988). According to Sweeten et al. (1988), the WC of the pen surface should be in the range of 26% to 31% and 35% to 41% for loose surface manure and less than 25-mm deep manure, respectively, for controlling the dust to limits of 150 and 260 $\mu g/m^3$ for total suspended particulates (TSP). These TSP limits were based on the national ambient air quality standards (NAAQS) during the 1980s. Other researchers have also suggested that the pen surface WC should be maintained at 25% to 35 % on the basis of odor and dust control as well as economy of treatment (Auvermann et al., 2006; DPI&F, 2003). From laboratory experiments, Miller and Woodbury (2003) also concluded that pen surface WC and organic matter content are key factors that contribute to dust emission from pen surfaces.

The following methods for controlling PM emissions from cattle feedlots have been investigated or recommended: pen surface sprinkling, frequent pen scraping, stocking density manipulation, and topical application of crop residues (Bonifacio et al., 2011; Razote et al., 2006; Auvermann, 2003; Romanillos, 2000; Sweeten, 1979; Carroll et al., 1974). Pen surface sprinkling is one of the most common ways of controlling dust. Previous research (e.g., Carroll et al., 1974; Bonifacio et al., 2011) reported mean PM_{10} control efficiencies ranging from 32% to 80% for sprinkler systems for cattle feedlot. However, sprinkler system is costly in installation and operation, and both of water and energy resources; it also requires frequent application of water, while water limits exist in many regions (Harner et al., 2008; Pimentel et al., 1997). Frequent pen scraping can be used to remove the loose manure that contributes to dust emission (Auvermann et al., 2006; Davis et al., 2004). Stocking density (i.e., number of animals per unit of pen area) may be adjusted to compensate for increases in net evaporative demand, shifting the moisture balance in favor of PM control. Effectiveness of increased stocking density, however, is likely to decrease as daily net evaporation increases; it may also induce behavioral problems and reduce overall feed-to-gain performance (Rahman et al., 2008; Auvermann et al., 2006; Mitloehner, 2000). Another potential method for reducing emission is topical application of crop residues and other materials on the pen surface to enhance its moisture holding capacity and reduce evaporative loss; the presence of crop residues may also lower the effect of hoof's

shearing action by serving as cushion (Auvermann et al., 2006; Razote et al., 2006; Davis et al., 2004).

Research is needed to evaluate the effectiveness of surface treatments and other methods in controlling PM emission rate. Auvermann (2003) and Razote et al. (2006) have developed experimental chambers for measuring PM emission potential of pen surfaces. The chambers were based on the vertical action of cattle hooves on the pen surface. Results indicated that the impact energy of cattle hooves affected the PM_{10} emission potential more than the depth of the manure layer (Razote et al., 2006). However, the mode of hoof action on the pen surface has both vertical and horizontal components. Future investigation is need for the emissions associated with the horizontal component of hoof action on the pen surface (Razote et al., 2006; Auvermann, 2003).

As an extension of the work by Razote et al. (2006), which was based on the vertical action of cattle hooves on the pen surface, this research considered the horizontal shearing action of cattle hooves on the pen surface. The objectives of this study were to (1) develop a repeatable laboratory method, based on the horizontal component of hoof action on a pen surface, for measuring the PM_{10} emission potential of pen surfaces; and (2) compare the relative effectiveness of surface treatments in reducing PM_{10} emission potential.

5.3 Materials and Methods

5.3.1 Test chamber

The laboratory apparatus was developed based on the weight-drop test chamber that was developed by Razote et al. (2006). Figure 5.1 shows a schematic diagram of the apparatus. It had a 3.7-m-long bench-top enclosure with a 0.61 m × 0.61 m cross section, mounted over a simulated feedlot pen surface, four mock cattle hooves, and samplers for PM_{10}. The simulated feedlot pen surface had a layer of loose, dry manure (0.51 m × 0.41 m × 0.1 m) with a compacted base soil (0.51 m × 0.81 m × 0.91 m) underneath. The four mock hooves (dried cattle hooves) had an average height, length and width of 9.3 ± 0.3 cm, 9.9 ± 0.2 cm, and 8.9 ± 0.1 cm, respectively (Fig. 5.2c). They were moved horizontally over a distance of 0.24 m on the manure layer through a compressed air hydraulic cylinder that was mounted on the apparatus. By changing valve settings in the cylinder (Fig. 5.2), the speed of the hooves was controlled. The

force exerted by the hooves on the manure layer was measured using a pre-calibrated load cell that was connected to the back of the hydraulic cylinder (Fig. 5.2a).

The chamber was equipped with five high-volume PM_{10} samplers (Model 1200, Thermo Electron, Atlanta, GA). One PM_{10} sampler was placed at the inlet side of the chamber to account for the background PM_{10} concentration; four PM_{10} samplers were connected to the outlet end of the chamber to collect the PM_{10} that were emitted as the hooves moved through the simulated pen surface (Fig. 5.1).

The manure sample used in the test chamber was taken from a feedlot and was dried and sieved to remove the large clods. Standard laboratory analysis of this sample at the Kansas State University Soil Testing Laboratory indicated an organic matter content of approximately 8%, based on the total carbon content, and sand, silt, and clay contents of 66%, 12%, and 22%, respectively.

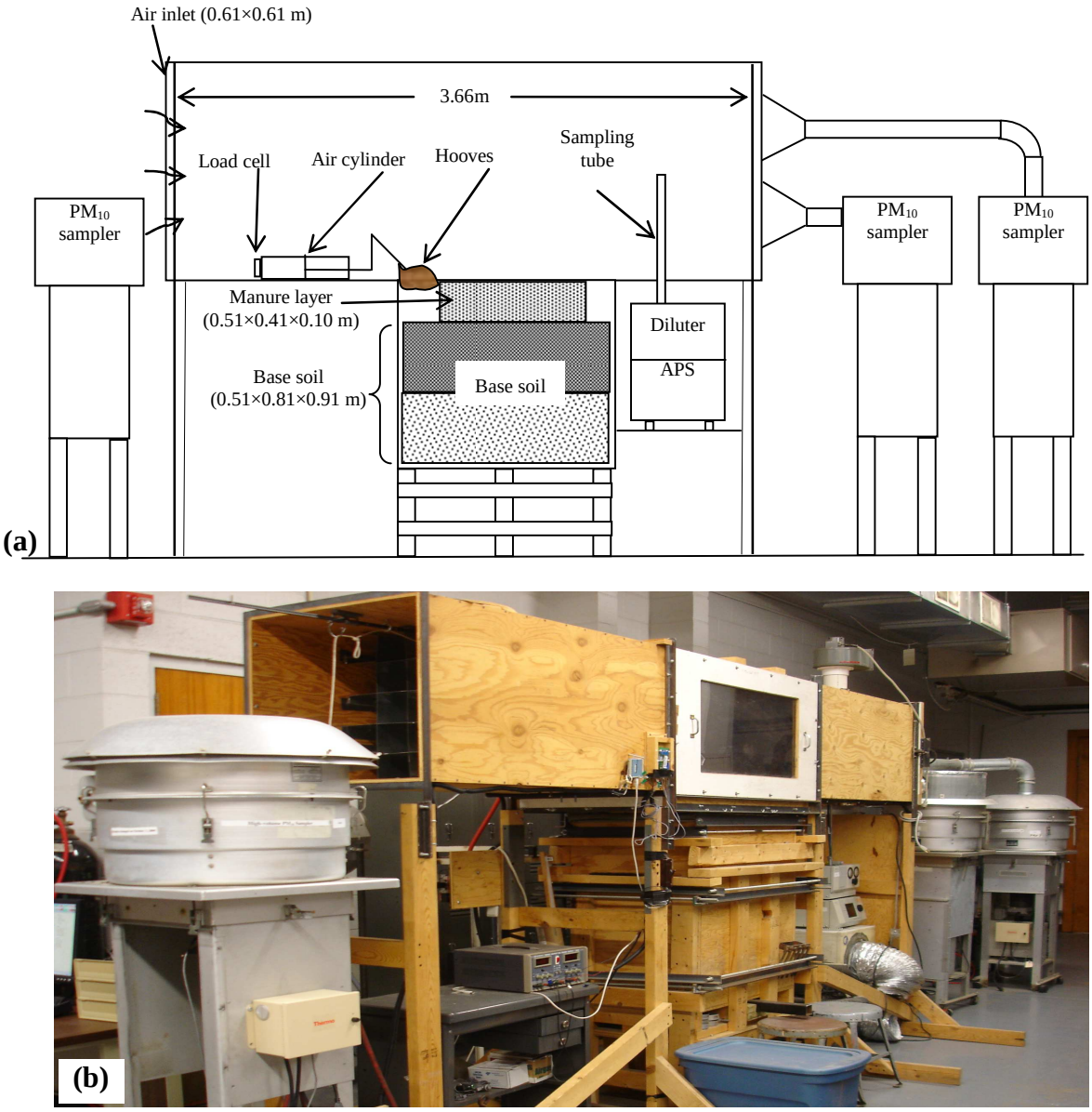

Figure 5.1 Laboratory apparatus: (a) schematic diagram (not drawn to scale) and (b) photograph.

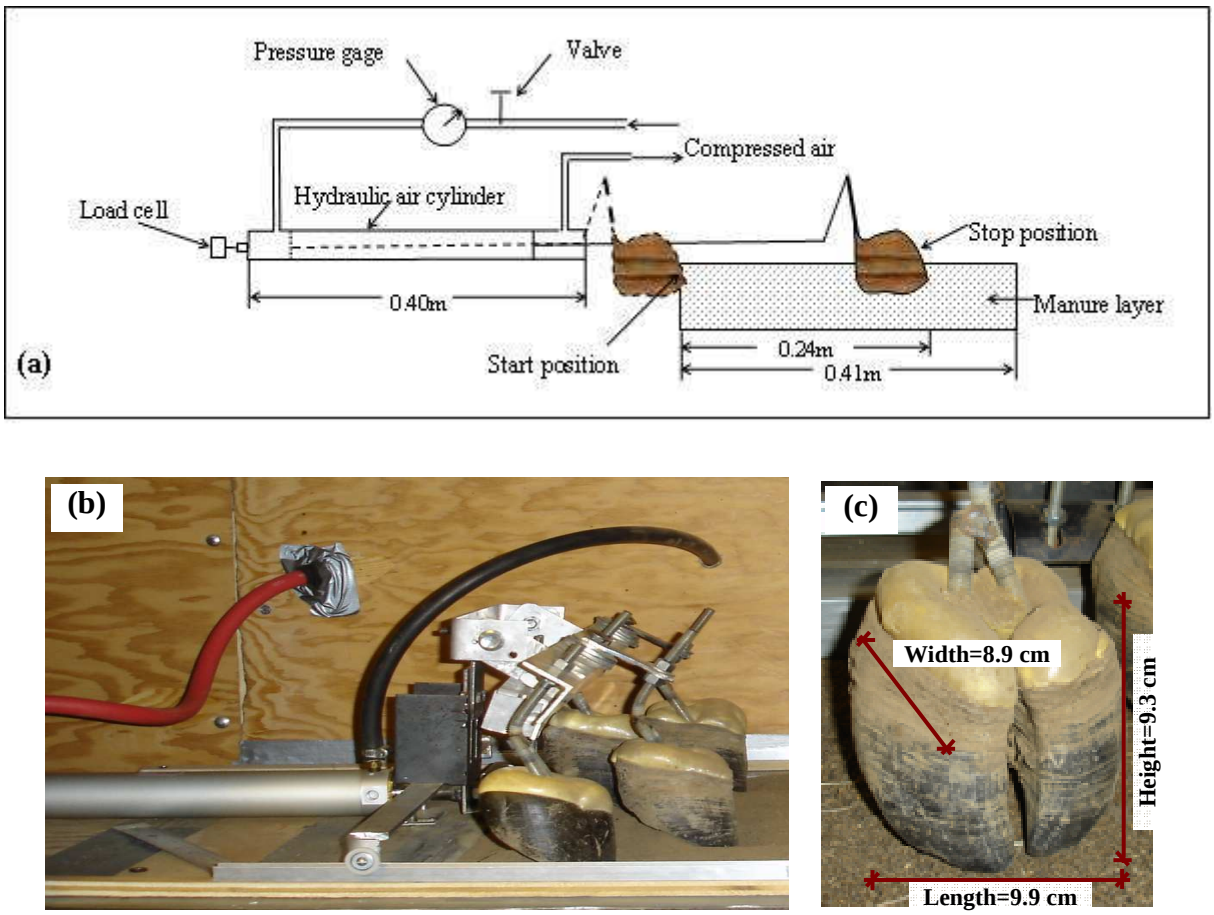

Figure 5.2 Hoof action system: (a) schematic diagram (not drawn to scale), (b) photograph of the hoof action system, and (c) photograph of a hoof showing average dimensions.

5.3.2 Experiments

This study first investigated effects of hoof speed and depth of penetration on the PM_{10} emission potential of the simulated pen surface. Three levels of hoof speed [i.e., high (0.57 ± 0.01 m/s), medium (0.29 ± 0.01 m/s), and low (0.25 ± 0.01 m/s)] and three levels of depth of penetration (i.e., 1.3, 2.5, and 5.1 cm) were considered (Table 5.1). Each treatment combination of hoof speed and depth of penetration had three replicates. The WC of the manure layer and those of the materials applied on the simulated pen surface were determined by using the ASTM D 2216-98 oven-drying method (ASTM, 2002). The mean WC of the loose manure layer, as measured by the oven-drying method, was 8.1 % wet basis (w.b.), ranging from 7.3% to 9.4% w.b. (Table 5.1). From these tests, the combination of hoof speed and depth of penetration that

resulted in the highest PM_{10} emission potential was identified and used in the second set of experiments.

Table 5.1 Experimental parameters.

Test	Factors Investigated	Speed Setting[†]	Depth of Hoof Penetration (cm)	Amount of Material Applied on the Simulated Pen Surface	Water Content of the Manure Layer (% wet basis)
1	Speed and Depth of penetration	Low	1.3, 2.5, 5.1	0	8.1
		Medium	1.3, 2.5, 5.1	0	8.1
		High	1.3, 2.5, 5.1	0	8.1
2	Surface treatments[‡]:				
	Wheat straw	High	5.1	0, 241, 482, 723 g/m^2	7.6
	Sawdust	High	5.1	0, 241, 482, 723 g/m^2	7.3
	Hay	High	5.1	0, 241, 482, 723 g/m^2	7.5
	Rubber mulch	High	5.1	0, 1415, 2834, 4253, 9217 g/m^2	9.6
	Water	High	5.1	3.2, 6.4 mm	9.5

[†] Speed settings: high – 0.57(± 0.01) m/s, medium – 0.29(± 0.01) m/s, and low – 0.25(± 0.01) m/s.

[‡] For wheat straw and hay, the average lengths were 163 (50 to 300) mm and 210 (50 to 310) mm, the average widths were 3.7 (1.4 to 9.3) mm and 1.7 (0.7 to 5.2) mm, and the average thicknesses were 0.7 (0.2 to 1.9) mm and 0.4 (0.2 to 0.8) mm; Sawdust had a geometric mean diameter (GMD) of 3.2 mm and geometric standard deviation (GSD) of 1.4; rubber mulch had a GMD of 8.7 mm and GSD of 1.8.

In the second set of experiments, the effectiveness of surface treatments with independent candidate materials in controlling PM_{10} emission potential was evaluated (Table 5.1; Fig. 5.3). Mulches are well known as protective cover to retain moisture and reduce erosion. Organic residues, including unprocessed wheat straw, sawdust, and unprocessed hay were applied on the pen surface in this study since they can act as a composting system (Chalker-Scott, 2008) together with soil/manure; the rubber mulch (made of recycled tires) was also used in this study because it is permanent, stable, and safe (Chalker-Scott, 2010). The minimum amounts of mulches applied in this study were pre-determined to roughly cover the surface of the manure layer. The amounts were then increased to fully cover the surface of manure layer. The amounts

of wheat straw (WC=7.6% w.b.; bulk density=9.3 kg/m^3), sawdust (WC=6.8% w.b.; bulk density=77 kg/m^3), and hay (WC=8.3% w.b.; bulk density=6.6 kg/m^3) were 241, 482, and 723 g/m^2, respectively. Corresponding thicknesses were approximately 3, 5, and 7 cm for wheat straw, 0.5, 0.7, and 1 cm for sawdust and 4, 7, and 10 cm for hay. For the rubber mulch (bulk density=350 kg/m^3), which was much heavier compared to the other materials, amounts were 1,415, 2,834, 4,253, and 9,217 g/m^2 and corresponding thicknesses were approximately 0.7, 1.3, 2, and 3 cm. These materials were uniformly placed on the surface of the manure layer. In this study, water application treatment was also evaluated and compared with the performance of the mulches. Predetermined amounts of water (about 380 mL and 720 mL) were applied uniformly on the manure layer with a manual sprayer. The wetted surface was allowed to stand for 30 min after sprinkling to allow the applied water to gradually infiltrate into the manure layer at 3.2 and 6.4 mm, similar to typical water application rates in commercial feedlots.

An untreated dry manure sample (i.e., with no candidate abatement materials applied on the surface) served as the control. All tests used the high-speed setting and 5.1-cm-depth of hoof penetration into the manure layer, since this combination resulted in the highest PM_{10} emission potential from the first set of experiments. Each surface treatment consisted of three replications. After each test, the manure layer and material applied on the surface were removed and replaced with new samples.

Figure 5.3 Surface treatment with (a) wheat straw, (b) sawdust, (c) hay, (d) rubber mulch, and (e) water application.

5.3.3 Particulate sampling

Each PM_{10} sampler was operated at a sampling flow rate of 1.13 m^3/min. The combined flow rates of the four samplers generated airflow within the chamber that was equivalent to approximately 0.22 m/s average wind speed, as measured by an omnidirectional probe (model 8475, TSI, Inc., Shoreview, MI) (Razote et al., 2006). The samplers were operated for 11 min, after which, the filters were immediately removed and placed in the conditioning chamber.

Filters in the PM_{10} samplers were 20 cm × 25 cm, type A/E, glass-fibers (Gelman Sciences, Ann Arbor, MI). They were conditioned in a conditioning chamber (25 ^{o}C, 40% relative humidity) for 24 h before weighing (for both pre-sampling and post-sampling weights) to minimize the humidity effect on filter weights. The PM_{10} emission potential (in mg) was determined as the mass difference between the PM_{10} collected on the four downstream samplers and that collected on the upstream sampler. The room air temperature and atmospheric pressure were measured during all the tests. The temperature ranged from 20°C to 27°C with an average of 24°C; the pressure ranged from 0.95 atm to 1 atm with an average of 0.97 atm.

For tests involving hay (which proved to have the highest reduction in emission potential), an Aerodynamic Particle Sizer (APS) Spectrometer (model 3021, TSI, Inc., St. Paul, MN) with a diluter (model 3302A, TSI, Inc., St. Paul, MN) was used to measure particle size distribution at the center of the chamber. The APS measures particle size distribution from 0.5 to 20 µm by determining the time-of-flight of individual particles in an accelerating flow field (Volckens and Peters, 2005). The APS was operated continuously during each test at a sampling flow rate of 5 L/min and averaging time of 20 s.

5.3.4 Force measurement

A pre-calibrated load cell as shown in Figure 5.2a was used to measure the force of hooves exerted on the manure layer. The total force (F_1) exerted on the simulated pen surface was recorded for each replicate. To determine the track resistance, the force (F_0) without any manure layer was measured prior to start of each test. The force (F) that the hooves exerted on the manure layer was considered as the difference between F_1 and F_0 (i.e., $F=F_1-F_0$).

5.3.5 Data analysis

PM_{10} emission potential (in mg) for each replicate was determined as the mass difference between PM_{10} collected on the four downstream high-volume PM_{10} samplers and that collected on the upstream PM_{10} sampler. For particle size distribution, geometric mean diameter (GMD) and geometric standard deviation (GSD), as well as the mass concentration for different size ranges, were determined from the APS data. Density of particles used for the APS was 1.8 g/cm^3, based on measurements with a multipycnometer (Quantachrome Instruments, Boynton Beach, FL). Analysis of Variance (ANOVA), the General Linear Model procedure, and Tukey multiple comparisons test in SAS (SAS v9.1, Cary, NC) were used in analyzing PM_{10} emission potential, GMD, and GSD at the 5% level of significance (SAS, 1990).

5.4 Results

5.4.1 Effects of speed and depth of penetration

For each speed setting, in general, the emission potential increased significantly ($P<0.05$) with increasing depth of penetration (Table 5.2), except for the low speed setting in which the 2.5-cm and 5.1-cm depth were not significantly different ($P>0.05$). These results suggest that the depth of penetration of the hooves, greatly affected the PM_{10} emission potential associated with the horizontal component of hoof action on the pen surface. As the depth of hoof penetration on the loose manure surface increased, there is an increase in the amount of soil/manure in contact with the moving hoof resulting in more soil/manure moved and more particles suspended in the air.

For each depth of penetration, the emission potential generally increased with increasing hoof speed (Table 5.2). The faster the hoof speed, the higher the energy exerted by the hoof on the soil/manure layer causing particles to be displaced at greater distances. This greater movement of the soil/manure layer caused larger particles to be displaced and smaller particles suspended in the air. The highest PM_{10} emission potential (48.7 mg) was observed at the high speed setting and deepest penetration (5.1 cm); this was about 14 times the smallest emission potential (3.4 mg), which was observed for the case involving the low speed setting and shallowest depth of penetration (1.3 cm).

Table 5.2 Effects of hoof speed and depth of penetration into the manure layer on PM_{10} emission potential of the simulated pen surface [†,‡].

Depth of Hoof Penetration into the Manure Layer (cm)	PM_{10} Emission Potential (mg) *					
	High Speed (m/s)		Medium Speed (m/s)		Low Speed (m/s)	
	Mean	SE [#]	Mean	SE [#]	Mean	SE [#]
1.3	11.28 Aa	1.08	6.44 Ba	0.98	3.36 Ca	0.47
2.5	26.87 Ab	3.38	9.96 Bb	0.50	8.82 Cb	0.77
5.1	48.68 Ac	3.85	26.31 Bc	2.55	8.61 Cb	1.02

[†]Each data point is the average of three replicates.

[‡]For the same hoof speed, mean values with the same lower case letters are not significantly different at the 5% level; for the same depth of hoof penetration into the manure layer, mean values with the same upper case letters are not significantly different at the 5% level.

[#] SE represents standard error.

*Amount of PM_{10} suspended in the air with one stroke of hoof movement on a pen surface of 0.51 m × 0.41 m × 0.1 m.

Forces exerted on the manure layer by the hooves were affected by the depth of penetration and hoof speed as shown in Figure 5.4. The depth of hoof penetration had greater effects on the force, since there were significant differences in forces at all levels of depth. The force increased with increasing depth of penetration. Significant differences in force were observed between low speed and medium speed as well as high speed ($P<0.05$), while there was no significant difference in force between the medium and high speed setting ($P>0.05$). The power exerted by the hooves on the manure layer, product of force and speed, was also positively correlated with the PM_{10} emission potential with R^2 of 0.90 as shown in Figure 5.5.

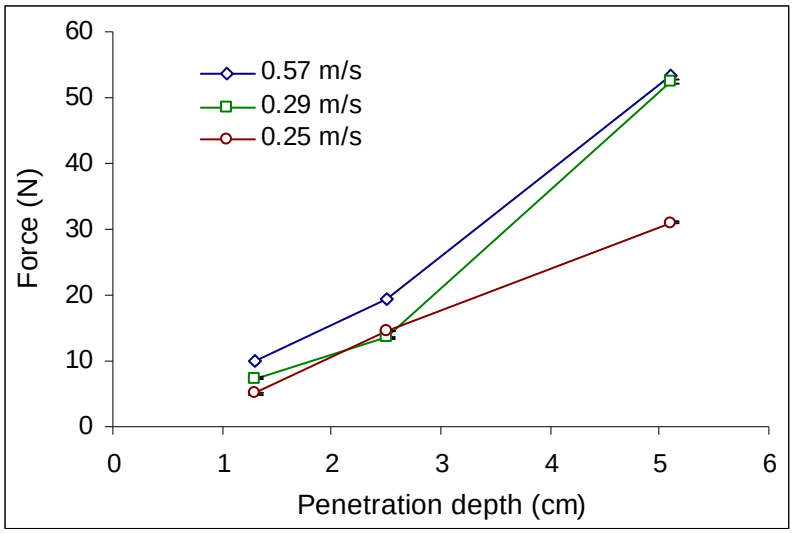

Figure 5.4 Mean force of hooves on the simulated pen surface as affected by hoof speed and depth of penetration. Each data point is the average of three replicates; error bars represent standard error.

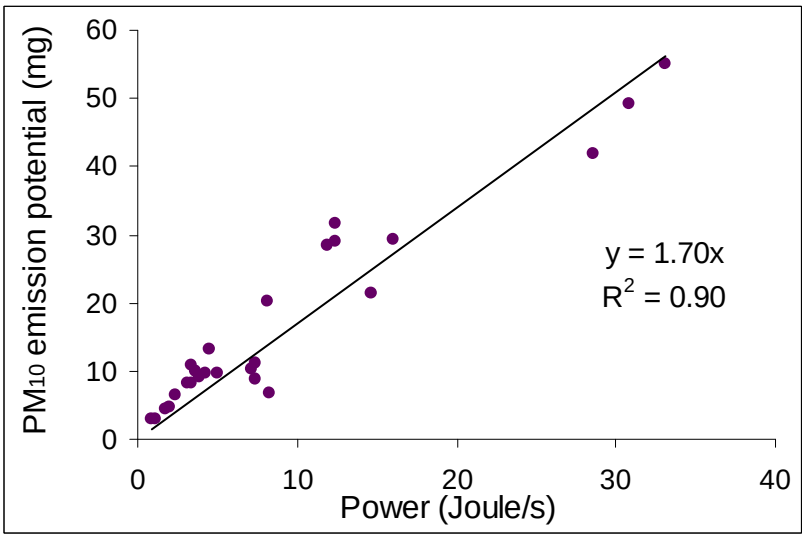

Figure 5.5 Mean PM_{10} emission potential of the simulated pen surface as affected by hoof power.

Results obtained above indicate that PM_{10} emission potential could be closely related with cattle live weight and degree of activity. Energetic actions of cattle on the loose manure layer may cause high PM_{10} emission. With the same speed of movement on a loose manure layer, heavier cattle may cause higher PM_{10} emission compared with light-weight cattle. Consequently, the type and age of cattle may be considered in dust control strategies, and control methods may focus on (1) frequent scraping of the pen surface to reduce the depth of loose

manure layer in contact with cattle hooves and/or (2) reducing cattle activity, especially during late afternoon hours when cattle tends to be more active.

5.4.2 Surface treatments

Compared with the control (i.e., untreated manure layer), application of wheat straw, sawdust, and hay significantly reduced the PM_{10} emission potential of the manure layer (Table 5.3), except for wheat straw and sawdust when applied at the smallest amount (i.e., 241 g/m^2). Also, the PM_{10} emission potential decreased with increasing amount of material applied on the manure layer, except for sawdust which had lower PM_{10} emission potential (25.6 mg) when applied at 723 g/m^2 compared with that (30.5 mg) applied at 482 g/m^2. In general, application of hay on the manure layer resulted in the smallest PM_{10} emission potential, although it was not significantly different from that of sawdust at the 241 and 482 g/m^2 levels. Also, there was no significant difference between straw and sawdust ($P>0.05$) in the PM_{10} emission potential of the manure layer. Of all cases, application of hay at the highest amount (i.e., 723 g/m^2) resulted in the smallest PM_{10} emission potential of the manure layer – this reduction was equivalent to a mean percentage reduction in PM_{10} emission potential of 77%.

Table 5.3 Effect of surface treatments (wheat straw, sawdust, hay) on PM_{10} emission potential of the simulated pen surface[†, ‡].

Amount	**Wheat straw**		**Sawdust**		**Hay**	
(g/m^2)	Mean	SE[*]	Mean	SE[*]	Mean	SE[*]
0	43.3 A a	6.0	43.3 A a	6.0	48.7 A a	3.8
241	39.4 A ab	1.1	37.3 AB ab	9.8	25.5 B b	0.1
482	30.7 A bc	3.1	25.6 AB b	1.4	18.3 B bc	2.1
723	23.6 A c	1.8	30.5 A b	2.2	11.1 B c	0.2

[†]Emission tests were done with hoof speed at high level and depth of penetration of 5.1cm. Each data point is the average of three replicates.

[‡] For the same amount of material applied on the surface, mean values with the same upper case letters are not significantly different at the 5% level; for the same type of material applied on the surface, mean values with the same lower case letters are not significantly different at the 5% level.

For tests involving application of rubber mulch on the simulated surface, results showed no significant reduction in PM_{10} emission potential of the surface (Table 5.4). This might be due to the size and weight of the rubber mulch; as the hooves moved, the rubber mulch was displaced along with the manure layer and did not provide an effective barrier in capturing the emitted dust. The extra movement of the materials might have caused additional dust to be generated resulting in higher emission compared with the control. In addition, the manure layer used for the tests involving the rubber mulch was taken from a batch of soil/manure sample different from the one used in other tests. Compared to the untreated or control for the other surface treatments, the untreated soil/manure layer (i.e., control) for the rubber mulch tests had relatively low PM_{10} emission potential (17.5 mg), which could have also affected the effectiveness of rubber mulch. Consequently, another set of tests for hay was conducted with the soil/manure sample the same as that used for rubber mulch. The reductions in PM_{10} emission potential at 241 g/m^2, 482 g/m^2, and 723 g/m^2 levels were 55%, 56%, and 64%, respectively. These values were close to those from the first set of tests involving hay.

As expected, application of water decreased the emission potential of the soil/manure layer (Table 5.4). Also, the higher the amount of water applied, the greater was the reduction in PM_{10} emission potential. Application of 6.4 mm of water resulted in a mean percentage reduction in PM_{10} emission potential of 69%.

Table 5.4 Effects of application of rubber mulch and water on PM_{10} emission potential of the simulated pen surface [†, ‡].

Treatment	Amount applied on the surface	PM_{10} Emission Potential (mg) *	
		Mean	SE
Rubber mulch	0 g/m^2	17.5 a	1.2
	1415 g/m^2	16.3 a	2.7
	2834 g/m^2	18.5 a	2.2
	4253 g/m^2	15.5 a	1.3
	9217 g/m^2	13.5 a	0.9
Water	0 mm	37.7 b	2.3
	3.2 mm	22.0 c	2.1
	6.4 mm	11.7 d	2.2

[†] Emission tests were done with hoof speed at high level and depth of penetration of 5.1cm. Each data point is the average of three replicates.

[‡] For each treatment, column means with the same letter are not significantly different at the 5% significant level.

*Amount of PM_{10} suspended in the air with one stroke of hoof movement on a pen surface of 0.51 m × 0.41 m × 0.1 m.

Maximum reductions in PM_{10} emission potential using wheat straw, sawdust, and water were 46% (with amount applied of 723 g/m^2), 41% (with amount applied of 482 g/m^2), and 69% (with 6.4 mm penetration into the manure layer), respectively. The maximum reduction in PM_{10} emission potential with application of rubber mulch was only 23% (with amount applied of 9217 g/m^2). Generally, from among the candidate abatement materials tested, hay reduced PM_{10} emission potential better than all other materials at all application rates. Reduction in PM_{10} emission potential with application of hay (48% to 77%) was comparable to that of water sprinkling (42% and 69% for 3.2 mm and 6.4 mm of water applied, respectively).

Hay had greater effectiveness in reducing PM_{10} emission compared with other materials in this study, because hay had long fibers that were interlocked to each other forming a continuous blanket on top of the manure layer. When the mock hooves moved horizontally through the layer, they displaced the manure layer in their paths forming valley ridges on both sides and in front of the hooves. Even after the hooves have moved through the hay and manure layer, the fibers were held together and still covered the surface of the manure layer including the

ridges, capturing most of the dust generated. Although wheat straw had long fiber, the fibers were thicker than those of hay and did not interlock. Therefore, for the same amount applied on the surface, wheat straw had relatively less flatter and had less surface area than hay, resulting in less effective capture of particles. Sawdust and rubber did not provide effective barriers to capture dust particles. Although, at the highest application rate they both totally covered the surface, they were both loose and easily displaced and mixed with the loose manure layer by the moving hooves, lowering their effectiveness in reducing PM_{10} emission potential. In addition, the extra movement of the heavier rubber when displaced by the hooves may cause regeneration of dust.

The GMD varied with time for the surface treatment involving hay at 723 g/m^2 and untreated surface (Fig. 5.6). Note that it took from 0.5 to 1.0 s to move the hooves a distance of 0.24 m over the manure layer. After the hooves were moved, the GMD increased rapidly within the first 3 min and then gradually decreased to near background level as shown in Figure 5.6.

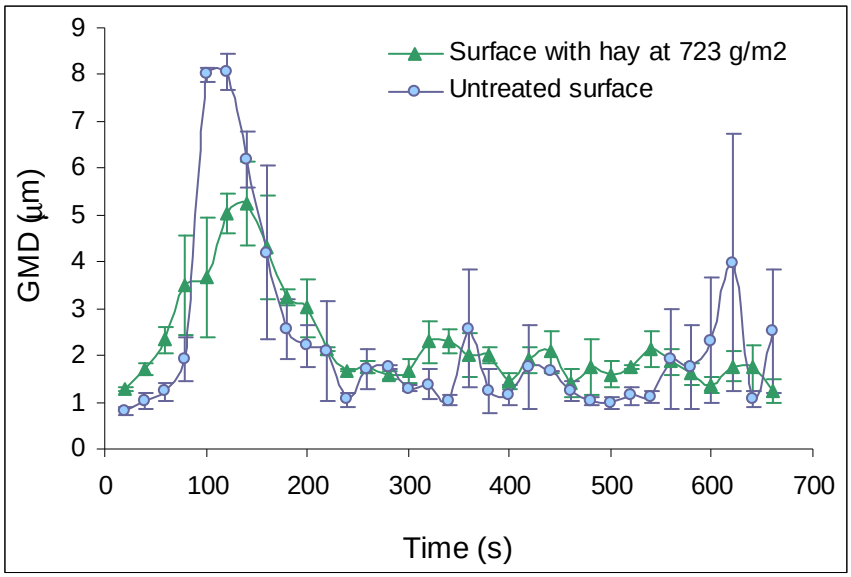

Figure 5.6 Plot of geometric mean diameter (GMD) of particulates as measured by the Aerodynamic Particle Sizer Spectrometer for the surface treated with hay at 723 g/m^2 and the untreated surface; error bars represent standard error.

The maximum GMD values and corresponding GSD values for the manure layer treated with hay and control are summarized in Table 5.5. The mean maximum GMD for the untreated surface (i.e., control), 8.2 µm, was significantly higher ($P<0.05$) than those for the surfaces treated with hay. The amount of hay applied did not significantly influence the GMD ($P>0.05$).

In addition, surface treatment with hay reduced concentrations for all particle sizes from 0.5 to 20 µm as shown in Figure 5.7, which presents the mass concentrations of particles emitted from the simulated pen surface during the period in which GMD was highest. As expected, reduction in concentration was higher for the larger particles because they can be easily entrapped by the hay fibers, while the smaller particles can go through the spaces between the fibers.

Table 5.5 Maximum geometric mean diameter (GMD) and corresponding geometric standard deviation (GSD) values, as measured by the Aerodynamic Particle Sizer spectrometer, for surface treatment with hay[†,‡].

Amount	**GMD (µm)**		**GSD**	
(g/m^2)	Mean	SE	Mean	SE
0	8.2 a	0.25	2.1	0.00
241	6.1 b	0.38	2.0	0.12
482	5.9 b	0.19	1.9	0.19
723	6.5 b	0.09	1.9	0.06

[†] Emission tests were done with hoof speed at high level and depth of penetration of 5.1cm. Each data point is the average of three replicates.

[‡] Mean values with the same letter within a column are not significantly different at the 5% level.

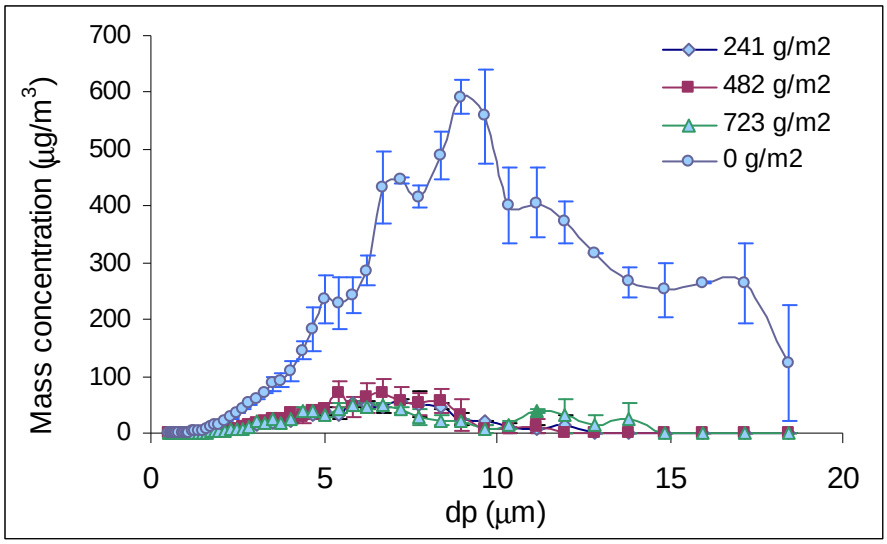

Figure 5.7 Effect of application of hay on the mass concentration of particles (with size distribution of 0.5 to 20 µm) emitted from the simulated pen surface, as measured by the Aerodynamic Particle Sizer spectrometer. Each data point is the average of three replicates; error bars represent standard error.

5.5 Discussion

Water sprinkling is the most common method of controlling dust in cattle feedlots. Ledbetter (2005) indicated that about 3.2 mm of total net water was applied per day at 80% of the pen surface area in one of the feedlots in west Texas using a sprinkler system. Bonifacio et al. (2011) evaluated the effectiveness of a sprinkler system in a cattle feedlot in Kansas with a maximum water application rate of 5 mm/day. Results showed that the control efficiency for PM_{10} based on 24-h mean concentration ranged from 32% to 80% with an overall mean of 53%; the effect of water application (less than 5 mm per day) using the sprinkler system lasted about one day or less. In comparison, in this research, percentage reductions in the PM_{10} emission potential were 42% and 69% for water applications of 3.2 mm and 6.4 mm, respectively. While, water is effective in controlling PM emission in feedlots, installation and operation of a sprinkler system or traveling water guns are expensive (Bonifacio et al., 2011; Harner et al., 2008; Amosson et al., 2006, 2007) and water resource might be limited (Pimentel, et al., 1997). The estimated cost of water sprinkler systems ranged from $0.60 to $2.40 per marketed head per year depending on feedlot turnover rate and type of sprinkler system (Harner et al., 2008) without consideration of the cost of water and energy resources used during sprinkler operation. Furthermore, excess water used for dust control can create anaerobic conditions in the manure

pack resulting in odor problems. In addition, Mader et al. (2007) indicated that cattle acclimatization to being sprinkled can result in slight hyperthermia even during cooler days when sprinkling would normally not be utilized.

Thus, application of hay or other mulch materials on the pen surface might be good alternative methods to control dust emission from cattle feedlots. Also, surface mulches will help retain and preserve moisture by slowing evaporation (PM10 Inc., 2007). In a study on crop residues, Klocke et al. (2009) observed that surface coverage and amount of dry matter of crop residues influenced soil water evaporation and that evaporation was reduced nearly 50% compared with bare soil. With the reduction in water evaporation, application of mulches also has the potential to reduce the amount of supplemental water needed for sprinkler systems for effective dust control. Surface mulches also can protect the manure layer from rain by reducing its impact and slowing runoff speed (PM10 Inc., 2007); however, that effect would need to be balanced against the more traditional management objective of ensuring rapid pen drainage to reduce odors and avoid muddy, performance-sapping conditions on the surface. Consequently, additional investigation is needed to determine the feasibility of applying mulches on the pen surface of cattle feedlots. Factors to consider are availability, amount and frequency of application, and cost, among others. Auvermann et al. (2006) indicated that because manure is continually excreted by cattle, some kinds of materials must be applied frequently on pen surfaces to be consistently effective in reducing PM emission. Additional labor costs would be necessary if the candidate abatement material is applied manually.

PM_{10} emission potentials resulting from this study are relative values that can be used to assess effectiveness of dust-abatement measures. Field studies should be conducted to verify results obtained from this study, evaluate ease and practicality of the method, and assess potential synergistic effects of surface mulches and water sprinkling.

5.6 Conclusions

This study developed a simple, repeatable method for evaluating and quantifying the relative particulate control efficiencies of potential abatement measures for open cattle feedlots. Results showed that PM_{10} emission potential increased with increasing speed of hooves and depth of hoof penetration on the manure layer. Results also showed that topical application of mulches or water application significantly reduced the PM_{10} emission potential of the simulated pen surface. Of the candidate abatement materials tested, hay and water were the most effective in reducing the PM_{10} emission potential, with control efficiencies for hay ranging from 48% for an application rate of 241 g/m^2 to 77% for hay for an application rate of 723 g/m^2 and control efficiencies for water of 42% (for an application rate of 3.2 mm of water) and 69% (for an application rate of 6.4 mm).

5.7 References

Amosson, S.H., F. Bretz, L. New, and L.K. Almas. 2007. Economic analysis of a traveling gun for feedyard dust suppression. Mobile, Ala.: Presentation at Southern Agricultural Economics Association Annual Meeting. Available at: http://ageconsearch.umn.edu/bitstream/34881/1/sp07am02.pdf. (verified 6 Apr. 6, 2011).

Amosson, S.H., B. Guerrero, and L.K. Almas. 2006. Economic analysis of solid-set sprinklers to control dust in feedlots. Orlando, Fla.: Presentation at Southern Agricultural Economics Association Annual Meeting. Available at: http://ageconsearch.umn.edu/bitstream/35341/1/sp06am01.pdf. (verified Apr. 6, 2011)

ASTM. 2002. D2216-98: Standard test method for laboratory determination of water (moisture) content of soil and rock by mass. In *Annual Book of American Society for Testing Materials Standards*. Philadelphia, Penn.: ASTM.

Auvermann, B.W., R. Bottcher, A. Heber, D. Meyer, C.B. Parnell, Jr., B. Shaw, and J. Worley. 2006. Particulate matter emissions from animal feeding operations. In *Animal Agriculture and the Environment: National Center for Manure and Animal Waste Management White Papers*, 435-468. J.M. Rice, D.F. Caldwell, F.J. Humenik, eds. St. Joseph, Mich.: ASABE.

Auvermann, B.W. 2003. A mechanistic model of fugitive emissions of particulate matter from cattle feedyards: Part I. Introductory evaluation. In *Proc. Air Pollution from Agricultural Operations III Conference*, 257-266. St. Joseph, Mich.: ASAE.

Bonifacio, H.F., R.G. Maghirang, E.B. Razote, B.W. Auvermann, J.P. Harner, J.P. Murphy, L. Guo, J.M. Sweeten, and W.L. Hargrove. 2011. Particulate control efficiency of a water sprinkler system at a beef cattle feedlot in Kansas. *Trans. ASABE* 54(1): 295-304.

Carroll, J.J., J.R. Dunbar, R.L. Givens, and W.B. Goddard. 1974. Sprinkling for dust suppression in a cattle feedlot. *California Agric.* 28(3):12-14.

Chalker-Scott, L. 2010. *The informed gardener blooms again*. Seattle, Wash.: University of Washington Press.

Chalker-Scott, L. 2008. Dust mulches. *MasterGardener*. Available at: http://www.puyallup.wsu.edu/~linda%20chalker-scott/horticultural%20myths_files/Myths/magazine%20pdfs/Dust%20mulches.pdf. (verified 8 April. 2011).Davis, J.G., T.L. Stanton, and T. Haren. 2004. Feedlot manure management. Management, Livestock Series. No. 1.220. Fort Collins, Colo.: Colorado State University Cooperative Extension. Available at: http://www.cde.state.co.us/artemis/UCSU20/UCSU2062212202002INTERNET.pdf. Accessed 15 February 2010.

DPI&F. 2003. Feedlot waste management series: dust control. Queensland, Australia: Queensland Government, Department of Employment, Economic Development and Innovation. Available at: http://www2.dpi.qld.gov.au/environment/5243.html. Accessed 1 March 2009.

Harner, J., R.G. Maghirang, and E.B. Razote. 2008. Water requirements for controlling dust from open feedlots. In *Mitigating Air Emissions from Animal Feeding Operations Conference*. Ames, Iowa: Iowa State University. Available at: http://www.ag.iastate.edu/wastemgmt/Mitigation_Conference_proceedings/CD_proceedings/Animal_Housing-Treatment/Harner-Dust_control.pdf. (verified Apr. 6, 2011).

Ledbetter, K. 2005. Settling dust around feedyards. *The Cattleman*. Available at: http://findarticles.com/p/articles/mi_qa5420/is_200509/ai_n21378761/ . Accessed 02 March 2009.

Mader, T.L., M.S. Davis, and J.B. Gaughan. 2007. Effect of sprinkling on feedlot microclimate and cattle behavior. *Int. J. Biometeorol.* 51(6):541-551.

Miller, D. N. and B. L. Woodbury. 2003. Simple protocols to determine dust potentials from cattle feedlot soil and surface samples. *J. Environ. Qual.* 32(5): 1634-1640.

Mitloehner, F.M. 2000. Behavioral and environmental management of feedlot cattle. PhD diss. Lubbock, Tex..: Texas Tech University.

Pimentel, D., J. Houser, E. Preiss, O. White, H. Fang, L. Mesnick, T. Barsky, S. Tariche, J. Schreck, and S. Alpert. 1997. Water resources: agriculture, the environment, and society. *BioScience* 47(2): 97-106.

PM10 Inc. 2007. Erosion control - mulching. Palm Desert, CA: PM10 Inc. Available at: http://www.pm10inc.com/erosion-control-mulching.html. Accessed 1 April 2010.

Rahman, S., S. Mukhtar, and R.Wiederholt. 2008. Managing odor nuisance and dust from cattle feedlots. Fargo, N.D.: North Dakota State University Extension Service. Available at: http://www.ag.ndsu.edu/pubs/h2oqual/watnut/nm1391.pdf. Accessed 15 March 2010

Razote, E.B., R.G. Maghirang, J.P. Murphy, B.W. Auvermann, J.P. Harner III, D.L. Oard, W.L. Hargrove, D.B. Parker, and J.M. Sweeten. 2007. Air quality measurements from a water-sprinkled beef cattle feedlot in Kansas. ASABE Paper No. 07-4108. St. Joseph, Mich.: ASABE.

Razote E.B., R.G. Maghirang, B.Z. Predicala, J.P. Murphy, B.W. Auvermann, J.P. Harner III, and W.L. Hargrove. 2006. Laboratory evaluation of the dust emission potential of cattle feedlot surfaces. *Trans. ASABE* 49(4): 1117-1124.

Romanillos, A. 2000. Assessing the effect of stocking density on fugitive PM_{10} emissions from cattle feedyards and development of a cattle feedyard emission factor. MS thesis, College Station, Tex.: Texas A&M University.

SAS. 1990. SAS/STAT user's guide. Ver. 9.1. Cary, N.C.: SAS Institute Inc.

Sweeten, J.M. 1979. Water works for dust control. *Feedlot Manage.* 20(6): 28-31.

Sweeten, J.B., C.B. Parnell, R.S. Etheredge, and D. Osborne. 1988. Dust emissions in cattle feedlots. *Vet. Clin. North Am. Food Anim. Pract.* 4(3): 557-578.

Volckens, J., and T.M. Peters. 2005. Counting and particle transmission efficiency of the aerodynamic particle sizer. *J. Aerosol Sci.* 36(12): 1400-1408.

CHAPTER 6 - Numerical Simulation of Airflow and Particle Collection by Vegetative Barriers

6.1 Abstract

Vegetative barriers have the potential to mitigate particulate matter (PM) and gaseous emissions from open sources, including cattle feedlots; however, limited data are available on their effectiveness in capturing PM and gaseous pollutants. This study was conducted to predict airflow and particle collection efficiency of vegetative barriers. The applicability of computational fluid dynamics (CFD) in modeling airflow around and through porous barriers was first evaluated by simulating airflow passing a porous fence (1.2 m high × 0.01 m thick, 50% porosity), using standard and realizable k-ε turbulence models. Predicted air velocities compared favorably with available experimental data. The CFD model was then applied to simulate airflow and particle collection by trees (2.2 m high × 1.6 m wide) with known surface area density as a function of height. Predicted particle collection efficiencies for the trees generally agreed with available experimental data and ranged from less than 1% for 0.875-µm particles to approximately 32% for 15-µm particles. Further work is being conducted to investigate the effects of the structure of vegetative barriers on particle collection.

6.2 Introduction

Previous researches have measured high dust concentrations in the vicinity of open beef cattle feedlots during dry weather conditions (Razote et al., 2008; Purdy et al., 2007; Sweeten et al., 1988). Particulate matter (PM) generated from cattle feedlots has potential to cause health problems in humans and livestock (Rogge et al., 2006; Purdy et al., 2004; Sweeten et al., 2000; Reynolds et al., 1998). Cost-effective methods to reduce PM concentrations from cattle feedlots are needed.

Particulate control methods for cattle feedlots generally fall into two major categories. The first is reducing emission rate and includes varying stocking density (Auvermann and Romanillos, 2000a, 2000b), modifying cattle behavior relative to feeding schedule (Miller and Berry, 2005), sprinkler systems (Sweeten et al., 1988; Sweeten et al., 1998; Bonifacio et al.,

2011), manure harvesting (Auvermann and Romanillos, 2000a), and pen surface treatments (Razote et al., 2006). The second involves edge-of-feedlot or downwind control techniques, including shelterbelts (artificial or natural) to remove and/or disperse particles (Adrizal et al., 2008). Davis et al. (2004) indicated that trees planted along the perimeter of a feedlot will provide shelter from the wind largely containing any fugitive dust. Currently, no data are available on effectiveness of shelterbelts in removing or dispersing PM emitted from cattle feedlots.

Research on porous barriers (i.e., windbreaks, shelterbelts, vegetative barriers) started in 1930s and focused on reduction of wind speed and modification of microclimate based on field measurements, wind tunnel studies, or numerical simulations (Lin, 2006; Dierickx et al., 2003; Raupach et al., 2001; Cleugh, 1998; Wang and Takle, 1995; Wilson, 1985). Porous barriers have been used primarily to control snow and sand accumulation and pesticide drift. They are also recognized to mitigate fugitive dust and odors by mixing them with clean air, although the process is still not fully understood (Lin, 2006; Malone, 2004).

Tortuous airflows and surface roughness are major factors for the collection of PM by porous barriers. Tortuous airflows lead to higher turbulence and increased mixing of PM, and surface roughness increases the likelihood of particles impacting on foliage surfaces (Tiwary et al., 2005). Early studies have led to considerable progress in understanding airflow and turbulence characteristics (Boldes et al., 2001). Full understanding of aerodynamics of windbreaks is not available, even for relatively simple artificial barriers. Natural barriers are irregular and difficult to characterize structurally. Besides variable topographical settings, wind speed and direction change constantly in natural settings along with conditions of atmospheric stability (Lin, 2006; Wang and Takle, 1995). Raupach et al. (2001) noted that questions related to particle entrapment by porous barriers are how much of the oncoming flow passes through porous barriers and what fraction of particles in these flows is deposited onto porous barriers. In addition, prominent recirculation and flow separation if existing behind the barriers which tend to interface with the main flow and lead to misrepresentative particle concentration data need to be predicted before conducting field experiments since particle concentrations measured in highly distorted wake flows may be considered inadequate (Tiwary et al., 2005).

Field investigations on airflow and particle collection by vegetative barriers in cattle feedlots are time consuming and expensive. Numerical simulation with computational fluid

dynamics (CFD) can augment field investigations. The traditional Gaussian type of particulate dispersion models are only suitable for flat surfaces and do not apply to porous barriers (Lin, 2006). Therefore, new models are needed to predict the pattern of particle-laden airflow and the distribution of particle concentrations resulting from vegetative barriers or fences. CFD models have been successfully applied in studying aerodynamic phenomena (Bitog et al., 2009).

Field tests and wind tunnel experiments have been conducted to investigate effects of natural and/or artificial windbreaks (Packwood, 2000; Wang and Takle, 1995; Wilson, 1985). Considerable progress in understanding airflow and turbulence characteristics has been achieved; however, because of external and internal structures of vegetative barriers, it is difficult to fully understand aerodynamics of windbreaks (Lin, 2006). Besides the influence of vegetative barriers on airflow, vegetative barriers also affect particle concentration. Some of the oncoming particle-laden airflow passes over the barriers while some flows through them in which particles are filtered from the flow by deposition onto vegetation elements (leaves, trunks, twigs) (Petroff et al., 2008; Raupach, et al., 2001). Determining a suitable resistance model for a given geometry of barrier, given an estimated value of volumetric porosity, is the main problem for modelers (Packwood, 2000).

This study was conducted to determine effects of vegetative barriers on airflow and particle concentration using CFD. Specific objectives were to simulate the airflow through porous fences and trees and predict particle collection efficiency of trees.

6.3 Methods

In general, the CFD simulation process has three stages: pre-processing, solving, and post-processing (Tu et al., 200). Gambit (ver. 2.3, Lebanon, NH, FLUENT, Inc.) was employed during pre-processing to develop the geometry of flow domain. FLUENT (ver. 6.3, FLUENT, Inc., Lebanon, NH) was used as the main module to perform CFD calculations. Post-processing, which involves organization and interpretation of predicted results, involved use of Excel (Microsoft Corporation, Redmond, WA) and Tecplot (ver. 360 2009, Tecplot, Inc., Bellevue, WA).

6.3.1 Simulation of airflow around a porous fence

Several numerical simulation studies (Rosenfeld et al., 2010; Bourdin and Wilson, 2008; Santiago et al., 2007; Wilson and Yee, 2003) have used experimental data for a thin fence windbreak conducted by Bradley and Mulhearn (1983). The fence was a vertical slat of wood (1.2 m × 0.08 m × 0.01 m) woven in a sheep netting of mesh 0.15 m×0.15 m. To evaluate the applicability of the turbulence model, boundary conditions, and porous barrier prediction, this study also chose the Bradley and Mulhearn (1983) data as benchmark to study the airflow across a porous fence.

6.3.1.1 Computational domain

A 2D computational domain (Fig. 6.1) was used for the simulation and it was divided into a number of smaller subdomains. The discrete values of the flow properties such as air velocity and particle concentration were determined and described in each of these cells (Tu et al., 2008).

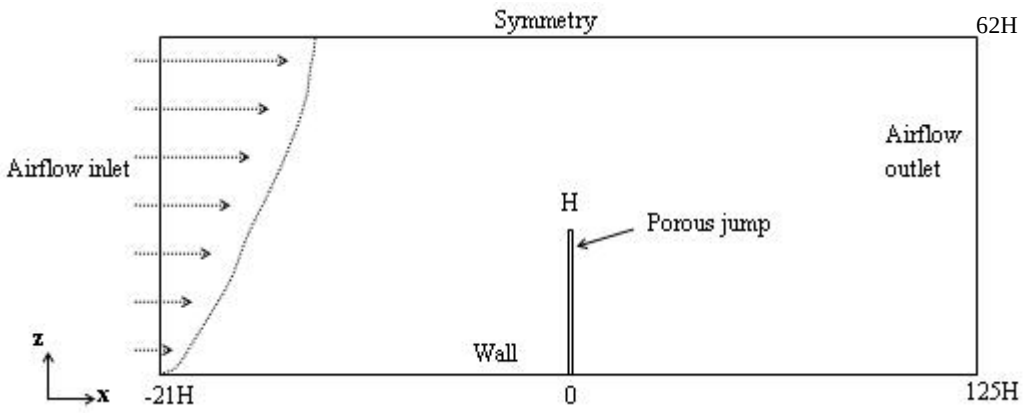

Figure 6.1 Schematic diagram of the geometry and domain for porous fence and (not drawn to scale).

The grids were generated by using straight edges. The origin of the horizontal axis (x=0) was defined to lie at the location of the fence. For convenience, computational domains were denoted as $\left[\frac{X_{up}}{H}, \frac{X_{down}}{H}, \frac{Z}{H}, W\right]_{N_x, N_z}^{R}$ where H and W are barrier height and width (Table 6.1), respectively; X_{up} is horizontal distance from the airflow inlet to the upwind edge of the barrier; X_{down} is horizontal distance from the origin to the airflow outlet; Z is distance from the

ground to the upper boundary of the domain; R represents the stretching ratio from the barrier to outer boundaries, which generated non-uniform grid results with finer grids near the barrier region and coarser grids further away from the barrier to reduce computational time and improve the accuracy; and N_x and N_z denote the number of cell columns and rows for the barriers (uniform vertical and horizontal spacing), respectively.

Table 6.1 Input values for the CFD models.

Parameter	Symbol	Value
Height of vegetative barrier (m)	H	1.2 (for fence) 2.2 (for tree)
Width of vegetative barrier (m)	W	0.01 (for fence) 1.6 (for tree)
Air density (kg/m^3)	ρ	1.225
Air dynamic viscosity (N·s/ m^2)	μ	1.79×10^{-5}
Air temperature (K)	T	293
Atmospheric pressure (Pa)	P	101325
Turbulence model constant	$C_{1\varepsilon}$	1.44
Turbulence model constant	$C_{2\varepsilon}$	1.92
Turbulence model constant	C_{μ}	0.09
Turbulent Prandtl number for k	σ_k	1.0
Turbulent Prandtl number for ε	σ_ε	1.3
von Karman constant	κ	0.4187
Particle density (kg/m^3)	ρ_p	1050
Mean free path (μm)	λ	0.066
Boltzmann constant (N·m/K)	ζ	1.38×10^{-23}
Turbulent Schmidt number	Sc_t	0.7
Polhausen coefficient	C_{Pol}	1.32

The computational domain was set as $\left[-21,\ 125,\ 62,\ 0.01\right]_{1,\ 10}^{1.2}$, in accordance with Bourdin and Wilson (2008). The statistics of the computational grids are listed in Table 6.2. Figure 6.2 shows the computational grids near the fence.

Table 6.2 Computational grids for the porous fence and trees.

		Porous Fence	Trees
Cells		2220	58000
Faces		4537	116722
Nodes		2318	58722
***x* coordinate (m)**	min	-25.2	-66
	max	150	110
***z* coordinate (m)**	min	0	0
	max	74.4	17.6
Volume (m^3)	min	6.4×10^{-3}	5.3×10^{-3}
	max	308	21
Face area (m^2)	min	6×10^{-2}	4×10^{-2}
	max	25	0.2

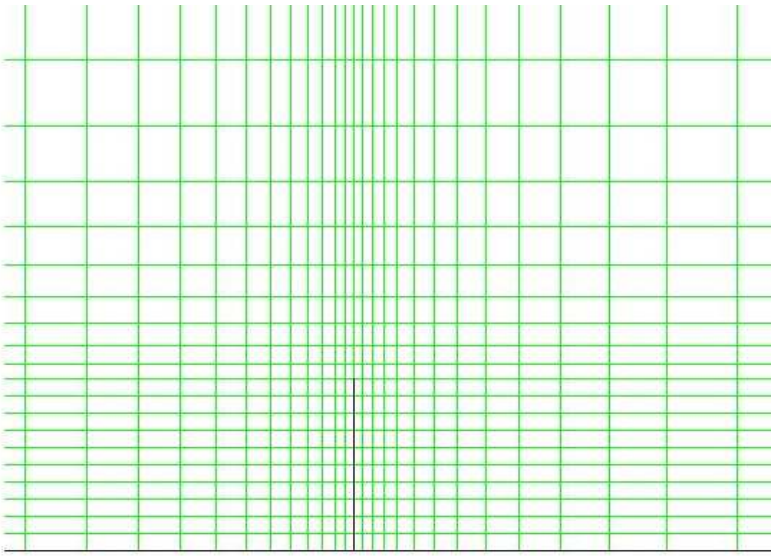

Figure 6.2 Computational grids generated near the fence.

6.3.1.2 Governing equations and numerical solver

The 2D Reynolds-averaged Navier-Stokes (RANS) equations were the governing equations for the continuous flow field. Airflow was assumed steady, incompressible, and isothermal, and the neutrally stratified turbulent atmospheric surface layer was assumed. Equations for continuity and the momentum conservation are as follows (Tu et al., 2008; Nunn, 1989):

$$\frac{\partial u_i}{\partial x_i} = 0 \tag{6.1}$$

$$\rho u_j \frac{\partial u_i}{\partial x_j} = -\frac{\partial P}{\partial x_i} + \frac{\partial}{\partial x_j}\left(\mu \frac{\partial u_i}{\partial x_j}\right) + S_i \tag{6.2}$$

where x_i, x_j is Cartesian coordinate (m); u_i and u_j are velocity components in the stream wise (u) and vertical directions (v) (m/s); ρ is air density (kg/m^3); P is pressure (Pa); μ is air dynamic viscosity (N·s/m^2); and S_i is source term. S_i was assumed to be zero everywhere except for the porous barrier which was treated as a momentum sink and discussed in Section 6.3.1.4. Values of ρ, P, and μ are listed in Table 6.1.

Standard and realizable $k-\varepsilon$ models were used in this study based on previous studies (Rosenfeld et al., 2010; Bourdin and Wilson, 2008; Lin, 2006; Tiwary et al., 2005). The transport equations for the standard $k-\varepsilon$ model (FLUENT Inc., 2006) are as follows:

$$\frac{\partial}{\partial x_i}(\rho k u_i) = \frac{\partial}{\partial x_j}\left[\left(\mu + \frac{\mu_t}{\sigma_k}\right)\frac{\partial k}{\partial x_j}\right] + G_k + G_b - \rho\varepsilon - Y_M \tag{6.3}$$

$$\frac{\partial}{\partial x_i}(\rho \varepsilon u_i) = \frac{\partial}{\partial x_j}\left[\left(\mu + \frac{\mu_t}{\sigma_\varepsilon}\right)\frac{\partial \varepsilon}{\partial x_j}\right] + C_{1\varepsilon}\frac{\varepsilon}{k}(G_k + C_{3\varepsilon}G_b) - C_{2\varepsilon}\rho\frac{\varepsilon^2}{k} \tag{6.4}$$

where G_k represents generation of k due to mean velocity gradients, calculated as

$$G_k = -\rho\overline{u_i' u_j'}\frac{\partial u_j}{\partial x_i} \tag{6.5}$$

G_b is generation of k due to buoyancy, calculated as

$$G_b = \beta g_i \frac{u_t}{Pr_t}\frac{\partial T}{\partial x_i} \tag{6.6}$$

Pr_t is turbulent Prandtl number for energy and equal to 0.85; g_i is component of the gravitational vector in the i^{th} direction; and β, the coefficient of thermal expansion, is defined as $\beta = -\frac{1}{\rho}\left(\frac{\partial \rho}{\partial T}\right)_P$. Y_M in Equation 6.3 represents the contribution of the fluctuating dilatation in compressible turbulence to the overall dissipation rate; $C_{1\varepsilon}$ and $C_{2\varepsilon}$ in Equation 6.4 are constants; $C_{3\varepsilon}$ in Equation 6.4 is constant calculated as $C_{3\varepsilon} = \tanh\left|\frac{v}{u}\right|$, in which $C_{3\varepsilon} = 1$ for buoyant shear layers that main flow direction is aligned with the direction of gravity and $C_{3\varepsilon} = 0$ for buoyant shear layers that are perpendicular to the gravitational vector; and σ_k and σ_ε are turbulent Prandtl numbers for k and ε, respectively. The Boussinesq hypothesis is employed to relate Reynolds stresses to mean velocity gradients. The turbulent (or eddy) viscosity, μ_t, is computed by combining k and ε as

$$\mu_t = \rho C_\mu \frac{k^2}{\varepsilon} \tag{6.7}$$

Model constants have the following default values: $C_{1\varepsilon}$ =1.44, $C_{2\varepsilon}$ =1.92, C_μ =0.09, σ_k =1.0, σ_ε =1.3 (Table 6.1).

The realizable $k-\varepsilon$ model (FLUENT Inc., 2006) differs from the standard $k-\varepsilon$ model in two ways: (1) it has a new formulation for turbulent viscosity; and (2) the transport equation for ε is based on an exact equation for the transport of the mean-square velocity fluctuation. The expression for the normal Reynolds stress in an incompressible strained mean flow is obtained by combining the Boussinesq relationship and the eddy viscosity definition as

$$\overline{u_i^2} = \frac{2}{3}k - 2\frac{\mu_t}{\rho}\frac{\partial U}{\partial x_i} \tag{6.8}$$

To ensure realizability, namely positivity of normal stresses and Schwarz inequality for shear stresses ($\overline{u_i' u_j'} \le \overline{u_i'^2 u_j'^2}$), C_μ is sensitized to mean flow and turbulence (k, ε).

The pressure-based solver used the SIMPLE (Semi-Implicit Method for Pressure-Linked Equations) method to introduce pressure into continuity equation. The entire set of simulations was run using second-order upwind scheme. For local residuals of continuity, momentum,

turbulence, and scalars, the absolute criterion of convergence was set to 0.0001 over 1000 iterations. In most cases, from 500 to 700 iterations were needed to achieve convergence.

6.3.1.3 Boundary conditions

Boundary conditions in this study are shown in Figure 6.1 (El Gharbi et al., 2009; Bourdin and Wilson, 2008; Santiago et al., 2007). At the upper boundary, symmetry boundary condition was imposed. Outlet airflow was considered fully developed and treated as outflow. No slip shear condition was used on the ground with roughness height, z_0 (m). z_0 is empirical constant, where z_0 /H=0.0017 (Bourdin and Wilson, 2008). The standard wall function was applied for the near-wall treatment.

The inlet velocity profile used in the simulation corresponded to the logarithmic profile (Bourdin and Wilson, 2008; Santiago et al., 2007):

$$u_{in} = \frac{u_*}{\kappa}\ln\left(\frac{z}{z_0}\right) \qquad (6.9)$$
$$v_{in} = 0$$

where u_{in} and v_{in} are inflow velocity at stream wise and vertical directions (m/s), respectively; z is height from the ground (m); κ is von Karman constant; u_* is friction velocity far upstream from the barrier. For the porous fence, u_* was set as 0.4 m/s (Bourdin and Wilson, 2008).

The magnitude of turbulent kinetic energy (k_{in}) and dissipation (ε_{in}) at the inlet can significantly influence the CFD solution. In the absence of measurement of k_{in} and ε_{in}, the following equations (Bourdin and Wilson, 2008; Santiago et al., 2007) were used based on the assumption of equilibrium boundary layer:

$$k_{in} = \frac{u_*^2}{\sqrt{C_\mu}} \qquad (6.10)$$

$$\varepsilon_{in} = \frac{u_*^3}{\kappa z} \qquad (6.11)$$

6.3.1.4 Simulation of fence as momentum sink

Aerodynamically, porous barriers are wind momentum sinks (i.e., pressure loss) when the rough surface interacts with airflow above and within it. Momentum is absorbed from the flow

by both form and skin-friction drags on elements and transported mainly by turbulent diffusion to produce the leeward wind speed reduction (Bourdin and Wilson, 2008; FLUENT Inc., 2006; Lin, 2006; Tiwary et al., 2005; Wang and Takle, 1995; Raupach and Thom, 1981).

Porous barriers can be treated as a pressure discontinuity surface by applying porous medium condition (porous jump for fence and porous zone for tree). The porous medium may be normally modeled with a viscous loss term (I) and inertial loss term (II), as shown in Equation 6.12 (FLUENT Inc., 2006). The model was added to the standard fluid flow equation as momentum sink.

$$S_i = -\left(\underbrace{\frac{\mu}{\alpha} u_i}_{\text{I}} + \underbrace{C_2 \frac{1}{2} \rho |u| u_i}_{\text{II}} \right) \tag{6.12}$$

where α is permeability (m^2), C_2 is inertial resistance (m^{-1}), and S_i is equivalent to pressure gradient and the pressure drop is related to the porosity of the porous medium.

The porous jump condition is one-dimensional simplification of the porous medium model (FLUENT Inc., 2006). For turbulent flow and modeling of a perforated plate, the viscous loss term can be ignored (Bourdin and Wilson, 2008; FLUENT Inc., 2006). Consequently, the face permeability in the user inputs for the porous jump model in FLUENT was set as $1e^{+20}$ m^2. C_2 is related to the resistance coefficient or pressure loss coefficient (k_r) of the porous barrier and can be expressed as Equation 6.13 (Bourdin and Wilson, 2008; FLUENT Inc., 2006; Tiwary et al., 2005; Wilson, 1985).

$$C_2 = \frac{k_r}{W} \tag{6.13}$$

k_r is a dynamic parameter that depends not only on porosity but also on the shape of the barrier elements, i.e., barriers of equal porosity may have different k_r and different effects (Wang and Takle, 1995). For the porous fence, k_r was set to 4 (Bourdin and Wilson, 2008; Santiago et al., 2007; Wilson, 1985). With a thickness of 0.01 m, the pressure-jump coefficient, C_2, was then set as 400. Inputs for porous jump models in FLUENT are summarized in Table 6.3.

Table 6.3 User inputs for porous medium models in FLUENT.

	Porous fence	Tree
Model	Porous jump	Porous zone
User inputs in FLUENT	Face permeability (m^2)=$1e^{+20}$	Direction-1 vector: X=0, Y=1
	Porous medium thickness (m)=0.01	Inertial resistance: Direction-1 (m^{-1})=0 Direction-2 (m^{-1})=$\frac{C_d d_{SA}}{W}$ (using UDF)
	Pressure-jump coefficient (m^{-1})=400	Power low model: C0=0, C1=0 Fluid porosity: Porosity=1 (all fluid)

6.3.2 Simulation of airflow and particle transport for the trees

The airflow around and through a row of trees was simulated considering their external and internal structures. An Eulerian-based model of particle transport through the trees was explored in this study, in which the number concentrations of different sized particles were calculated using a modified User-Defined Scalars (UDS) equation by implementing User-Defined Functions (UDFs) in FLUENT. Fluid flow was first solved without the presence of particles, and then particle flow was calculated based on the solution of fluid flow (Wang and Lin, 2006).

6.3.2.1 Computational domain

Computational domain size and geometry of the row of trees (Fig. 6.3) were based on research on Hawthorn trees by Tiwary et al. (2005). The origin of the horizontal axis (x=0) was defined to lie at the downwind edge of the tree. The computational domain was set as $\left[-30,\ 50,\ 8,\ 1.6\right]_{10,\ 16}^{1.01}$. The length of edge of each cell within the tree was $\Delta x = \frac{W}{N_x}$ in x direction and $\Delta z = \frac{H}{N_z}$ in y direction. Information on the computational grids are listed in Table 6.2. Figure 6.4 shows the distribution of generated rectangular grids near and within the tree.

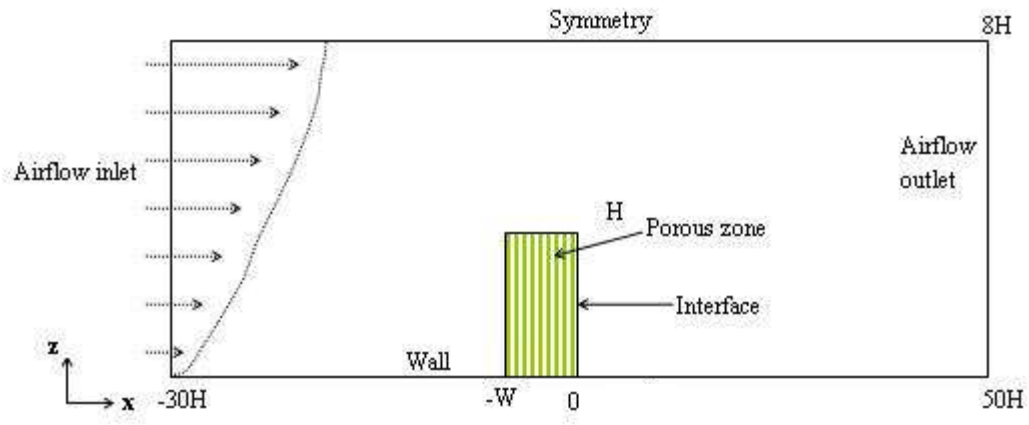

Figure 6.3 Schematic diagram of the geometry and domain for the row of trees (not drawn to scale)

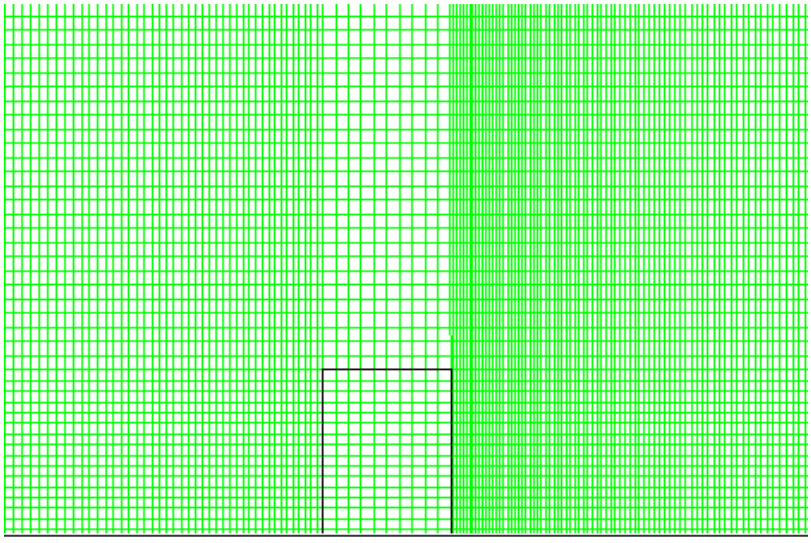

Figure 6.4 Computational grids generated near and within the row of trees.

6.3.2.2 Governing equations and numerical solver

The governing equations for airflow and assumptions were similar to those for the porous fence. Equations 6.1 and 6.2 were also used for continuity and the momentum conservation. The source term S_i in Equation 6.2 was also assumed zero everywhere except for the tree, which was treated as a momentum sink. Standard and realizable $k-\varepsilon$ models were also used. For local residuals of continuity, momentum, turbulence and scalars, the absolute criteria of convergence was set to 0.0001 over 1000 iterations. In most cases, from 600 to 1300 iterations were needed to achieve convergence.

6.3.2.3 Boundary conditions

Boundary conditions for the trees are shown in Figure 6.3 (El Gharbi et al., 2009; Tu et al., 2008; Mohebbi and Baroutian, 2007; Tiwary et al., 2005; Richards and Hoxey, 1993). Similar to the fence, symmetry boundary condition was imposed at the upper boundary and outlet airflow was treated as outflow. No slip shear condition was used on the ground with roughness height, z_0 (m). In this study, z_0 was assumed to be 0.0086 H based on the studies of Tiwary et al. (2005) and Packwood (2000). The standard wall function was applied for the near-wall treatment. The inlet velocity profile used in the simulation corresponded to the logarithmic profile as in Equation 6.9, in which u_*=0.0548U_{0H}. U_{0H} was air velocity at x/H=-10 and z/H=1. A value of 2.3 m/s was used for U_{0H} based on experimental data in Tiwary et al. (2005). Equations 6.10 and 6.11 were also used for the magnitudes of turbulent kinetic energy (k_{in}) and dissipation (ε_{in}) at the inlet.

6.3.2.4 Simulation of the trees as momentum sink

The row of trees was treated as a porous zone and also simulated based on Equations 6.12 and 6.13 (FLUENT Inc., 2006; Tiwary et al., 2005; Wilson, 1985). For ambient airflow, viscous loss term in Equation 6.12 was ignored (Tiwary et al., 2005). Thus, viscous resistance in the user inputs of FLUENT for the porous zone model was set as 0. The k_r, related to C_2, was the product of leaf area density d_{SA} (m^{-1}) and drag coefficient C_d (normal range of 0.1 to 0.5) (Rosenfeld et al., 2010; Melese Endalew et al., 2009; Tiwary et al., 2005; Wilson, 1985). Consequently, the inertial resistance at the z-direction was set as $C_2 = \frac{C_d d_{SA}}{W}$. The d_{SA} values were extracted from Tiwary et al. (2005) and fitted into functions related to heights from the ground (Fig. 6.5). Inputs for the porous zone model in FLUENT are summarized in Table 6.3.

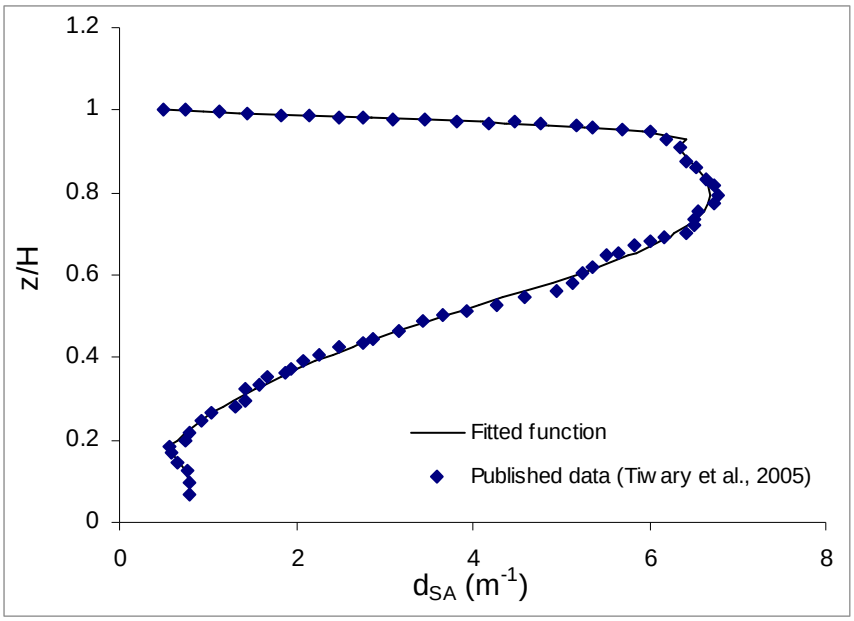

Figure 6.5 Surface area density (d_{SA}) as a function of height.

6.3.2.5 Particle transport

Processes of particle deposition onto vegetative barriers include transport of particles by turbulence and sedimentation and collection by the different elements of the barriers, including stems, twigs, and leaves. Particle collection by the element combines the collection efficiency due to diffusion, impaction, and interception, while other processes like diffusiophoresis, thermophoresis or electrophoresis, which are less important for natural plant surfaces (Petroff et al., 2008; Peters and Eiden, 1992; Bache, 1979), were neglected. The overall collection efficiency of a single element is equivalent to the sum of the components. The collection efficiency of these mechanisms depends on wind speed, canopy structure, together with many physical and physico-chemical parameters (Petroff et al., 2008).

The particle-laden airflow was treated as a two-phase mixture of air and particles. The Euler-Euler approach was used because of its computational efficiency and relative ease of integration into Eulerian-based CFD codes. In this approach, both phases were considered as two continua and treated mathematically by solving conservation equations for both phases. Similar to previous studies (Zhang et al., 2008; Portela and Oliemans, 2006; Predicala, 2003; Vlachos et al., 2002), one-way coupling was assumed because of relatively small particle concentration, i.e., presence of particles does not influence airflow. Spherical polystyrene

particles with density of 1050 kg/m^3 and diameters (d_p) of 0.875 µm, 1.5 µm, 2.75 µm, 4.25 µm, 6.25 µm, 8.75 µm, 12.5 µm, and 15 µm, based on Tiwary et al. (2005) data, were considered in this study.

The particle number concentration (N) was solved by a modified scalar transport equation coupled with the flow field as Equation 6.14 (Zhang et al., 2008; FLUENT Inc., 2006; Hinds, 1999):

$$\frac{\partial(u_i N_k)}{\partial x_i} - \frac{\partial}{\partial x_i}\left(\Gamma_k \frac{\partial N_k}{\partial x_i}\right) = -U_{sk}\frac{\partial N_k}{\partial x_i} + S_k \qquad k = 1, 2, ..., 8 \tag{6.14}$$

where N_k is number concentration of the kth group of particles with known diameter (i.e., 0.875, 1.5, 2.75, 4.25, 6.25, 8.75, 12.5, and 15 µm); Γ_k is diffusivity coefficient of particles in air; and U_{sk} is particle settling speed of the kth group of particles, defined as

$$U_{sk} = C_c \tau_p g \tag{6.15}$$

where C_c is slip correction factor, g is gravitational acceleration (m/s^2), and τ_p is particle relaxation time. C and τ_p are defined in Equations 6.16 and 6.17, respectively.

$$C_c = 1 + \frac{\lambda}{d_p}\left[2.34 + 1.05\exp\left(-\frac{0.39 d_p}{\lambda}\right)\right] \tag{6.16}$$

where λ is the mean free path (µm).

$$\tau_p = \frac{\rho_p {d_p}^2}{18\mu} \tag{6.17}$$

Γ_k in Equation 6.14 combines the laminar and turbulent diffusion components, Γ_D and Γ_T ($\Gamma_k = \Gamma_D + D_T$). The laminar diffusion coefficient, Γ_D, is calculated using the Stoke-Einstein equation as

$$\Gamma_D = \frac{\zeta T C_c}{3\pi\mu d_p} \tag{6.18}$$

where ζ is Boltzmann constant; T is absolute temperature (K); and µ is dynamic viscosity of the air. The turbulent diffusion coefficient, Γ_T, is defined as

$$\Gamma_T = \frac{\nu_t}{Sc_t} \tag{6.19}$$

where ν_t is turbulent viscosity and Sc_t is turbulent Schmidt number. The turbulent Schmidt number is a measure of the relative diffusion of momentum and mass due to turbulence. Because it is an empirical constant that is relatively insensitive to the molecular fluid properties, Sc_t was set 0.7 for all cases (Table 6.1) (Zhang et al., 2008; Hinds, 1999).

In Equation 6.14, S_k is the source term. Outside the barriers, its value is zero. Inside the barriers, on the other hand, it represents particle flux change per volume. The total particle flux to the tree can be determined using (Tiwary et al., 2005):

$$F = \int_0^H \int_{-W}^0 u(x,z)(N_{in} - N_{out})dxdz \tag{6.20}$$

where $u(x,z)$ is face velocity profile of the grid cell, N_{in} is particle concentration entering a cell, and N_{out} is particle concentration emerging from the cell. The collection efficiency of the elements of the tree in each cell can be calculated as

$$CE_{cell} = \frac{N_{in} - N_{out}}{N_{in}} \tag{6.21}$$

Then, Equation 6.20 can be expressed as

$$F = \int_0^H \int_{-W}^0 u(x,z)CE_{cell}N_{in}dxdz \tag{6.22}$$

Consequently, the source term can be calculated as Equation 6.23 considering only the horizontal wind advection, i.e.

$$S_k = -\frac{uCE_{cell}N_{in}\Delta z}{V} \tag{6.23}$$

where V is cell volume. CE_{cell} was estimated by accounting for the difference collection mechanisms of the tree elements in each grid cell as described in Section 6.3.2.6.

6.3.2.6 Calculation of particle collection efficiency of vegetation elements

Tree elements, such as leaves, stems, and twigs can be treated as filter fibers. Particle collection is due to particle interaction with these elements. Specific geometrical properties (i.e., shape, size, and orientation) of each element contribute to collection. However, models do not reflect this variability and an implicit averaging operation over the elements has been applied in most cases (Petroff et al., 2008).

Two main particle collection mechanisms were considered in this study: Brownian diffusion and inertial impaction (Tiwary et al., 2005; Raupach et al., 2001; Hinds, 1999; Fuchs, 1964). Brownian diffusion is the dominant collection mechanism for very fine particles (Petroff et al., 2008; Hinds, 1999). The single element efficiency due to diffusion, E_D, is (Raupach et al., 2001)

$$E_D = \frac{\Gamma_D C_{Pol} \mathrm{Re}^{\frac{1}{2}} Sc^{\frac{1}{3}}}{d_e U_{cell}} \tag{6.24}$$

where C_{Pol} is the Polhausen coefficient equal to 1.32 for a two-sided flat plate; d_e is diameter of the element with an average of 6 mm ranging from 2 mm to 10 mm (Tiwary et al., 2005); U_{cell} is air velocity in each cell; Sc is Schmidt number, given by

$$Sc = \frac{\mu}{\Gamma_D \rho} \tag{6.25}$$

and Re is Reynolds number for flow around an element of cross-section d_e, defined as

$$Re = \frac{\rho d_e U_{cell}}{\mu} \tag{6.26}$$

Inertial impaction occurs when a particle with large inertia is unable to adjust quickly to follow the streamline and collides with the tree elements (Petroff et al., 2008; Hinds, 1999). Single element collection efficiency (E_I) due to inertial impaction is commonly expressed as Equation 6.27 (Tiwary et al., 2005; Raupach et al., 2001; Peters and Eiden, 1992).

$$E_I = \left(\frac{St}{St + 0.8} \right)^2 \tag{6.27}$$

Stokes number, St, is defined as

$$St = \frac{d_P{}^2 \rho_P U_{cell}}{18 \mu d_e} \tag{6.28}$$

Collection via diffusion should be estimated for each element type by using the d_{SA} and via impaction by using only the projected surface area, which is related to the angle (θ) between the element orientation and stream wise direction. The collection mechanism for leaves is different from that of other elements such as stems, because the orientation of leaves may be

changed by the wind (Tiwary et al., 2005); however, the angle variation of those elements was not considered in this study. Instead, a weighting factor r of 1.9 assuming $\theta = 90°$ (Tiwary et al., 2005) was applied to calculate the overall collection efficiency of all tree elements. The overall collection efficiency contributed by the tree within each grid cell was expressed as

$$CE_{cell} = r\left[1 - \exp\left(-d_{SA}(E_I + E_D)\Delta x\right)\right] \tag{6.29}$$

Particle collection by the tree at certain height was calculated by

$$CE = \frac{N_{up} - N_{down}}{N_{up}} \tag{6.30}$$

where N_{up} and N_{down} are number concentrations at the upwind and downwind sides of the tree at certain height, respectively.

6.3.3 User defined functions

With user-defined function (UDF) called 'DEFINE_PROFILE', the computational inlet flow expressed in Equations 6.9-6.11 and the inertial term C_2 in Equation 6.13 were calculated and compiled to FLUENT solver.

The particle phase transport equation (Eq. 6.14) was solved by a passive scalar transport equation solver in FLUENT with some modifications. A general steady scalar (convection-diffusion) transport equation for a passive scalar ϕ_i is (FLUENT Inc., 2006)

$$\frac{\partial \rho u_i \phi_k}{\partial x_i} - \frac{\partial}{\partial x_i}\left(\Gamma_k \frac{\partial \phi_k}{\partial x_i}\right) = S_{\Phi k} \qquad k = 1, 2, ..., N \tag{6.31}$$

It can be solved in FLUENT solver, in which the first and second items in the left side are convection and diffusion terms (Γ_k is the diffusion coefficient), respectively; and $S_{\Phi k}$ is the source term that can be supplied by the user for each of the N scalar equations.

In order to use the solver for Equation 6.31, Equation 6.14 can be re-written as Equation 6.32 (Zhang et al., 2008):

$$\frac{\partial\left[(u_i + U_{sk})N_k\right]}{\partial x_i} - \frac{\partial}{\partial x_i}\left(\Gamma_d \frac{\partial N_k}{\partial x_i}\right) = S_k \qquad k = 1, 2, ..., 8 \tag{6.32}$$

In this format, fluid density was excluded; Γ_d was calculated as Γ_k in Equation 6.31 with UDF called 'DEFINE_DIFFUSIVITY', and the diffusion coefficient on every grid point of the

computational domain can be calculated then; S_k was implemented as the source term using the UDF 'DEFINE_SOURCE'. The source term was handled explicitly as Equation 6.23.

Modification was needed for the convection term comparing the formats of Equation 6.32 and Equation 6.31. The convection and settling terms of Equation 6.14 were combined as the convection term and was solved implicitly. The convection term in its original scalar transport Equation 6.31 has the following form (FLUENT Inc., 2006):

$$\nabla \cdot \vec{\psi}\phi \tag{6.33}$$

where $\vec{\psi}$ is a vector field. In the default convection term, $\vec{\psi}$ by default is the product of density and velocity vector ($\vec{u}$):

$$\vec{\psi}_{default} = \rho\vec{u} \tag{6.34}$$

Using the UDF 'DEFINE_UDS_FLUX', the convection term in Equation 6.32 could be defined. However, the UDF needs to return the scalar value $\vec{\psi} \cdot \vec{A}$ to FLUENT, where $\vec{A}$ is the face normal vector of the cell face. In Equation 6.32, there is no ρ term and the settling term is added, then the returned $\psi \cdot \vec{A}$ becomes

$$\vec{\psi} \cdot \vec{A} = \frac{\vec{\psi}_{default} \cdot \vec{A}}{\rho} + \vec{U}_{sk} \cdot \vec{A} \tag{6.35}$$

Notice that ρ is density on the cell face and only the ρ value of the cell is recorded in the flow solver, so the face value ρ is calculated as the average of two neighboring cell values.

The second-order upwind scheme was used for convection terms, and the second-order central differencing method was used for diffusion terms. Once flow-field solutions were obtained, the velocity field was inputted to the particulate phase computing subroutines to solve Equation 6.32.

6.3.4 Data analysis

6.3.4.1 Airflow

Previous research indicated that vegetative barriers can provide shelter for some distance downwind and the efficiency may be determined by the way that wind speed and turbulent flow are modified (Raupach et al., 2001; Cleugh, 1998). Cleugh (1998) indicated that the effectiveness of a porous barrier as shelter can be quantified by the following parameters:

1) ratio of wind speed (normalized velocity) measured near the barrier (u) to a reference wind speed (u_0) that is not affected by the barrier;

2) minimum downwind speed ($u_{\min}$) and downwind distance ($x_{\min}$) to $u_{\min}$; and

3) distance (x_s) to $u/u_0 < c$, where c is an arbitrary factor and is often 0.7 or 0.8.

Simulation results of airflow obtained in this study, therefore, began from analyzing general airflow patterns around the barrier and then related parameters were compared with published experimental results. Based on published experimental data (Bourdin and Wilson, 2008; Bradley and Mulhearn, 1983), the upwind mean velocity at $z = 3.33H$ was chosen as the reference velocity (u_0) for both the fence and tree; and the normalized predicted velocities, u/u_0, at $z = 0.38H$ and $z = 1.88H$ were analyzed and compared with experimental data. Contours of the normalized horizontal velocity (u/u_0) around vegetative barriers were used to represent specific wind speed distributions of the airflow predicted by CFD models.

The sensitivity of predicted velocity to values of C_d and z_0 were assessed along with turbulent models. Normally, C_d ranges from 0.1 to 0.5 and 0.5 was used in the study of Tiwary et al. (2005). $z_0/H = 0.0086$ was applied in their study based on the study of airflow through fences conducted by Packwood (2000). This study applied these values and also adjusted them by -50% to determine their effects on airflow. Table 6.4 lists the cases tested for airflow analysis in this study.

Table 6.4 Study cases of airflow through the trees.

	$k-\varepsilon$ **model**	C_d	z_0 **/H**
Case 1	Standard	0.5	0.0086
Case 2	Realizable	0.5	0.0086
Case 3	Standard	0.25	0.0086
Case 4	Realizable	0.25	0.0086
Case 5	Standard	0.5	0.0043
Case 6	Realizable	0.5	0.0043

6.3.4.2 Particle collection efficiency

For the particle collection, simulation was based on field measurements of particle concentration taken at upwind and downwind of the tree (Tiwary et al., 2005). In the said study, two identical optical particle counters (OPCs) were placed at points of $(x = -W - 0.1\,H, z = 0.75\,H)$ and $(x = 0.1\,H, z = 0.75\,H)$ away from the tree. Predicted particle collection efficiencies (CEs) of the tree, which were calculated based on predicted concentration values at these two points, were compared with published experimental data using paired t-tests. In addition, to evaluate the rationality of the predicted concentration, horizontal variation of normalized particle concentration (N / N_0) for $d_p = 15\ \mu m$ at $z = 0.75\,H$ and vertical variation of N / N_0 for $d_p = 15\ \mu m$ at different locations predicted by CFD models were also analyzed in this study.

6.4 Results and Discussion

6.4.1 Airflow around the fence

Figure 6.6 shows the horizontal airflow streamlines around the fence. A roughly triangular shape of wind speed reduction zone was formed and extended to far downwind of the fence. A smaller portion of wind speed reduction area was also observed on the windward side of the fence. Streamlines above the fence sharply curved upward and showed slight downward curvature towards the ground, which are related to the displaced profile and mixing zone, respectively, in Figure 6.6. These agreed with the observations described by Judd et al. (1996), in which the flow is divided into six distinct zones (approach profile, displaced profile, bleed flow, quiet zone, mixing zone and re-equilibration zone). There was no recirculation region; this is

consistent with the observation by Wang and Takle (1995) and Bradley and Mulhearn (1983), that there was no evidence of a recirculating region when the porosity reached and exceeded 50%.

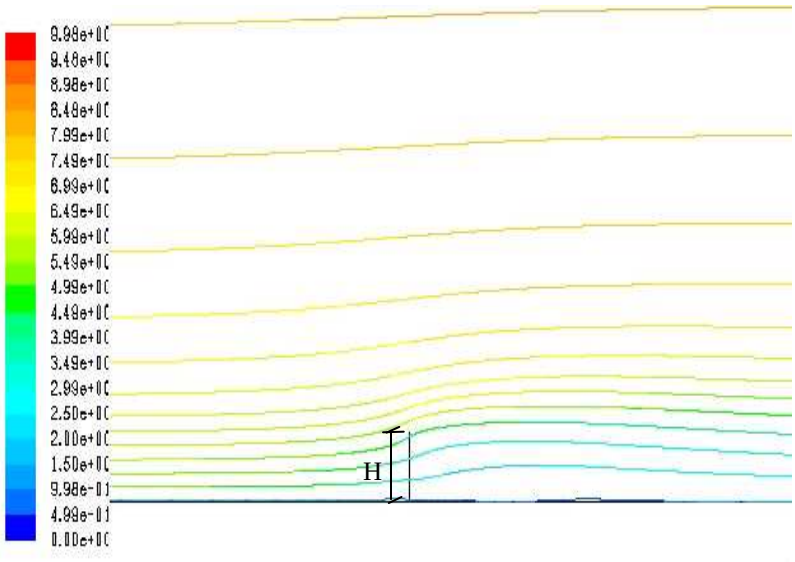

Figure 6.6 Predicted airflow streamlines (m/s) above and through the fence (colored by horizontal air velocity).

The normalized velocities (u/u_0) at $z = 0.38H$ and $z = 1.88H$ are shown in Figure 6.7. Also shown are published experimental data of Bradley and Mulhearn (1983). In general, predicted normalized velocities for the two turbulence models agreed well with published experimental data. The standard $k-\varepsilon$ model had better results at $z = 0.38H$ further downstream of the fence compared with the realizable $k-\varepsilon$ model; however, at $z = 1.88H$, the realizable $k-\varepsilon$ model had better results.

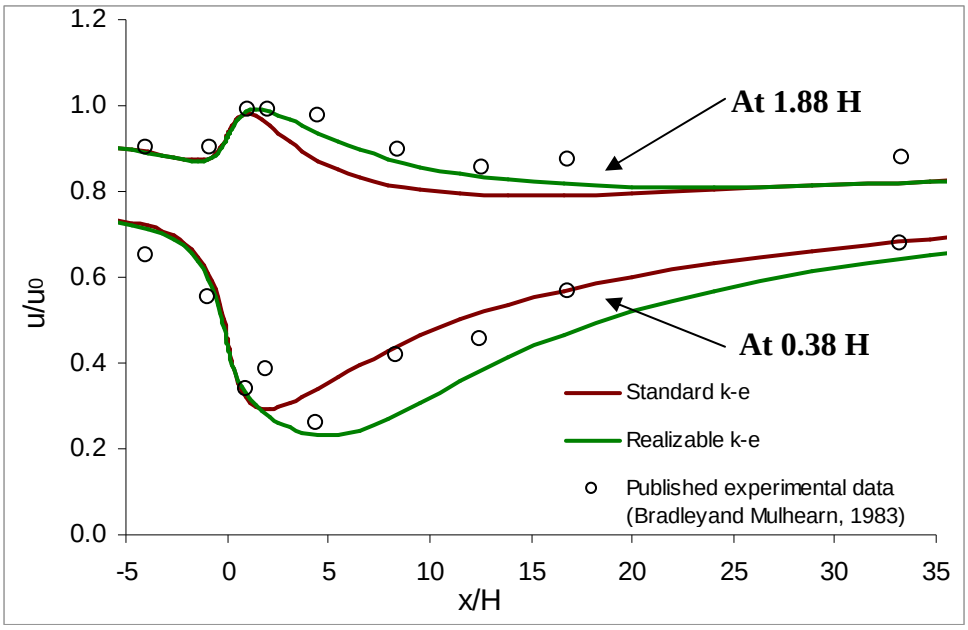

Figure 6.7 Comparison of normalized predicted air velocities though the fence with published experimental data (Bradley and Mulhearn, 1983).

Contours of the normalized horizontal velocity (u/u_0) predicted by both standard and realizable $k-\varepsilon$ models are shown in Figure 6.8. For the standard $k-\varepsilon$ model (Fig. 6.8a), the $u_{\min}$ ($u_{\min}/u_0 \le 0.2$) was in the area of $2\,H \le x_{\min} \le 5\,H$ and $z < 0.2H$, x_s was greater than $30H$ for u/u_0<0.7. For the realizable $k-\varepsilon$ model, the $u_{\min}$ ($u_{\min}/u_0 \le 0.2$) was in the area of $3\,H \le x_{\min} \le 9\,H$ and $z < 0.2\,H$, x_s was also greater than $30H$ for u/u_0<0.7. The realizable $k-\varepsilon$ model (Fig. 6.8b) predicted slightly lower velocity downwind of the fence and higher velocity over the fence compared with the standard $k-\varepsilon$ model (Fig. 6.8a).

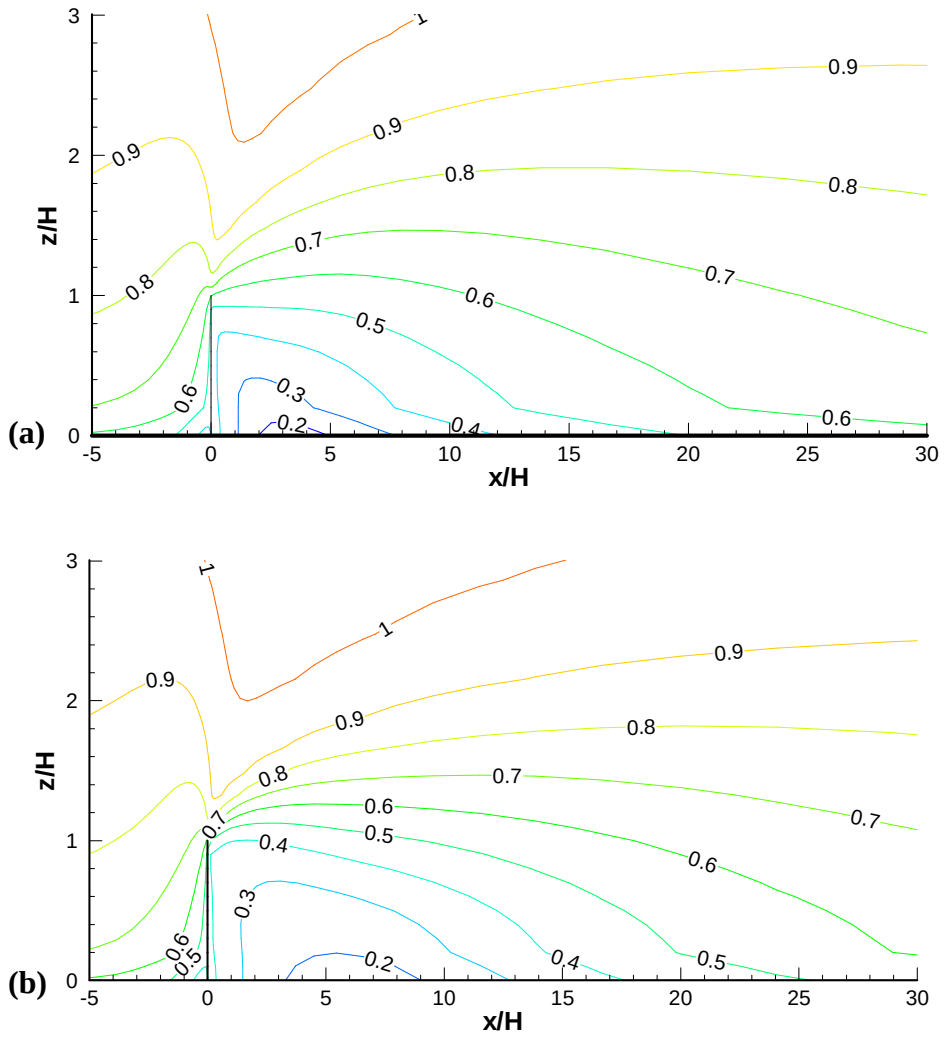

Figure 6.8 Contours of normalized horizontal velocity (u/u_0) near the fence predicted by (a) standard $k-\varepsilon$ model and (b) realizable $k-\varepsilon$ model.

6.4.2 Airflow around the trees and particle collection

6.4.2.1 Airflow

Figure 6.9 shows the flow streamlines around and through the trees. Similar to the porous fence, a roughly triangular shape of wind speed reduction zone downwind of the tree was also observed; the area was less than that for the fence and slight speed reduction was observed at the bottom and upwind of the tree. This was caused by the different resistance of the tree at different heights with low and/or no resistance at the bottom of the tree. Above the tree, flow streamlines

also curved upward and showed slight downward curvature towards the ground. There was no separating recirculation zone also.

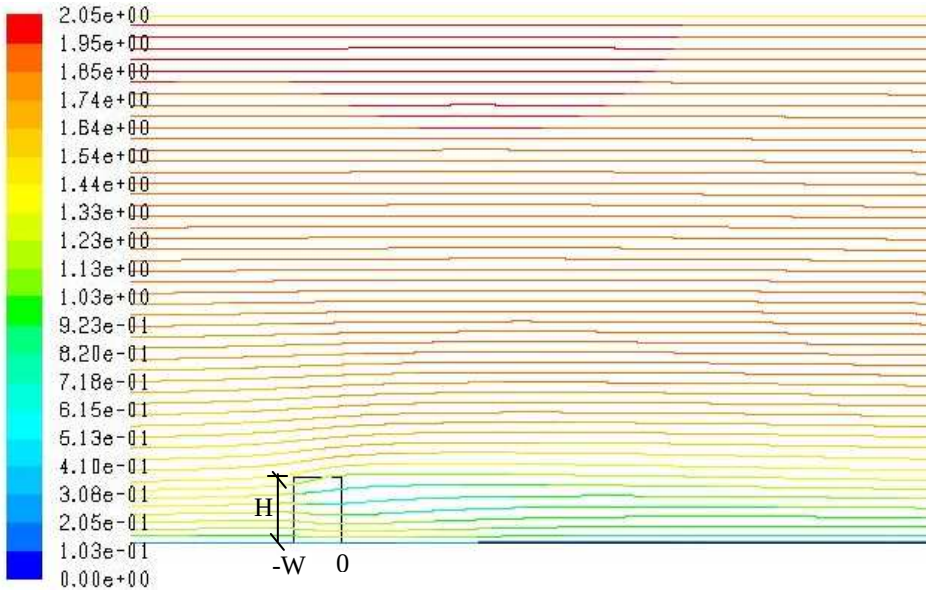

Figure 6.9 Flow streamlines (m/s) above and through the tree (colored by horizontal air velocity) predicted by realizable $k-\varepsilon$ model with $C_d = 0.5$ and $z_0 / H = 0.0086$ (Case 2).

Figure 6.10 shows predicted results on airflow for the six cases in Table 6.4. In general, at z=0.38 H, predicted u/u_0 values were greater when $C_d = 0.25$ than when $C_d = 0.5$ (Fig. 6.10a). At z=1.88 H, on the other hand, predicted u/u_0 values were not affected considerably by the C_d values. The z_0 / H had slight effect on the predicted u/u_0 values as shown in Figure 6.10b.

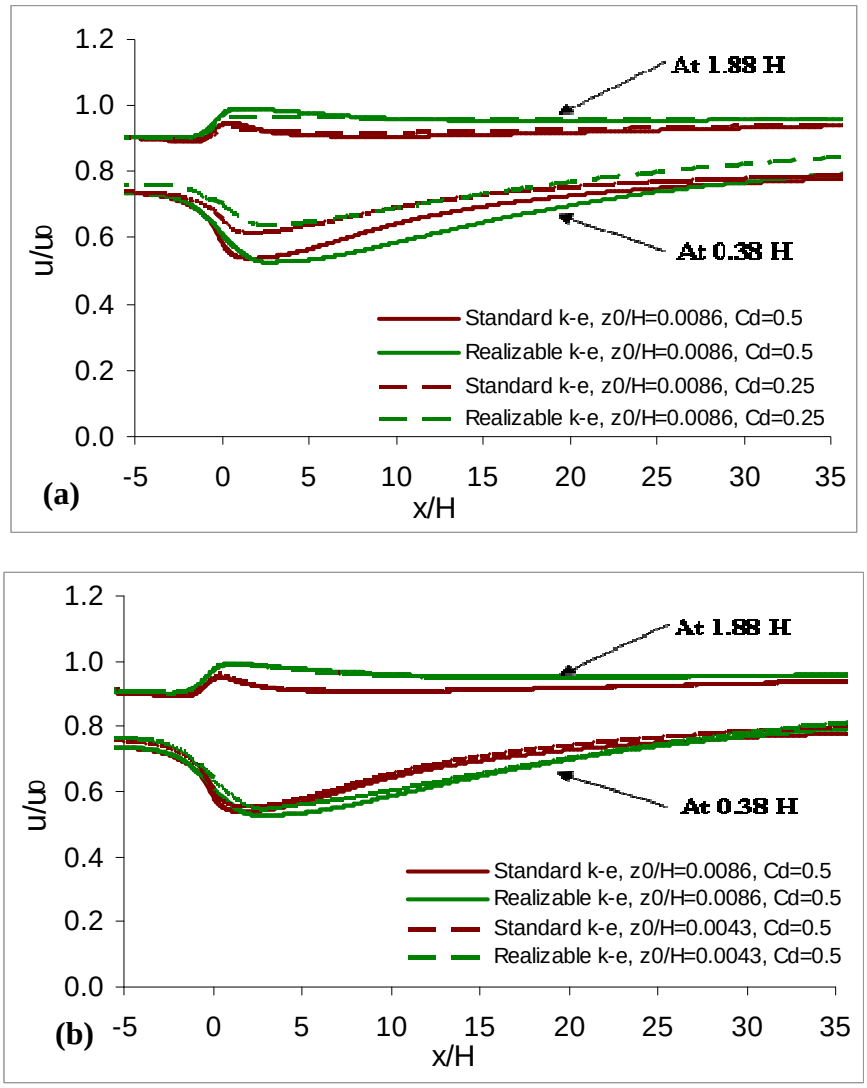

Figure 6.10 Comparison of predicted u/u_0 values by (a) varying C_d values at $z_0/H = 0.0086$ (Cases 1 and 2 vs. Cases 3 and 4); (b) varying z_0 values at $C_d = 0.5$ (Cases 1 and 2 vs. Cases 5 and 6) for the trees by different turbulent models.

Figure 6.11 shows predicted velocity profiles through the trees at $z = 0.75$ H. In this figure, the stream wise distance was normalized by the width of tree. The predicted velocities at the upwind edge of trees were reduced gradually with distance. Predicted velocity values were greater when $C_d = 0.25$ or $z_0/H = 0.0043$ than when $C_d = 0.5$ or $z_0/H = 0.0086$. These indicated the velocities through the tree were increased when the resistance was reduced and/or the inlet velocity was increased.

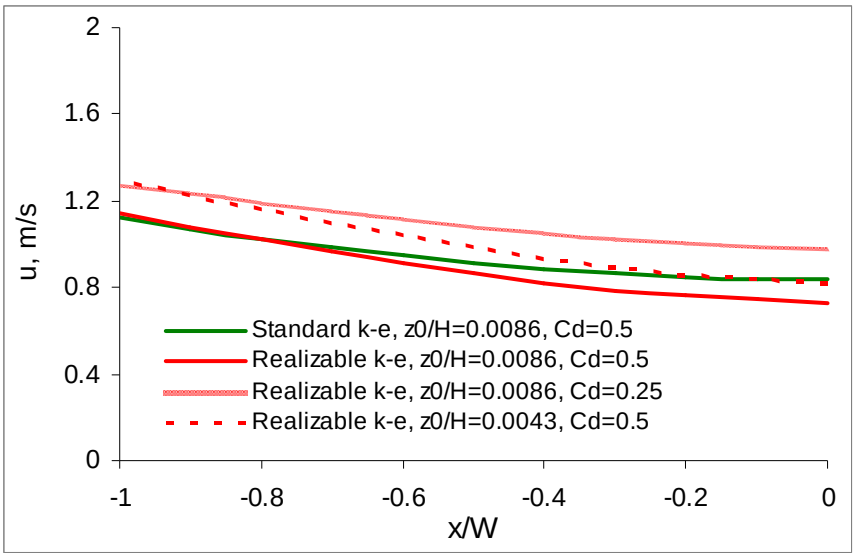

Figure 6.11 Predicted horizontal velocities of airflow through the trees at z=0.75H.

Figure 6.12 shows contours of predicted normalized velocities (u/u_0) around the trees, which represent specific wind speed distributions of u/u_0 predicted by realizable $k-\varepsilon$ model, with different C_d and z_0 values. In general, the three models had similar airflow patterns. There were two speed reduction zones. One was located at around $-5H$ and close to the ground as that for the fence. Another one was located within the upper part and at the downwind edge of the tree where k_r was higher. Predicted u/u_0 values increased within the lower part of the tree where k_r was lower or zero. In addition, the distribution of u/u_0 values varied with C_d and z_0 values.

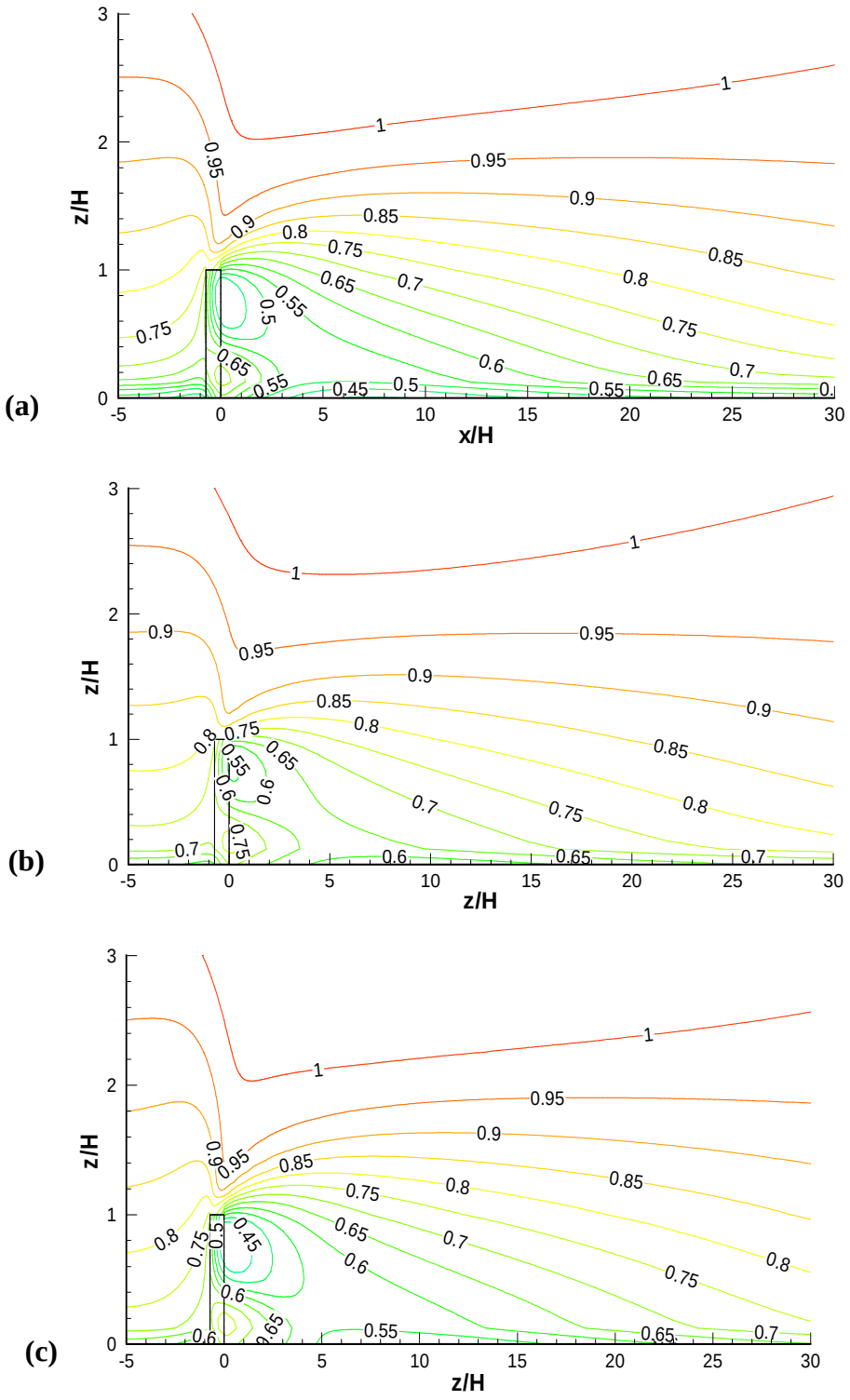

Figure 6.12 Contours of normalized horizontal velocity (u/u_0) around the trees predicted by realizable $k-\varepsilon$ model with (a) $C_d = 0.5$, $z_0/H = 0.0086$; (b) $C_d = 0.25$, $z_0/H = 0.0086$; and (c) $C_d = 0.5$, $z_0/H = 0.0043$.

6.4.2.2 Particle collection

Figure 6.13 shows the predicted CE values for the standard and realizable $k-\varepsilon$ models at $z_0 / H = 0.0086$ and $C_d = 0.5$ (i.e., Cases 1 and 2, respectively). With the realizable $k-\varepsilon$ model, predicted CE values were closer to experimental values, especially for particles with diameter greater than 5 µm, compared with the standard $k-\varepsilon$ model. However, both models underestimated the CE for large particles compared with experimental data. There was strong correlation between predicted CE and experimental values (Pearson correlations were greater 0.9); however, the P (T<=t) values were less than 0.05 for Case 1 and Case 2, indicating that there were significant differences between simulated and experimental values.

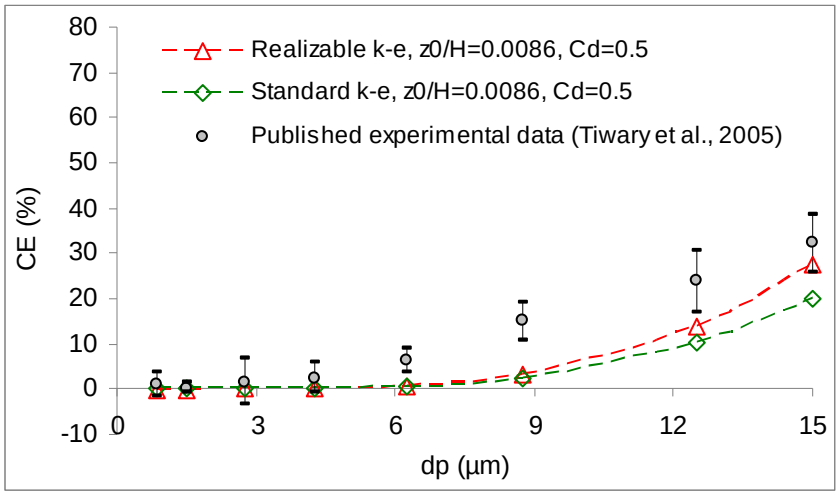

Figure 6.13 Published experimental collection efficiency (CE) of the tree (Tiwary et a., 2005) and values predicted by standard $k-\varepsilon$ (Case 1) and realizable (Case 2) models with $z_0 / H = 0.0086$, and $C_d = 0.5$.

Better agreements of predicted values and experimental data were observed when C_d =0.25 or z_0 / H =0.0043 (Fig. 6.14). Predicted CE values were within the range of experimental data, except for particles with $d_p = 6.25\ \mu m$ and $d_p = 8.75\ \mu m$, in which predicted values were slightly less than experimental data. Paired t-tests indicated that there were no significant differences between predicted values (Cases 4 and 6) and experimental data.

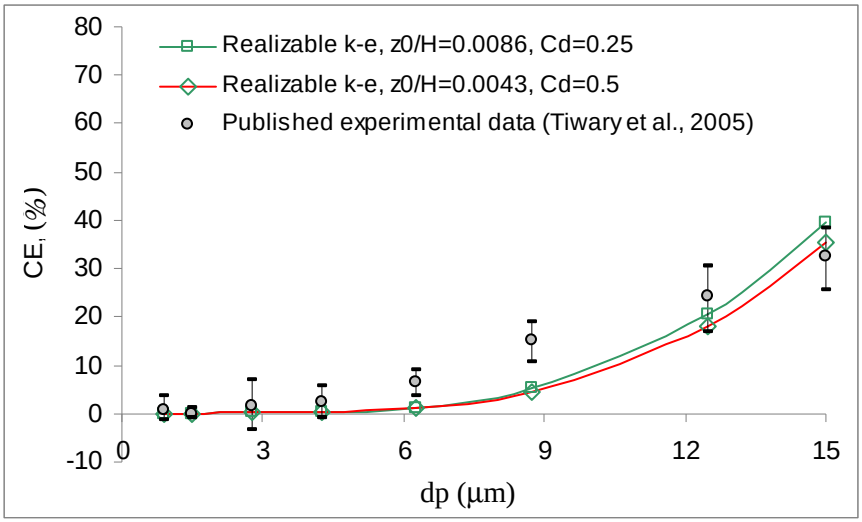

Figure 6.14 Published experimental collection efficiency (CE) of the tree (Tiwary et al., 2005) with that predicted by realizable $k-\varepsilon$ model with $C_d = 0.25, z_0 / H = 0.0086$ (Case 4) and $C_d = 0.5, z_0 / H = 0.0043$ (Case 6).

Horizontal variation of normalized particle concentration (N / N_0) for $d_p = 15\ \mu m$ at $z = 0.75\ H$ and vertical variation of normalized particle concentration (N / N_0) for $d_p = 15\ \mu m$ at different locations predicted by realizable $k-\varepsilon$ model with $C_d = 0.25$ and $z_0 / H = 0.0086$ (Case 4) are shown in Figures 6.15 and 6.16, respectively. Figure 6.15 shows slight variation of particle concentration upwind of the tree; it was reduced significantly through the tree and gradually recovered approximately to the upwind values. The near-surface particle concentration increased with increasing downwind distance because the flow above the barriers are mixed downwards into the sheltered region, eventually recovering approximately to their values far upwind (Raupach et al., 2001; Cleugh, 1998). Figure 6.16 shows that concentrations above the

barrier were slightly reduced, most likely due to the gravitational settling. However, concentrations were greatly reduced near and within the barrier, especially at the upper part and downwind edge of the tree. Higher reduction of concentration near the ground was observed at the stream wise direction around 10 H downwind of the tree.

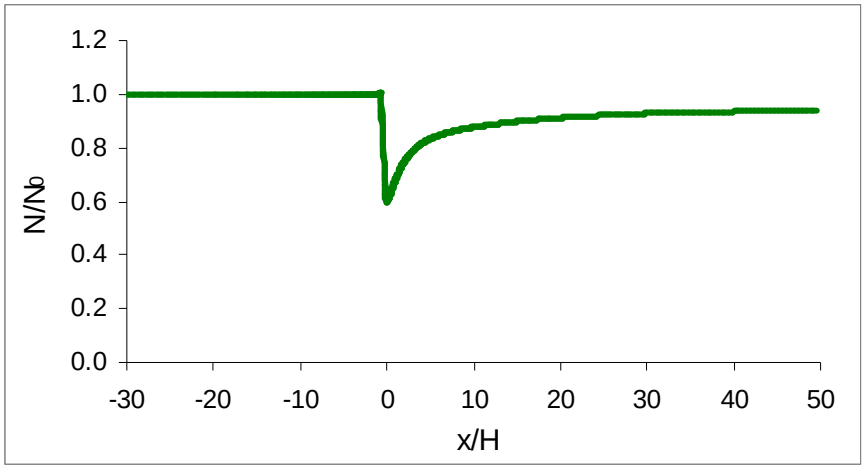

Figure 6.15 Horizontal variation of normalized particle concentration (N / N_0) of $d_p = 15\ \mu m$ at $z = 0.75\ H$ height predicted by realizable $k-\varepsilon$ model with $C_d = 0.25$ and $z_0 / H = 0.0086$ (Case 4).

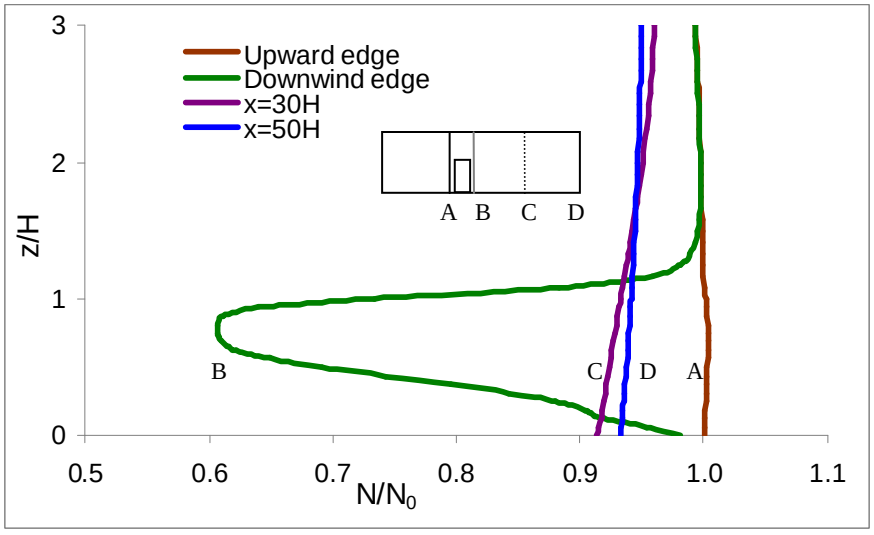

Figure 6.16 Vertical variation of normalized particle concentration (N / N_0) of $d_p = 15\ \mu m$ at different locations predicted by realizable $k-\varepsilon$ model with $C_d = 0.25$ and $z_0 / H = 0.0086$ (Case 4).

6.5 Conclusions

This study investigated the airflow around a porous fence using computational fluid dynamics (CFD). Predicted results agreed well with available experimental data. The CFD model was then applied to simulate airflow around and through a row of trees. In addition, an Eulerian-based model of particle transport was implemented in the CFD model to predict particle collection by the trees. Predicted particle collection efficiencies compared favorably with available experimental data. This study indicated the potential of numerical simulation with CFD to predict collection efficiency of vegetative barriers. Future work is needed to establish effects of the structure of vegetative barriers – geometry, species, number of rows - on particle collection.

6.6 References

Adrizal, P.H. Patterson, R.M. Hulet, R.M. Bates, D.A. Despot, E.F. Wheeler, P.A. Topper, D.A. Anderson, and J.R. Thompson. 2008. The potential for plants to trap emissions from farms with laying hens: 2. Ammonia and dust. *J. Appl. Poultry Res.* 17(3): 398-411.

Auvermann, B.W., and A. Romanillos. 2000a. Effect of increased stocking density on fugitive emissions of PM_{10} from cattle feedyards. In *Proc. International Meeting of the Air and Waste Management Association*. Pittsburgh, Penn.: Air and Waste Management Association.

Auvermann, B.W., and A. Romanillos. 2000b. Manipulating stocking density to manage fugitive dust emission from cattle feedyards. In *Proc. of the Innovative Technologies for Planning Animal Feeding Operations*, 61-70. Akron, Colo.: USDA-ARS Central Great Plains Research Station.

Bache, D.H. 1979. Particle transport within plant canopies-I. A framework for analysis. *Atmos. Environ.* 13(9): 1257-1262.

Bitog, J.P., I.B. Lee, M.H. Shin, S.W. Hong, H.S. Hwang, I.H. Seo, J.I. Yoo, K.S. Kwon, Y.H. Kim, and J.W. Han. 2009. Numerical simulation of an array of fences in Saemangeum reclaimed land. *Atmos. Environ.* 43(30): 4612-4621.

Boldes, U., J. Colman, and J.M. Di Leo. 2001. Field study of the flow behind single and double row herbaceous windbreaks. *J. Wind Eng. Ind. Aerodyn.* 89(7-8): 665-687.

Bonifacio, H.F., R.G. Maghirang, E.B. Razote, B.W. Auvermann, J.P. Harner, J.P. Murphy, L. Guo, J.M. Sweeten, and W.L. Hargrove. 2011. Particulate control efficiency of a water sprinkler system at a beef cattle feedlot in Kansas. *Trans. ASABE* 54(1): 295-304.

Bourdin, P., and J.D. Wilson. 2008. Windbreak aerodynamics: Is computational fluid dynamics reliable? *Boundary Layer Meteorol.* 126(2): 181-208.

Bradley, E.F., and P.J. Mulhearn. 1983. Development of velocity and shear stress distributions in the wake of a porous shelter fence. *J. Wind Eng. Ind. Aerodyn.* 15(1-3): 145-156.

Cleugh, H.A. 1998. Effects of windbreaks on airflow, microclimates and crop yields. *Agroforestry Syst.* 41(1): 55-84.

Davis, J.G., T.L. Stanton, and T. Haren. 2004. Feedlot manure management. Management, Livestock Series. No. 1.220. Fort Collins, Colo.: Colorado State University Cooperative Extension. Available at: http://www.cde.state.co.us/artemis/UCSU20/UCSU2062212202002INTERNET.pdf. Accessed 15 February 2010.

Dierickx, W., W.M. Cornelis, and D. Gabriels. 2003. Wind tunnel study on rough and smooth surface turbulent approach flow and on inclined windscreens. *Biosystems Eng.* 86(2):151-166.

El Gharbi, N., R. Absi, A. Benzaoui, and E.H. Amara. 2009. Effect of near-wall treatments on airflow simulations. Proceedings of 2009 International Conference on Computational Methods for Energy Engineering and Environment: ICCM3E. Sousse, Tunisia, 20-22 November, 2009, pp. 185-189.

FLUENT Inc. 2006. FLUENT 6.3 user's guide. Lebanon, N.H.: FLUENT Inc.

Fuchs, N.A. 1964. *The mechanics of aerosols*. Oxford: Pergamon Press.

Hinds, W.C. 1999. *Aerosol technology: properties, behavior and measurement of airborne particles*. 2nd ed. New York: John Wiley &Sons, Inc.

Judd, M.J., M.R. Raupach, and J.J. Finnigan. 1996. A wind tunnel study of turbulent flow around single and multiple windbreaks, part I: velocity fields. *Boundary Layer Meteorol.* 80: 127-165.

Lin, X. 2006. Simulation of odor dispersion around natural windbreaks. PhD diss. Ste-Anne-de-Bellevue, Quebec: McGill University.

Malone, B. 2004. Using trees to reduce dust and odor emissions from poultry farms. *In Proc. 2004—Poultry information Exchange*, 33-38. Surfers Paradise, Queensland, Australia.

Melese Endalew, A.M. Hertog, M.A. Delele, K. Baetens, T. Persoons, M. Baelmans, H. Ramon, B.M. Nicolai, and P. Verboven. 2009. CFD modeling and wind tunnel validation of airflow through plant canopies using 3D canopy architecture. *Int. J. Heat Fluid Flow* 30(2): 356-368.

Miller, D.N., and E.D. Berry. 2005. Cattle feedlot soil moisture and manure content: 1. Impacts on greenhouse gases, odor compounds, nitrogen losses, and dust. *J. Environ. Qual.* 34(2): 644-655.

Mohebbi, A., and S. Baroutian. 2007. Numerical modeling of particulate matter dispersion from Kerman cement plant, Iran. *Environ. Monit. Assess.* 130(1-3): 73-82.

Nunn, R.H. 1989. *Intermediate fluid mechanics*. New York: Hemisphere Pub. Co.

Packwood, A.R. 2000. Flow through porous fences in thick boundary layers: comparisons between laboratory and numerical experiments. *J. Wind Eng. Ind. Aerodyn.* 88(1): 75-90.

Peters, K., and R. Eiden. 1992. Modelling the dry deposition velocity of aerosol particles to a spruce forest. *Atmos. Environ.* 26(14): 2555-2564.

Petroff, A., A. Mailliat, M. Amielh, and F. Anselmet. 2008. Aerosol dry deposition on vegetative canopies. Part I: Review of present knowledge. *Atmos. Environ.* 42(16): 3625-3653.

Portela, L.M., and R.V.A. Oliemans. 2006. Possibilities and limitations of computer simulations of industrial turbulent dispersed multiphase flows. *Flow, Turbulence and Combustion* 77(1-4): 381-403.

Predicala, B.Z. 2003. Characterization and modeling of concentrations and emissions of particulate matter in swine buildings. PhD diss. Manhattan, Kan.: Kansas State University.

Purdy, C.W., R.N. Clark, and D.C. Straus. 2007. Analysis of aerosolized particulates of feedyards located in the Southern High Plains of Texas. *Aerosol Sci. Technol.* 41(5): 497-509.

Purdy, C.W., D.C. Straus, D.B. Parker, S.C. Wilson, and R.N. Clark. 2004. Comparison of the type and number of microorganisms and concentration of endotoxin in the air of feedyards in the Southern High Plains. *Atmos. J. Veterinary Res.* 65(1): 45-52.

Raupach, M.R., and A.S. Thom. 1981. Turbulence in and above plant canopies. *Ann. Rev. Fluid Mech.* 13: 97-129.

Raupach, M.R., N. Woods, G. Dorr, J.F. Leys, and H.A. Cleugh. 2001. The entrapment of particles by windbreaks. *Atmos. Environ.* 35(20): 3373-3383.

Razote, E.B., R.G. Maghirang, L. Guo, J.G. Tallada, B.W. Auvermann, J.P. Harner III, and W.L. Hargrove. 2008. TEOM measurements of PM_{10} and $PM_{2.5}$ concentrations at cattle feedlots in Kansas. ASABE Paper Number MC08108. St. Joseph, Mich.: ASABE.

Razote E.B., R.G. Maghirang, B.Z. Predicala, J.P. Murphy, B.W. Auvermann, J.P. Harner III, and W.L. Hargrove. 2006. Laboratory evaluation of the dust emission potential of cattle feedlot surfaces. *Trans. ASABE* 49(4): 1117-1124.

Reynolds, S.J., D.Y. Chao, P.S. Thorne, P. Subramanian, P.F. Waldron, M. Selim, P.S. Whitten, and W.J. Popendorf. 1998. Field comparison of methods for evaluation of vapor/particle phase distribution of ammonia in livestock buildings. *J. Agric. Safety Health* 4(2): 81-93.

Richards, P., and R. Hoxey. 1993. Appropriate boundary conditions for computational wind engineering models using the $k-\varepsilon$ turbulence model. *J. Wind Eng. Ind. Aerodyn.* 46-47:145-153.

Rogge, W.F., P.M. Medeiros, and B.R.T. Simoneit. 2006. Organic marker compounds for surface soil and fugitive dust from open lot dairies and cattle feedlots. *Atmos. Environ.* 40(1): 27-49.

Rosenfeld M., G. Marom, and A. Bitan. 2010. Numerical simulation of the airflow across trees in a windbreak. *Boundary Layer Meteorol.* 135(1): 89-107.

Santiago, J.L., F. Martin, A. Cuerva, N. Bezdenejnykh, and A. Sanz-Andres. 2007. Experimental and numerical study of wind flow behind windbreaks. *Atmos. Environ.* 41(30): 6406-6420.

Sweeten, J.M., C.B. Parnell, B.W. Shaw, and B.W. Auvermann. 1998. Particle size distribution of cattle feedlot dust emission. *Trans. ASAE* 41(5): 1477-1481.

Sweeten, J.B., C.B. Parnell, R.S. Etheredge, and D. Osborne. 1988. Dust emission in cattle feedlots. *Veterinary Clinics of North America: Food Animal Practice* 4(3): 557-578.

Sweeten, J.M., C.B. Parnell, B.W. Auvermann, B.W. Shaw, and R.E. Lacey. 2000. Livestock feedlots. In: *Air Pollution Engineering Manual*, W. T. Davis (ed.). New York: John Wiley & Sons.

Tiwary, A., H.P. Morvan, and J.J. Colls. 2005. Modelling the size-dependent collection efficiency of hedgerows for ambient aerosols. *J. Aerosol Sci.* 37(8): 990-1015.

Tu, J, G.H. Yeoh, and C. Liu. 2008. *Computational fluid dynamics: a practical approach.* Amsterdam: Butterworth-Heinemann.

Vlachos, N., E. Mourouglou, and A.G. Konstandopoulos. 2002. Development of fluent user-defined functions for the modeling of particle transport in non-isothermal gas flows. Advanced Process Modeling and Simulation Tools. Thermi, Thessaloniki, Greece: 2002 workshop of CPERI.

Wang, C., and Y. Lin. 2006. Numerical simulation of three dimensional gas-particle flow in a spiral cyclone. *J. Appl. Math. Mech*. 27(2): 247-253.

Wang, H., and E.S. Takle. 1995. A numerical simulation of boundary-layer flows near shelterbelts. *Boundary Layer Meteorol.* 75(1-2): 141-173.

Wang, H., E.S. Takle, and J. Shen. 2001. Shelterbelts and windbreaks: Mathematical modeling and computer simulations of turbulent flows. *Ann. Rev. Fluid Mech.* 33:549-586.

Wilson, J.D. 1985. Numerical studies of flow through a windbreak. *J. Wind Eng. Ind. Aerodyn.* 21(2): 119-154.

Wilson, J.D., and E. Yee. 2003. Calculation of wind disturbed by an array of fences. *Agric. For. Meteorol.* 115(1-2): 31-50.

Zhang, N., Z.C. Zheng, and R.G. Maghirang. 2008. Numerical simulation of smoke clearing with nanoparticle aggregates. *Int. J. Numer. Methods Eng.* 74(4): 601-618.

CHAPTER 7 - Conclusions and Recommendations

7.1 Summary and Conclusions

Emissions of particulate matter (PM) are an increasing concern for large open beef cattle feedlots. Research is needed to develop science-based information on PM emissions and abatement measures for mitigating those emissions. This research was conducted to (1) measure PM concentrations emitted from large cattle feedlots, (2) compare different samplers for measuring concentrations of PM with equivalent aerodynamic diameter of 10 µm or less (PM_{10}), (3) evaluate the relative effectiveness of pen surface treatments in reducing PM_{10} emissions, and (4) predict PM control efficiency of vegetative barriers.

The following conclusions were drawn from this research:

- Measurement of PM concentration with gravimetric samplers at feedlots KS1 and KS2 showed the downwind and net mass concentrations of PM with equivalent aerodynamic diameter of 2.5 µm or less ($PM_{2.5}$), PM_{10}, and total suspended particulates (TSP) varied seasonally. The mass concentrations of TSP and PM_{10} were closely related to the pen surface water content. The mass concentration of $PM_{2.5}$ also was related to the pen surface water content, but not to the same degree. For PM control, the water content of pen surface should be at least 20%. Measurement of the particle size distribution at the downwind perimeter of the feedlot with a cascade impactor showed geometric mean diameter ranging from 7 to 18 µm, indicating that particles that are emitted from the feedlots were generally large in size.
- Collocated PM_{10} samplers at feedlots KS1 and KS2 showed similar trends but significant differences in concentrations. In general, the TEOM tended to oversample PM_{10} (by approximately 6%) compared with the high-volume sampler. The low-volume PM_{10} sampler tended to undersample (by about 47%) compared with the high-volume sampler.
- Laboratory experiments showed PM_{10} emission potential due to the horizontal shearing action of cattle hooves increased with increasing speed of hooves and depth of hoof penetration into the uncompacted manure layer. Topical application of

mulches or water application significantly reduced PM_{10} emission potential of the simulated pen surface. Of the materials tested, hay and water were the most effective in reducing PM_{10} emission potential, with control efficiencies for hay ranging from 48% for an application rate of 241 g/m^2 to 77% for an application rate of 723 g/m^2. Control efficiencies for water ranged from 42% (for an application rate of 3.2 mm) to 69% (for an application rate of 6.4 mm).

- The applicability of computational fluid dynamics (CFD) in modeling airflow around and through porous barriers was evaluated by simulating airflow passing a porous fence in two-dimensional domain, using standard and realizable k-ε turbulence models. Predicted air velocities agreed well with published data. The CFD model was then applied to simulate airflow and particle collection by trees with known surface area density as a function of height. Predicted particle collection efficiencies for the trees generally agreed with published data and ranged from less than 1% for 0.875-µm particles to approximately 32% for 15-µm particles.

7.2 Recommendations for Further Study

Particulate matter emitted from cattle feedlots is influenced by numerous factors that must be examined closely to improve and/or develop effective control strategies. The following are recommended for future studies:

- Multiple-day, seasonal sampling of PM is needed to assess animal and worker exposure as well as improve the effectiveness of control strategies. In addition, standard PM measurements in open feedlots need to be established to facilitate comparison of results from different studies.
- Determine factors, such as weather conditions, pen surface water content, and cattle behavior, which can be used to predict the PM emission from feedlots.
- Further investigate potential methods to control pen surface water content in optimal range for both PM and odor control. Especially, the sprinkler system and pen surface treatment need much field or laboratory study to improve their effectiveness and capability.

- Establish effects of height, width, and shape of the trees on particle collection. In addition, experimental measurements must be conducted to validate the numerical prediction under feedlot conditions.